NACA

RESEARCH MEMORANDUM

WIND-TUNNEL INVESTIGATION AT A MACH NUMBER OF 2.01 OF THE AERODYNAMIC CHARACTERISTICS IN COMBINED PITCH AND SIDESLIP OF SOME CANARD-TYPE MISSILES HAVING CRUCIFORM WINGS AND CANARD SURFACES WITH 70° DELTA PLAN FORMS

By M. Leroy Spearman and Cornelius Driver

Langley Aeronautical Laboratory
Langley Field, Va.

NATIONAL ADVISORY COMMITTEE
FOR AERONAUTICS

WASHINGTON
August 23, 1954

NACA RM L54F09

~~CONFIDENTIAL~~

NATIONAL ADVISORY COMMITTEE FOR AERONAUTICS

RESEARCH MEMORANDUM

WIND-TUNNEL INVESTIGATION AT A MACH NUMBER OF 2.01 OF THE AERODYNAMIC CHARACTERISTICS IN COMBINED PITCH AND SIDESLIP OF SOME CANARD-TYPE MISSILES HAVING CRUCIFORM WINGS AND CANARD SURFACES WITH 70° DELTA PLAN FORMS

By M. Leroy Spearman and Cornelius Driver

SUMMARY

An investigation has been conducted in the Langley 4- by 4-foot supersonic pressure tunnel to determine the static longitudinal stability and control characteristics of several missiles at a Mach number of 2.01. The missiles had cruciform wings and canard surfaces of delta plan form with leading edges swept 70°. Two models were tested with body fineness ratios of 19.1 and 15.7. The tests were made through an incidence angle range from -2° to about 26° at various roll angles from 0° to 90°.

The present paper consists largely of a data presentation of the results obtained at combined angles of pitch and sideslip. In addition to the basic data presentation, appendixes are included in which the body-, wind-, and stability-axes systems are described and the transfer equations necessary to convert the basic data to other forms are shown.

INTRODUCTION

In connection with the development of missile configurations with canard control surfaces, an investigation has been conducted in the Langley 4- by 4-foot supersonic pressure tunnel to determine the longitudinal and lateral aerodynamic characteristics of a series of such configurations. The models had cruciform wings and canard controls of delta plan form with the leading edges swept 70° and were equipped with all-movable canard surfaces for both longitudinal and directional control and movable wing-tip ailerons for lateral control.

~~CONFIDENTIAL~~

The results of an investigation of the effects of body length (fineness ratios of 14.8, 15.7, 16.7, 17.7, and 19.1) on the longitudinal stability and control characteristics of these missiles at a Mach number of 2.01 are presented in reference 1. The aerodynamic characteristics of the canard surfaces in the presence of the fineness ratio 19.1 body at a Mach number of 1.61 are presented in reference 2. The results of an investigation made at a Mach number of 2.01 to determine the effects of large deflections of the canard control and deflections of the wing-tip controls on the aerodynamic characteristics of the configuration with a fineness ratio of 15.7 are presented in reference 3. The results of some additional tests made at a Mach number of 1.41 of the configuration with a fineness ratio of 15.7 and of the bodies with fineness ratios of 15.7 and 19.1 with very small-span wings are presented in reference 4.

The present paper consists of a data presentation of the results obtained at a Mach number of 2.01 for the configurations with fineness ratios of 15.7 and 19.1 at various roll angles from 0° to 90° through an incidence angle range from -2° to about 26°. A resolution of these results provides the aerodynamic characteristics for the missiles at angles of attack up to about 26° at zero angle of sideslip or at combined angles of attack and sideslip up to a maximum of about 16° for each. The results include those for the complete configurations (body-wing-canard) with wings both in line with the canard surfaces and indexed 45° with respect to the canard surfaces, as well as those for the body-wings, body-canards, and body-alone configurations. In addition to the basic-data presentation, some transfer equations are included that may be used to facilitate the preparation of various types of analysis figures.

SYMBOLS

The basic results of the tests are presented as coefficients of forces and moments referred to the body-axis system (fig. 1) with the moment reference point for all configurations located 6.25 body diameters forward of the base of the body (-19.5 percent of the wing mean aerodynamic chord).

C_N	normal-force coefficient, $-Z/qS$
C_C	chord-force coefficient, $-X/qS$
C_m	pitching-moment coefficient, $M'/qS\bar{c}$
C_Y	lateral-force coefficient, Y/qS
C_l	rolling-moment coefficient, L/qSb

C_n	yawing-moment coefficient, N/qSb
Z	normal force along Z-axis
X	chord force along X-axis
M'	pitching moment about Y-axis
Y	lateral force along Y-axis
L	rolling moment about X-axis
N	yawing moment about Z-axis
q	free-stream dynamic pressure, lb/sq ft
S	total wing area resulting from extending the wing leading edge and trailing edge to the body center line
$\bar{c}$	wing mean aerodynamic chord, in.
d	diameter of body, in.
b	span of wing, in.
l	length of body, in.
α	angle of attack, deg
β	angle of sideslip, deg
i	angle of incidence, deg
ϕ	angle of roll, deg
δ_H	horizontal canard deflection angle, deg
δ_a	aileron deflection angle, deg

Subscripts:

s	stability axis
B	body axis
w	wind axis

MODELS AND APPARATUS

Sketches of the models are shown in figure 2. The geometric characteristics of the models are presented in table I.

The body of the model was composed of a parabolic nose followed by the frustum of a cone which was faired into a cylinder. The body length was varied through the use of different lengths of the cylindrical portion. Resulting body fineness ratios were 15.7 and 19.1. Coordinates of the body are given in table II. The canard surfaces and the wing had delta plan forms with hexagonal sections and leading edges swept 70°. The ratio of exposed canard area to exposed wing area for the basic configuration was 0.10. The horizontal canard was motor driven and deflections could be set by remote control. Tip ailerons of triangular plan form were provided on one pair of wings only (normally in the horizontal plane). It was possible to rotate the rear portion of the body containing the cruciform wings so that the wings might either be alined with the canard surfaces or indexed 45° with respect to the canard surfaces.

Force measurements were made through the use of a six-component internal strain-gage balance. The model was mounted in the tunnel on a remotely controllable rotary-type sting. The angle-of-incidence range was from 0° to about 26° at various roll angles from 0° to 90°.

TESTS, CORRECTIONS, AND ACCURACY

The conditions for the tests were:

Mach number	2.01
Stagnation temperature, °F	110
Stagnation pressure, atmospheres	1.0
Reynolds number based on $\bar{c}$	3.47×10^6

The stagnation dewpoint was maintained sufficiently low (-25° F or less) so that no condensation effects were encountered in the test section.

The angle of incidence was corrected for the deflection of the balance and sting under load. The Mach number variation in the test section was approximately ±0.01 and the flow-angle variation in the vertical and horizontal planes did not exceed about ±0.1°. No corrections were applied to the data to account for these flow variations. The base pressure was measured and the chord force was adjusted to a base pressure equal to the free-stream static pressure.

The estimated errors in the individual measured quantities are as follows:

C_N	±0.004
C_C	±0.002
C_m	±0.0004
C_Y	±0.001
C_n	±0.0005
C_l	±0.0004
i, deg	±0.1
ϕ, deg	±0.1
δ_H, deg	±0.1
δ_α, deg	±0.1

RESULTS

The basic results are computed for a body-axis system and are presented as functions of the incidence angle i for various constant roll angles ϕ. It is, perhaps, more conventional to present aerodynamic data for a particular axis system for various angles of attack and angles of sideslip. The selection of an axis system and angle notation is a matter of judgment dependent upon what may be most convenient or most useful for a particular purpose. The axes systems commonly employed are the body, wind, and stability systems. A description of the angle notations and axes systems is presented in appendix A and the transfer equations necessary to convert the present results to other forms are presented in appendix B.

The figures are presented in the following manner:

	Figure
Body alone:	
$l/d = 15.7$	3(a)
$l/d = 19.1$	3(b)
Body-canard, $l/d = 15.7$:	
$\delta_H = 0$	4(a)
$\delta_H = 8$	4(b)
$\delta_H = 12$	4(c)

Through the use of the equations given in appendix B, it is possible to obtain the incidence angle i necessary for various constant roll angles ϕ to provide a varying angle of sideslip at various constant angles of attack. This procedure has been followed and the tabulated coefficients at combined angles of attack and sideslip for one configuration are given in table III.

Numerous types of analyses, of course, are possible but in order to expedite publication of these results, none are included in this data report.

Langley Aeronautical Laboratory,
National Advisory Committee for Aeronautics,
Langley Field, Va., May 27, 1954.

APPENDIX A

AXES SYSTEMS AND ANGLE DEFINITIONS

Presentation of basic results.- The basic results for this report are computed for the body-axes system and are presented as functions of the incidence angle i for various constant roll angles ϕ. The incidence angle (see fig. 1) is defined as the angle between the body X-axis and the relative wind (line of flight) in the plane containing the body X-axis and the line of flight. The roll angle ϕ is the angular displacement about the body X-axis of the body X,Z-plane from the plane containing the body X-axis and the line of flight. From these two angles alone it is possible to locate the body in space with respect to its line of flight.

Body axes.- The body axes are a system of axes fixed within the model with the origin at the center of gravity or moment reference point and the X-axis is an arbitrary axis in the vertical plane of symmetry and usually points along the body reference center line. The Y-axis is perpendicular to the vertical plane of symmetry and points along the horizontal plane. The Z-axis is in the vertical plane of symmetry and perpendicular to the X-axis.

Wind axes.- The wind axes are a system of axes in which the X-axis always points along the line of flight (into the relative wind). The Z-axis lies in the vertical plane containing the wind X-axis and is perpendicular to the wind X-axis, and the wind Y-axis is perpendicular to both the X- and Z-axes.

Stability axes.- The stability axes are a system of axes in which the X-axis is the intersection of the vertical plane of symmetry of the model with a plane perpendicular to the plane of symmetry and parallel with the line of flight. The stability Y-axis is perpendicular to the vertical plane of symmetry, and the stability Z-axis is in the vertical plane of symmetry and perpendicular to the stability X-axis. The stability axes system is, in effect, a combination of the body and wind axes in that the stability and wind axes are identical in the angle-of-attack plane when the yaw angle is zero and the stability and body axes are identical in the angle-of-yaw plane when the angle of attack is zero. Hence, the stability axes do not pitch with the model but do yaw with the model.

Angle system.- The angle of attack is defined as the angle between the body X-axis and the projection of the body X-axis on the plane containing the line of flight and the body Y-axis. The angle of sideslip is the angle between the line of flight and the projection of the body X-axis on the plane containing the line of flight and the body Y-axis.

APPENDIX B

TRANSFER EQUATIONS

The equations necessary to convert the angles of incidence and roll to angles of attack and sideslip are as follows:

$$\tan \alpha = \cos \phi \tan i$$

$$\sin \beta = \sin \phi \sin i$$

The transfer equations necessary to convert the forces and moments from the body axes are as follows:

From body axes to stability axes:

$$X_s = X_B \cos \alpha + Z_B \sin \alpha$$

$$Y_s = Y_B$$

$$Z_s = Z_B \cos \alpha - X_B \sin \alpha$$

$$L_s = L_B \cos \alpha + N \sin \alpha$$

$$M_s' = M_B'$$

$$N_s = N \cos \alpha - L \sin \alpha$$

From body axes to wind axes:

$$X_w = X_B \cos \alpha \cos \beta + Z_B \sin \alpha \cos \beta + Y_B \sin \beta$$

$$Y_W = Y_B \cos \beta - X_B \cos \alpha \sin \beta - Z_B \sin \alpha \sin \beta$$

$$Z_W = Z_B \cos \alpha - X_B \sin \alpha$$

$$L_W = L_B \cos \alpha \cos \beta + N_B \sin \alpha \cos \beta + M_B' \sin \beta$$

$$M_W' = M_B' \cos \beta - L_B \cos \alpha \sin \beta - N_B \sin \alpha \sin \beta$$

$$N_W = N_B \cos \alpha - L_B \sin \alpha$$

REFERENCES

1. Spearman, M. Leroy: Aerodynamic Characteristics in Pitch of a Series of Cruciform-Wing Missiles With Canard Controls at a Mach Number of 2.01. NACA RM L53I14, 1953.

2. Spearman, M. Leroy: Component Tests To Determine the Aerodynamic Characteristics of an All-Movable 70° Delta Canard-Type Control in the Presence of a Body at a Mach Number of 1.61. NACA RM L53I03, 1953.

3. Spearman, M. Leroy: Effect of Large Deflections of a Canard Control and Deflections of a Wing-Tip Control on the Static-Stability and Induced-Roll Characteristics of a Cruciform Canard Missile at a Mach Number of 2.01. NACA RM L53K03, 1953.

4. Spearman, M. Leroy, and Robinson, Ross B.: Aerodynamic Characteristics of a Cruciform-Wing Missile With Canard Control Surfaces and of Some Very Small Span Wing-Body Missiles at a Mach Number of 1.41. NACA RM L54B11, 1954.

TABLE I

GEOMETRIC CHARACTERISTICS OF MODEL

Wings:	
Span, in.	11.853
Chord at body center line, in.	17.069
Chord at body intersection, in.	13.407
Chord at aileron break line, in.	4.606
Area (leading and trailing edges extended to body center line), sq in.	104.8
Area (exposed), sq in.	64.2
Aspect ratio	1.404
Sweep angle of leading edge, deg	70
Thickness ratio at body center line	0.0147
Thickness ratio at aileron break line	0.0543
Leading-edge angle normal to leading edge, deg	15.6
Mean aerodynamic chord, in.	11.48
Aileron:	
Area, sq in.	3.201
Mean aerodynamic chord	3.071
Thickness ratio at break line	0.039
Canard surfaces:	
Area (exposed) sq in.	6.406
Aspect ratio	1.73
Sweep angle of leading edge, deg	70
Mean aerodynamic chord, in.	2.576
Ratio of exposed area to wing exposed area	0.1
Body:	
Maximum diameter, in.	2.666
Base area, sq in.	5.583
Length (long body), in.	50.833
Length (short body), in.	42.0
Fineness ratio (long body)	19.1
Fineness ratio (short body)	15.7

TABLE II

BODY COORDINATES

Body station, in.	Radius, in.	
0 (Nose)	0	
.297	.076	
.627	.156	
.956	.233	
1.285	.307	
1.615	.378	
1.945	.445	
2.275	.509	
2.605	.573	
2.936	.627	
3.267	.682	
3.598	.732	
3.929	.780	
4.260	.824	
4.592	.865	
4.923	.903	
5.255	.940	
5.587	.968	
5.920	.996	
6.252	1.020	
6.583	1.042	Conical section
11.542	1.333	Conical section
42.000	1.333	Cylindrical
50.833	1.333	Cylindrical

TABLE III

TABULATED RESULTS FOR VARIOUS ANGLES OF ATTACK AND SIDESLIP

[Complete model; $l/d = 15.7$; inline wings]

(a) $\delta_H = 0^\circ$.

ϕ	i	β	C_N	C_m	C_l	C_n	C_Y
$\alpha = 4^\circ$							
15	4.14	-1.07	0.109	-0.038	-0.0002	-0.004	0.021
25	4.41	-1.87	.106	-.039	-.0003	-.011	.042
35	4.88	-2.81	.118	-.041	-.0002	-.020	.071
45	5.65	-4.00	.124	-.040	-.0001	-.032	.112
60	7.96	-6.91					
70	11.56	-10.88	.116	-.033			
77	17.27	-16.85					
80	21.94	-21.64					
$\alpha = 8^\circ$							
15	8.28	-2.16	0.255	-0.085	-0.0013	-0.011	0.046
25	8.82	-3.75	.257	-.084	-.0017	-.025	.095
35	9.74	-5.62	.255	-.085	-.0019	-.043	.158
45	11.24	-8.00	.256	-.085	-.0005	-.066	.237
60	15.70	-13.68	.263	-.081	.0040	-.109	.441
70	22.34	-21.11		-.052			
$\alpha = 12^\circ$							
15	12.4	-3.26	0.39	-0.125	-0.0059	-0.015	0.072
25	13.2	-5.66	.392	-.125	-.0056	-.039	.153
35	14.55	-8.46	.397	-.124	-.0026	-.066	.253
45	16.73	-12.00	.397	-.117	.0005	-.095	.381
60	23.03	-20.21					
$\alpha = 16^\circ$							
15	16.54	-4.39	0.527	-0.147	-0.0080	-0.018	0.102
25	17.56	-7.62	.529	-.148	-.0077	-.052	.218
35	19.29	-11.35	.532	-.147	-.0057	-.083	.353
45	22.07	-16.00	.533	-.141	-.0003	-.120	.521
$\alpha = 20^\circ$							
15	20.65	-5.57	0.678	-0.166	-0.0149	-0.025	0.147
25	21.88	-9.63	.675	-.169	-.0144	-.061	.294
35	23.96	-14.30	.686	-.173	-.0127	-.094	.463
$\alpha = 24^\circ$							
15	24.75	-6.80	0.863	-0.195	-0.0140	-0.069	0.236
25	26.16	-11.73	.860	-.202	-.0156	-.099	.399

TABLE III.- Concluded

TABULATED RESULTS FOR VARIOUS ANGLES OF ATTACK AND SIDESLIP

[Complete model; $l/d = 15.7$; inline wings]

(b) $\delta_H = 12^\circ$

ϕ	i	β	C_N	C_m	C_l	C_n	C_Y
$\alpha = 4^\circ$							
15	4.14	-1.07	0.121	0.007	0.0005	-0.005	0.019
25	4.41	-1.87	.125	.006	.0012	-.012	.041
35	4.88	-2.81	.126	.005	.0020	-.020	.066
45	5.65	-4.00	.132	.004	.0033	-.031	.106
60	7.96	-6.91	.142	.002	.0064	-.057	.198
70	11.56	-10.88	.157	.005	.0092	-.087	.339
$\alpha = 8^\circ$							
15	8.28	-2.16	0.263	-0.045	-0.0006	-0.012	0.044
25	8.82	-3.75	.265	-.045	.0018	-.026	.088
35	9.74	-5.62	.267	-.045	.0028	-.042	.150
45	11.24	-8.00	.275	-.042	.0044	-.063	.236
60	15.70	-13.68	.291	-.041	.0080	-.102	.424
$\alpha = 12^\circ$							
15	12.40	-3.26	0.398	-0.090	-0.0027	-0.012	0.066
25	13.20	-5.66	.407	-.092	-.0017	-.038	.145
35	14.55	-8.46	.411	-.090	-.0006	-.064	.247
45	16.73	-12.00	.422	-.087	.0025	-.092	.373
$\alpha = 16^\circ$							
15	16.54	-4.39	0.538	-0.122	-0.0083	-0.012	0.090
25	17.56	-7.62	.550	-.121	-.0067	-.047	.203
35	19.29	-11.35	.555	-.121	-.0062	-.080	.339
45	22.07	-16.00	.562	-.121	-.0035	-.113	.510
$\alpha = 20^\circ$							
15	20.65	-5.57	0.695	-0.137	-0.0121	-0.025	0.122
25	21.88	-9.63	.700	-.141	-.0091	-.062	.262
35	23.96	-14.30	.706	-.151	-.0120	-.096	.444
$\alpha = 24^\circ$							
15	24.75	-6.80	0.870	-0.164	-0.0141	-0.051	0.184
25	26.16	-11.73	.857	-.173	-.0162	-.080	.348

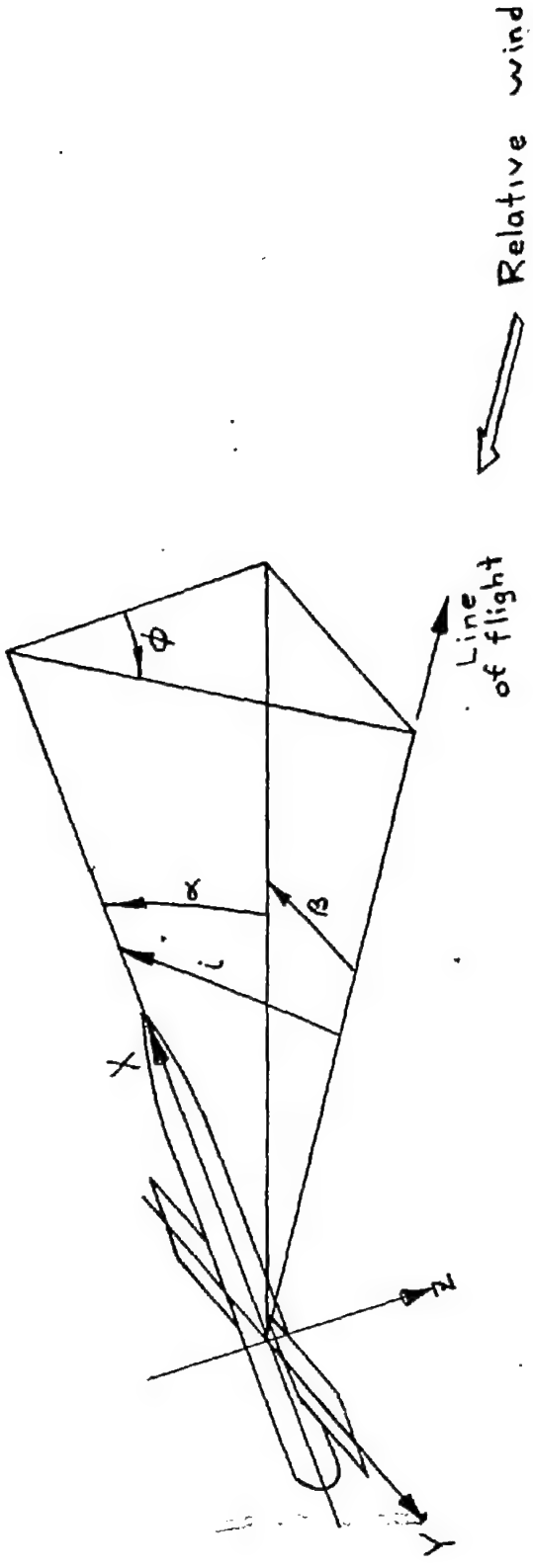

Figure 1.- Angle notation.

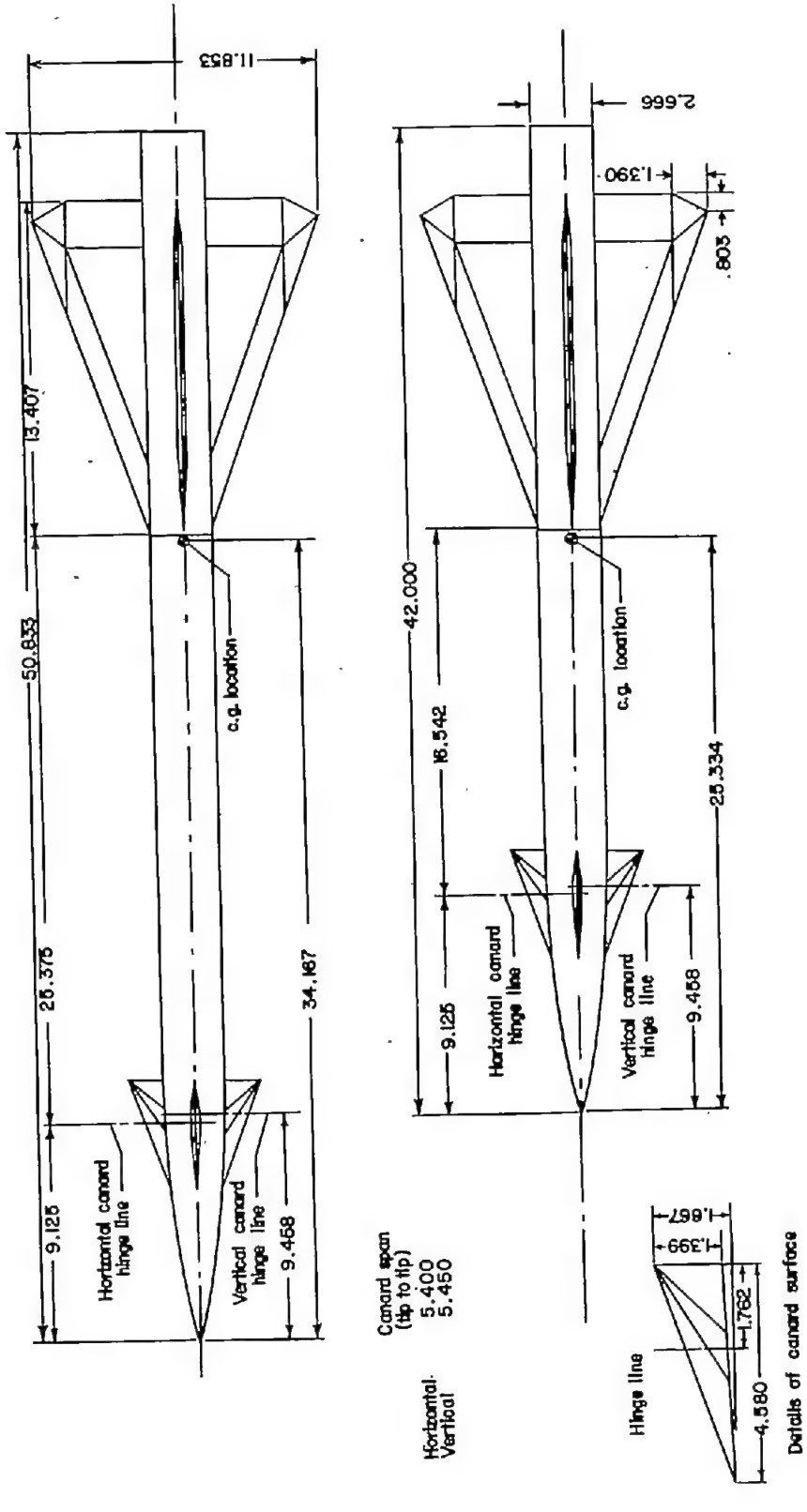

Figure 2.- Details of models. All dimensions are in inches.

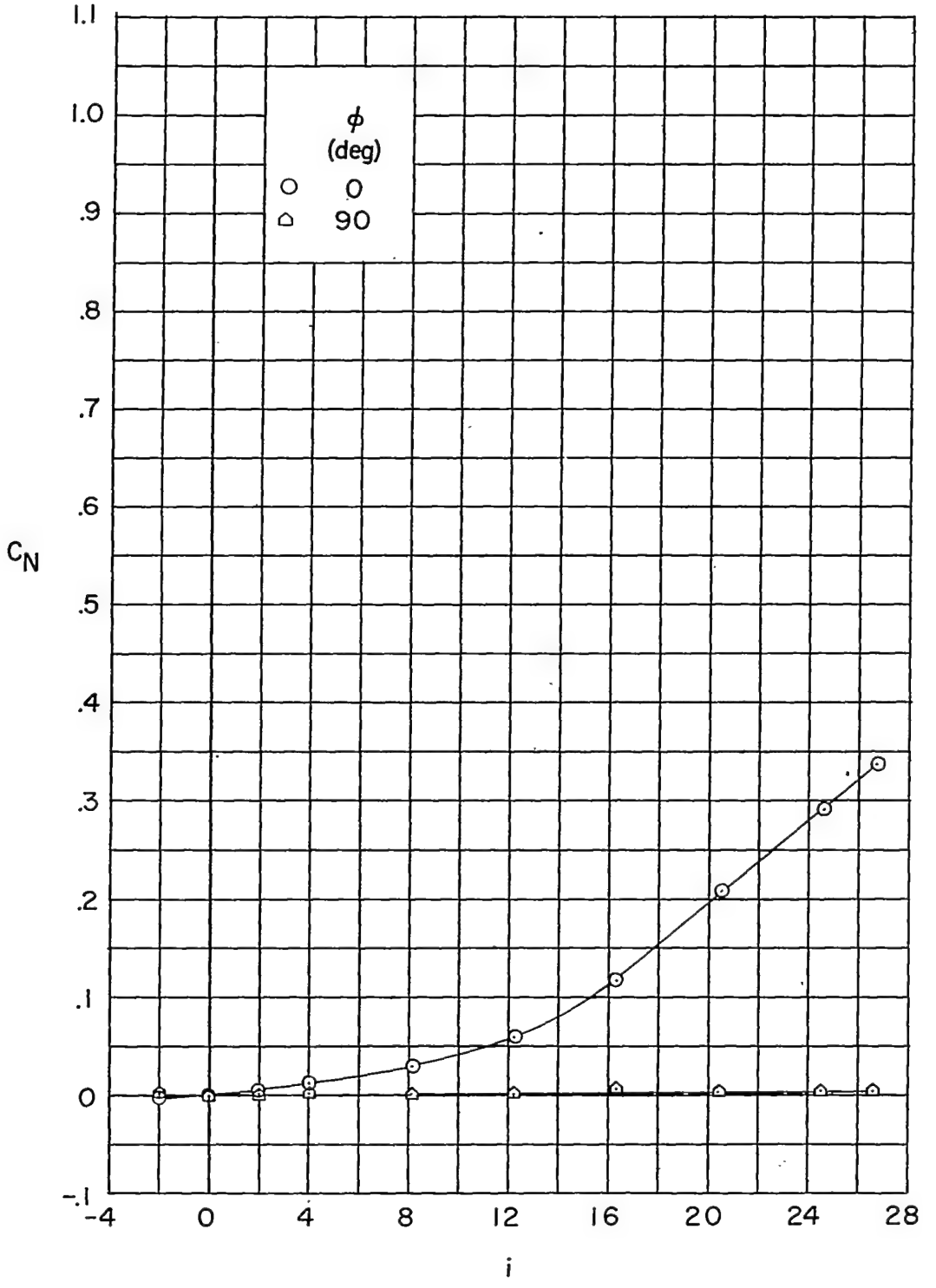

(a) $l/d = 15.7$.

Figure 3.- Body alone.

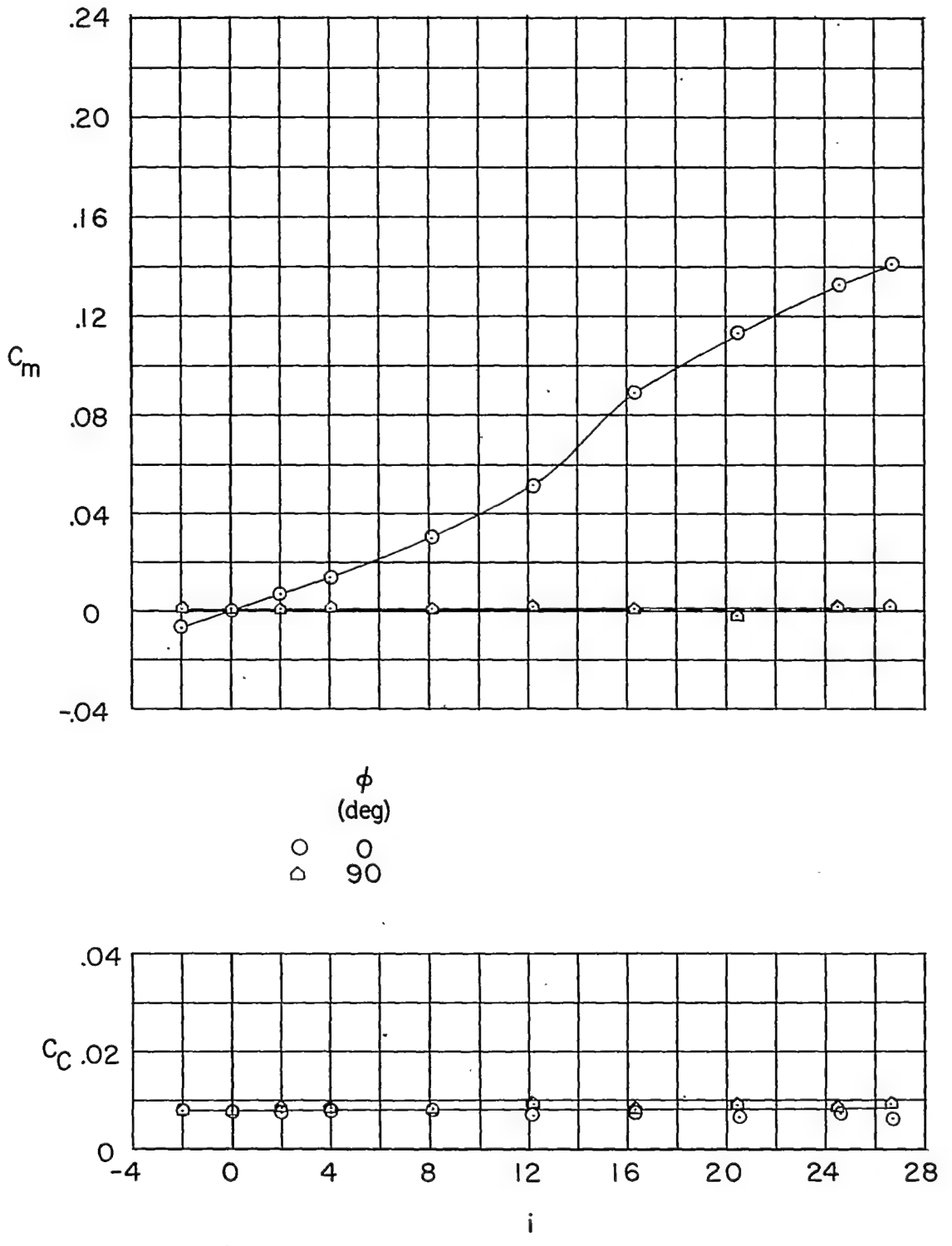

(a) Continued.

Figure 3.- Continued.

[redacted]

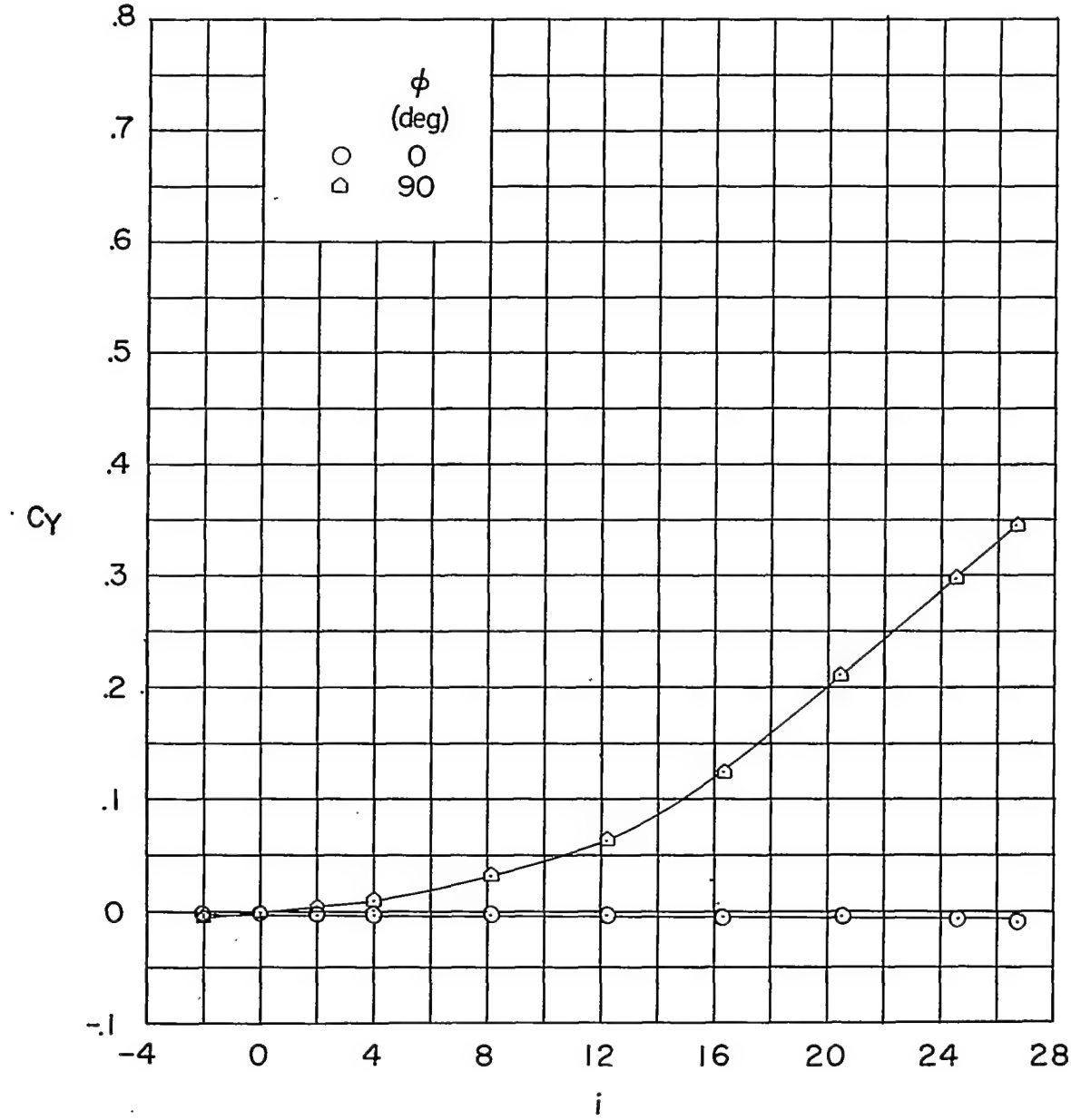

(a) Continued.

Figure 3.- Continued.

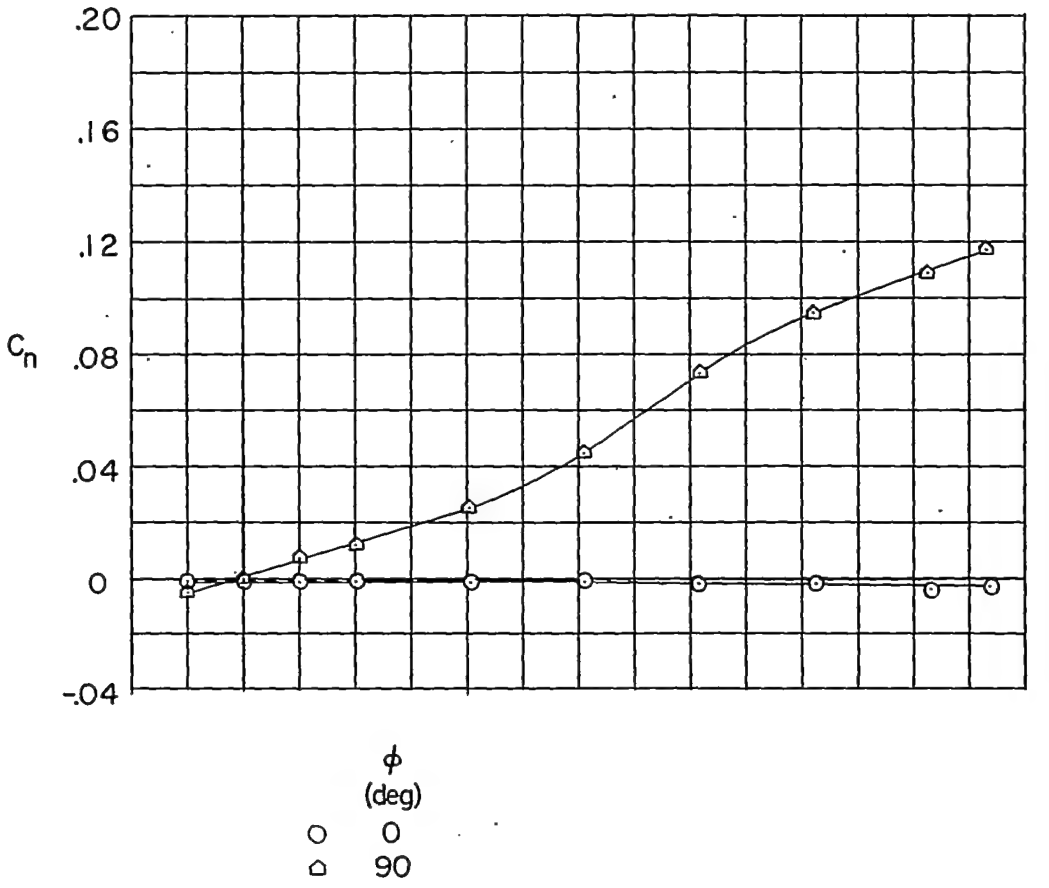

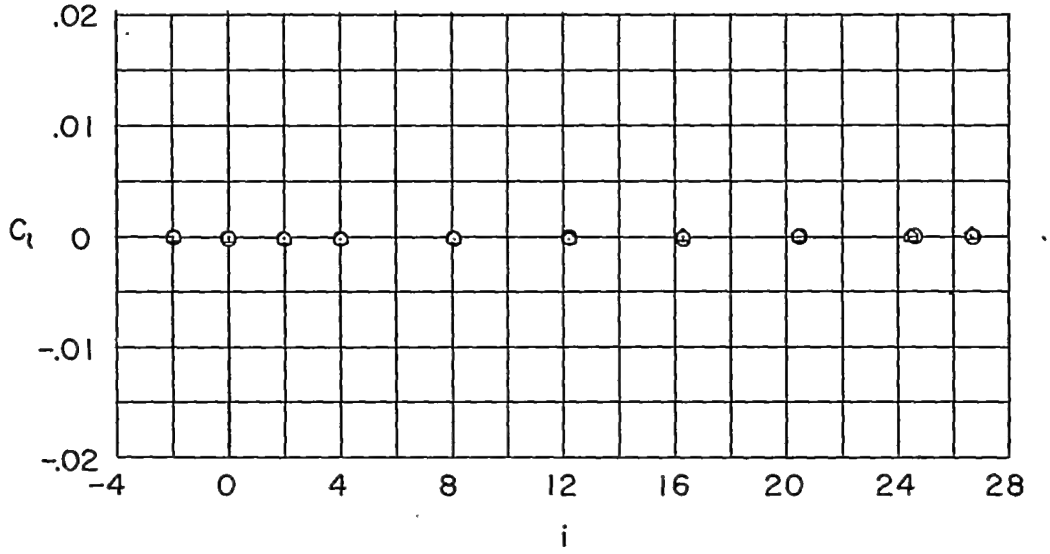

(a) Concluded.

Figure 3.- Continued.

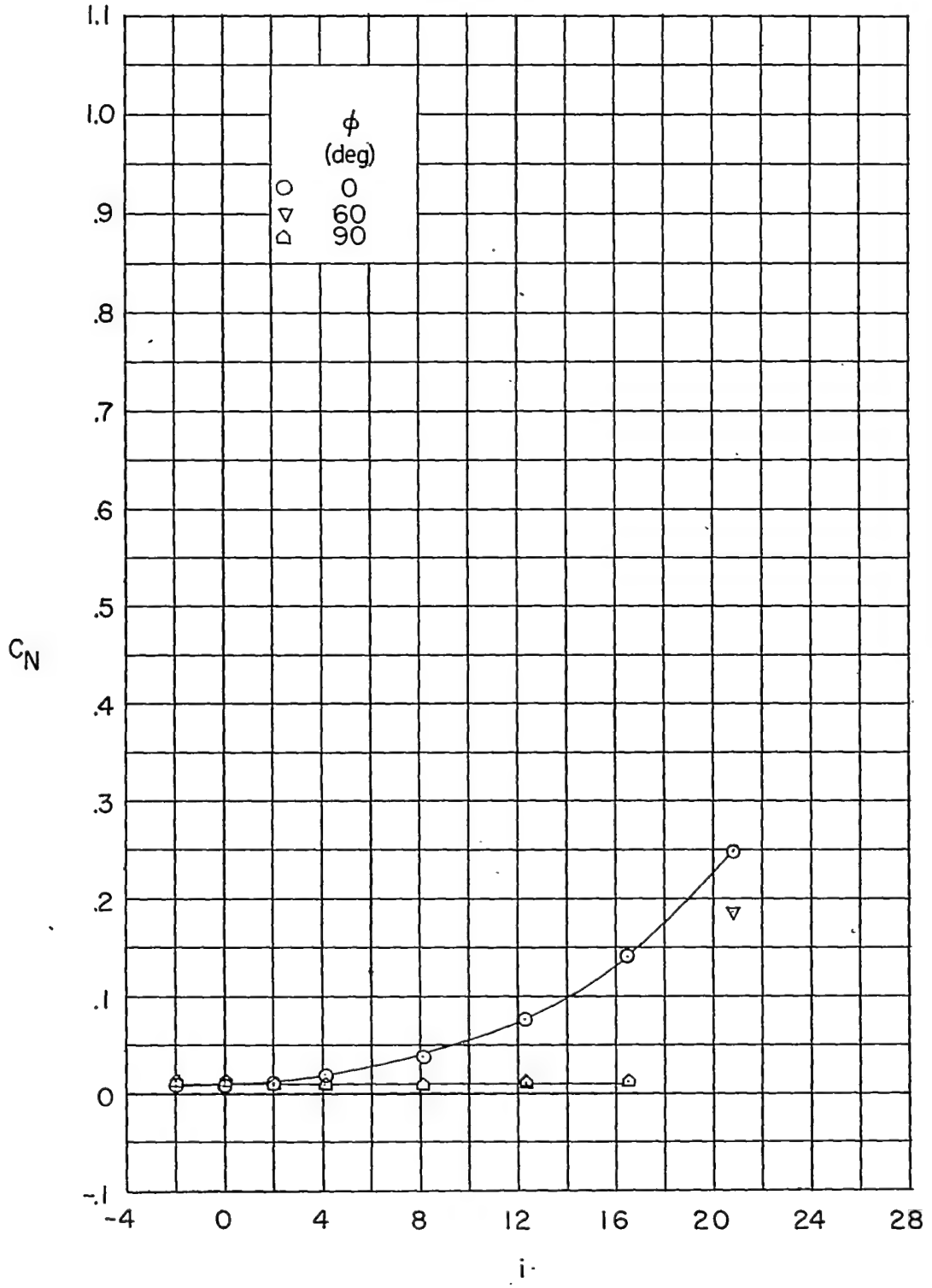

(b) $l/d = 19.1$.

Figure 3.- Continued.

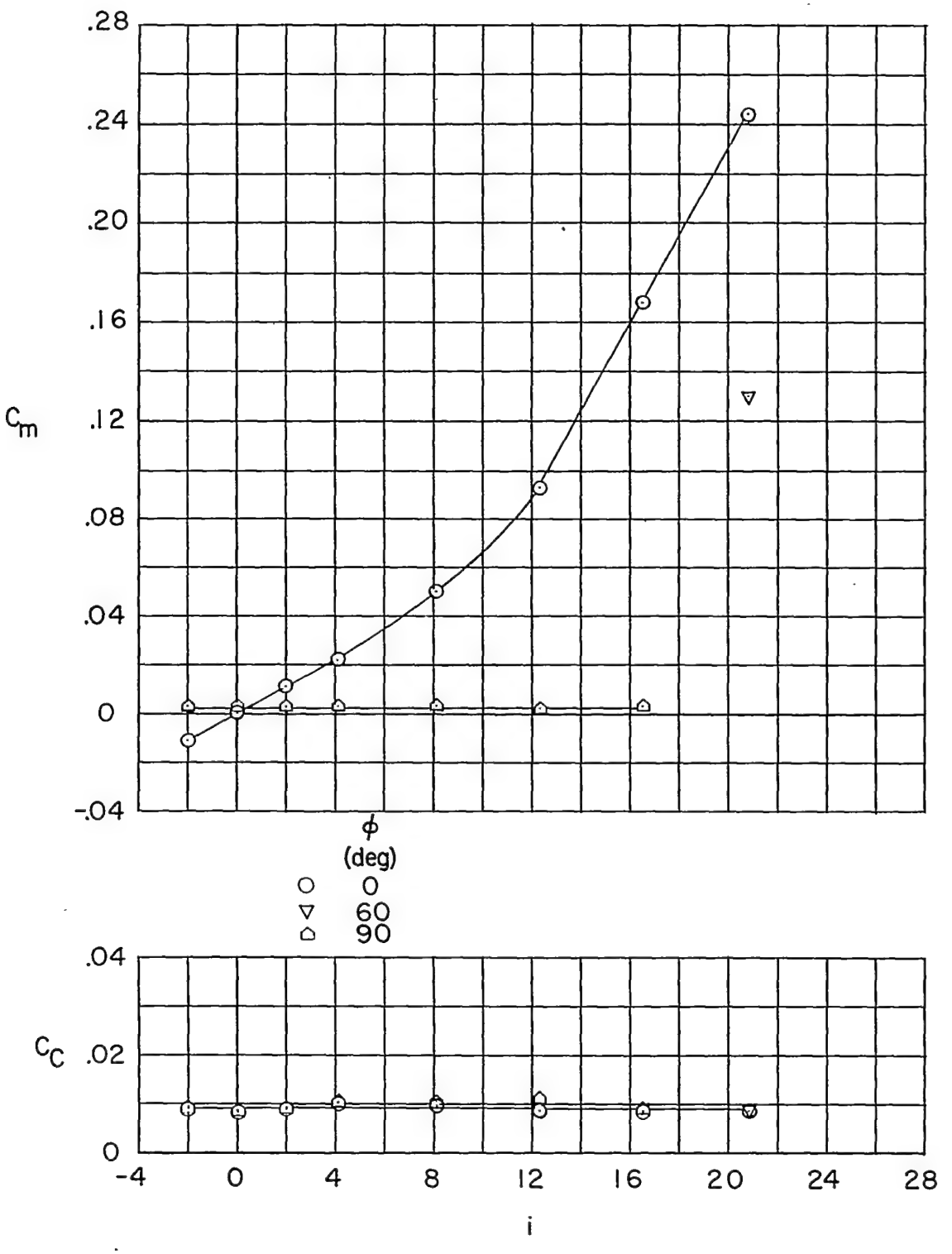

(b) Continued.

Figure 3.- Continued.

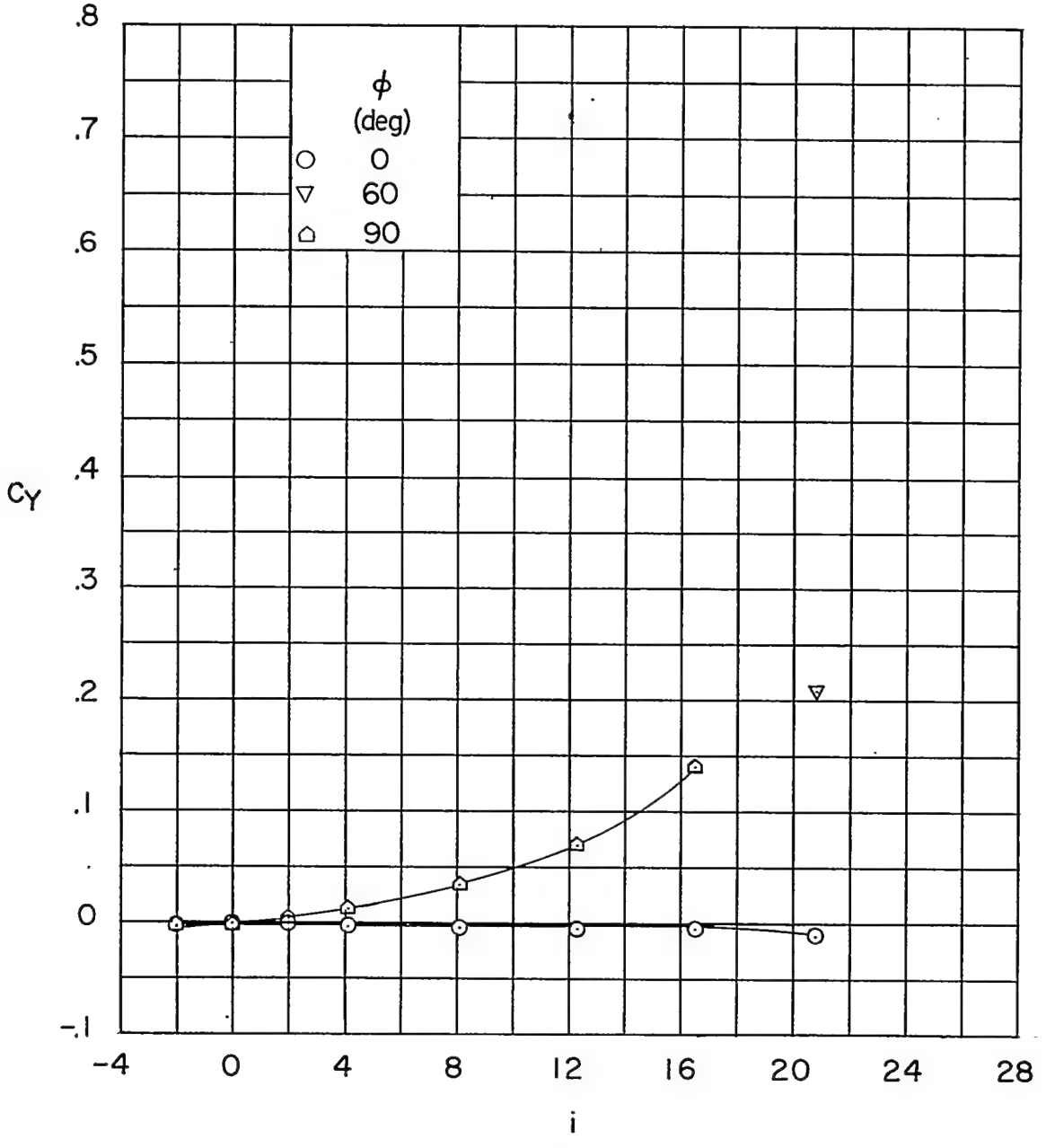

(b) Continued.

Figure 3.- Continued.

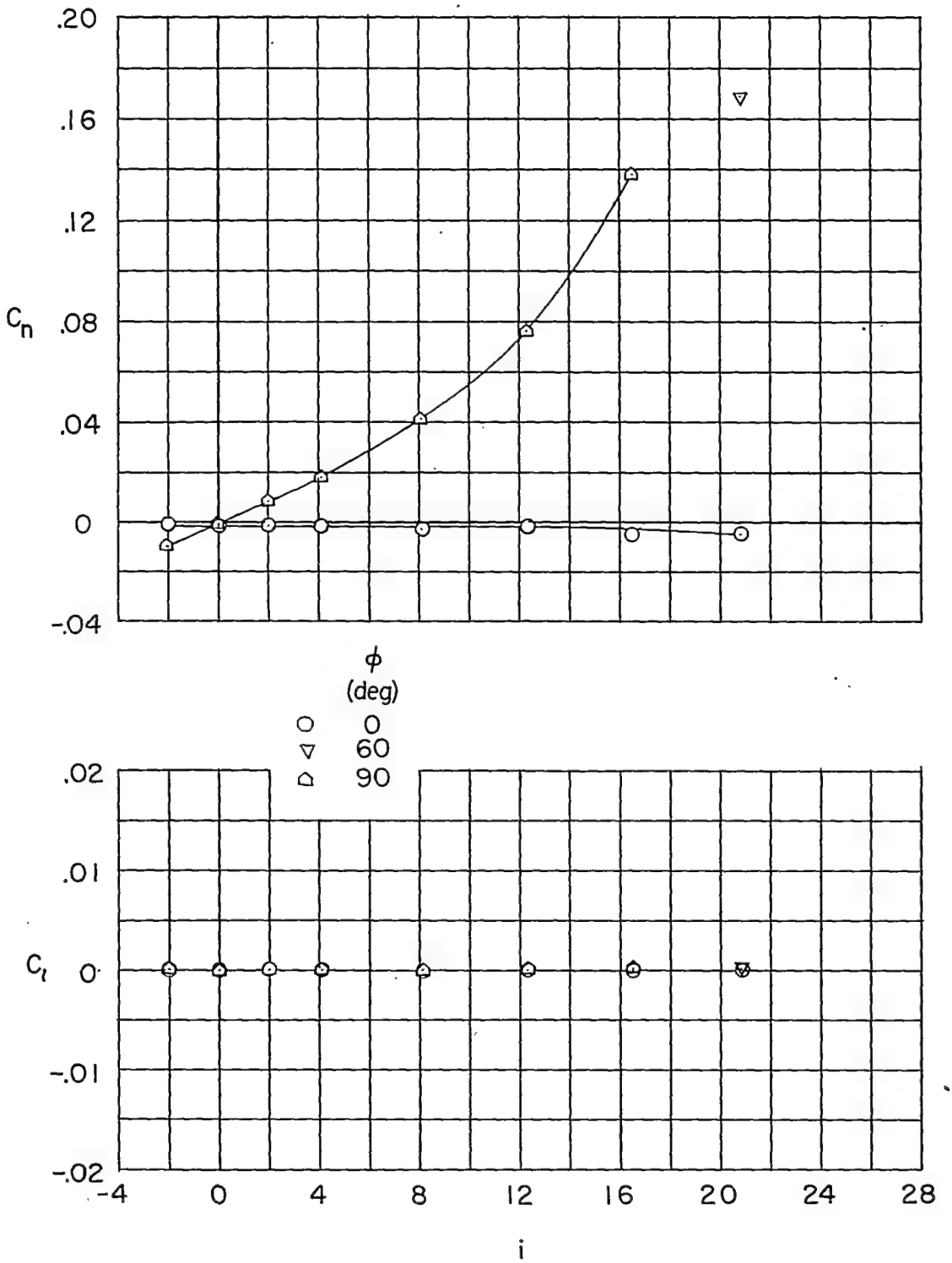

(b) Concluded.

Figure 3.- Concluded.

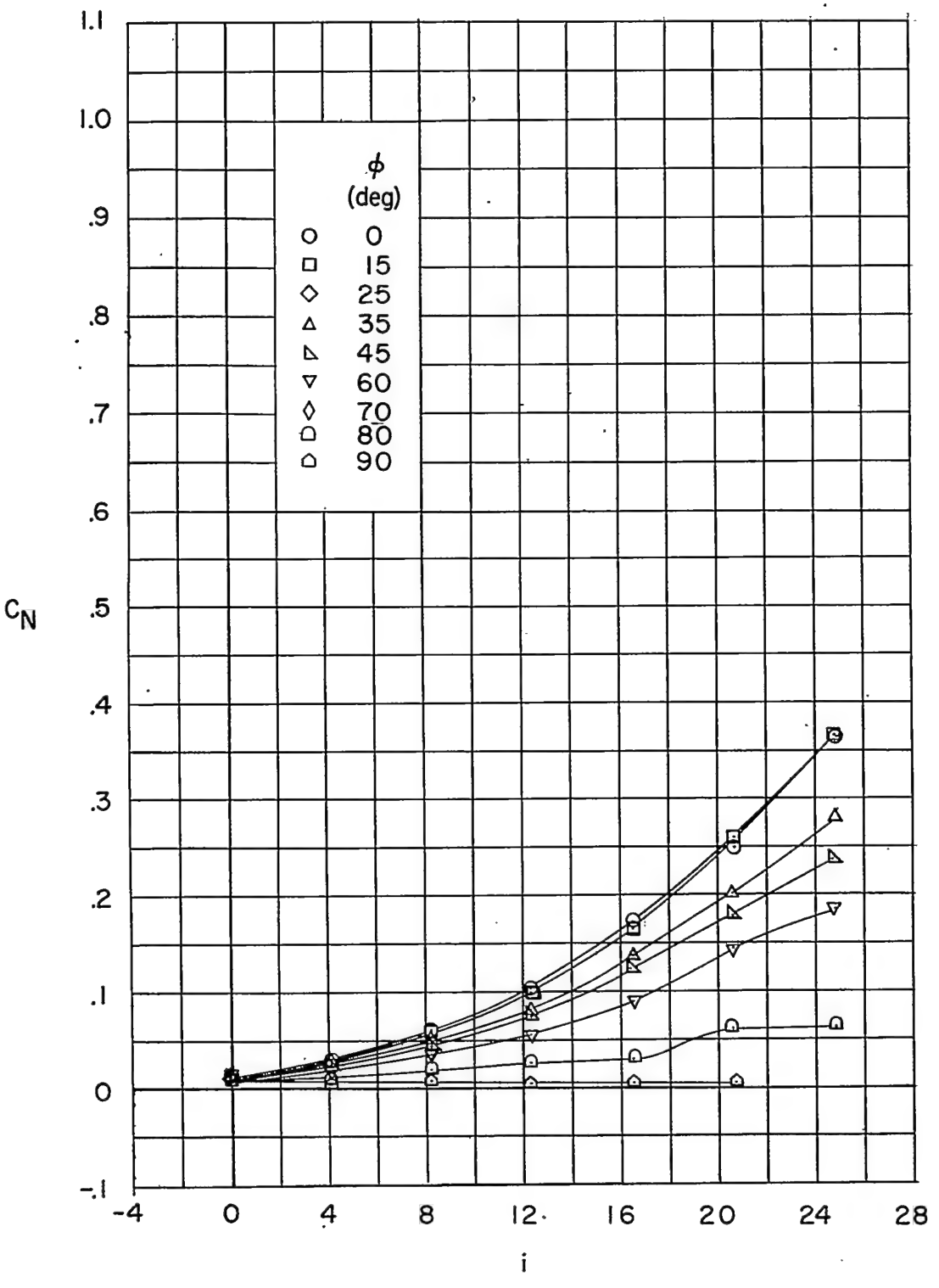

(a) $\delta_H = 0^o$.

Figure 4.- Body-canards. $l/d = 15.7$.

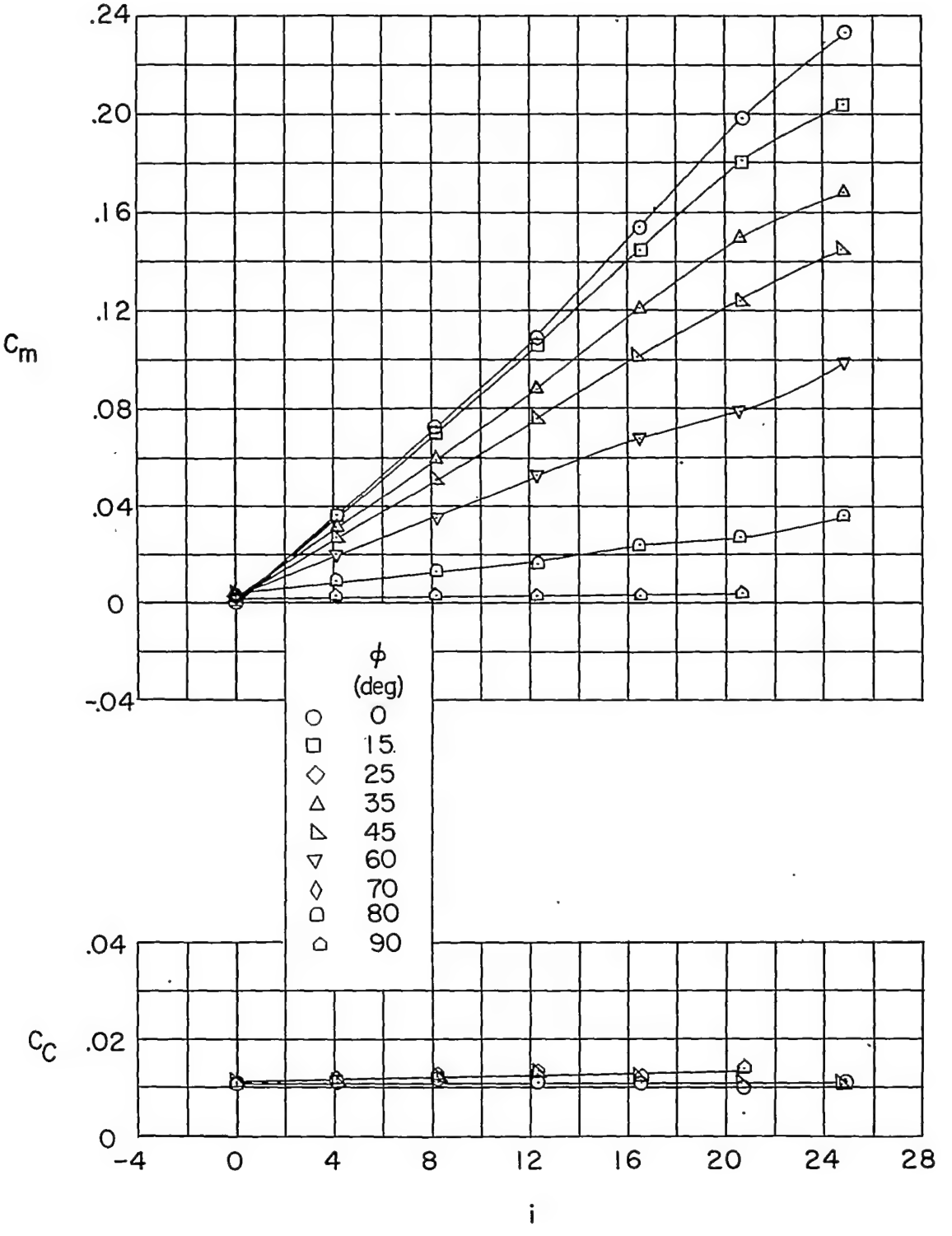

(a) Continued.

Figure 4.- Continued.

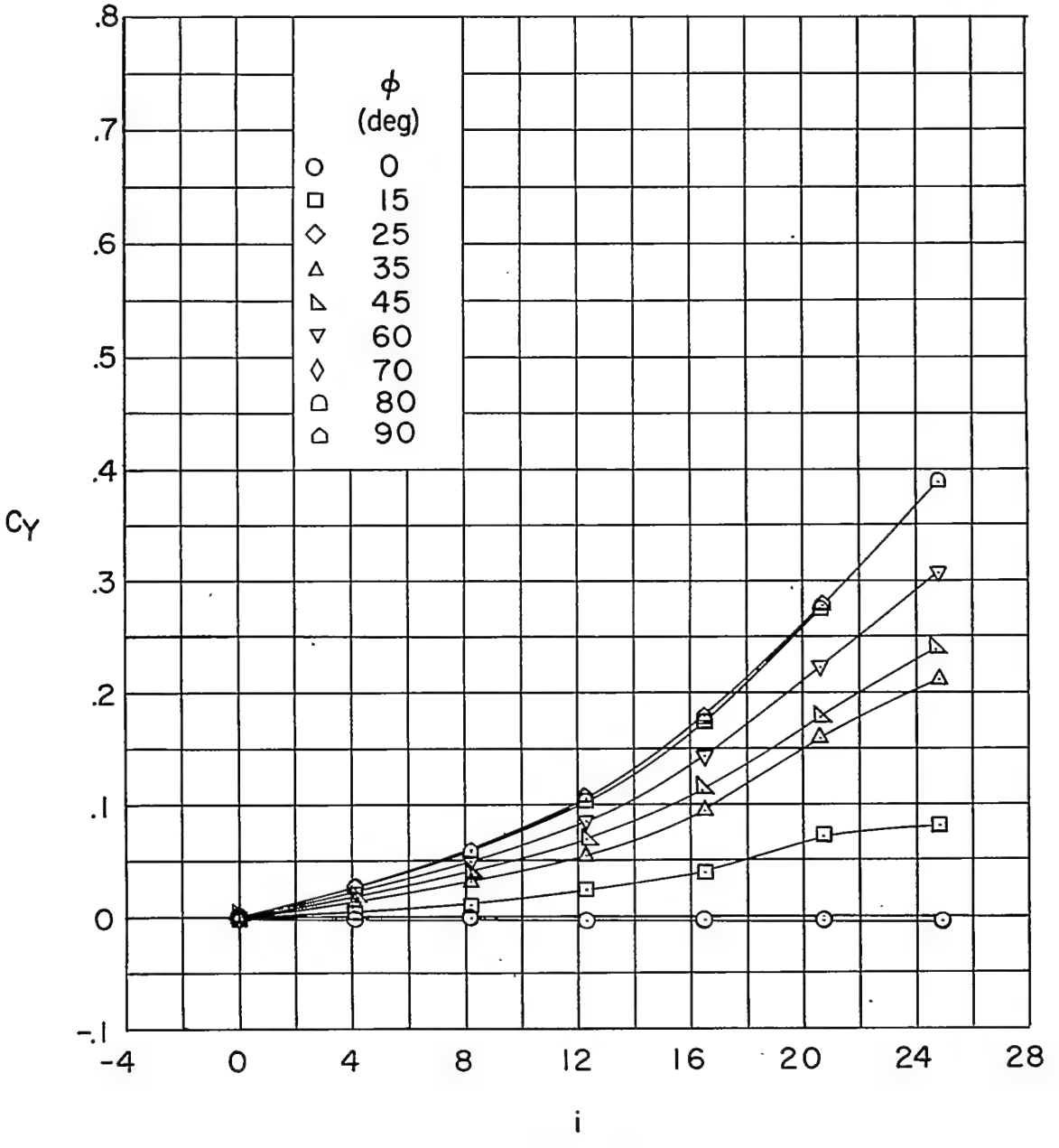

(a) Continued.

Figure 4.- Continued.

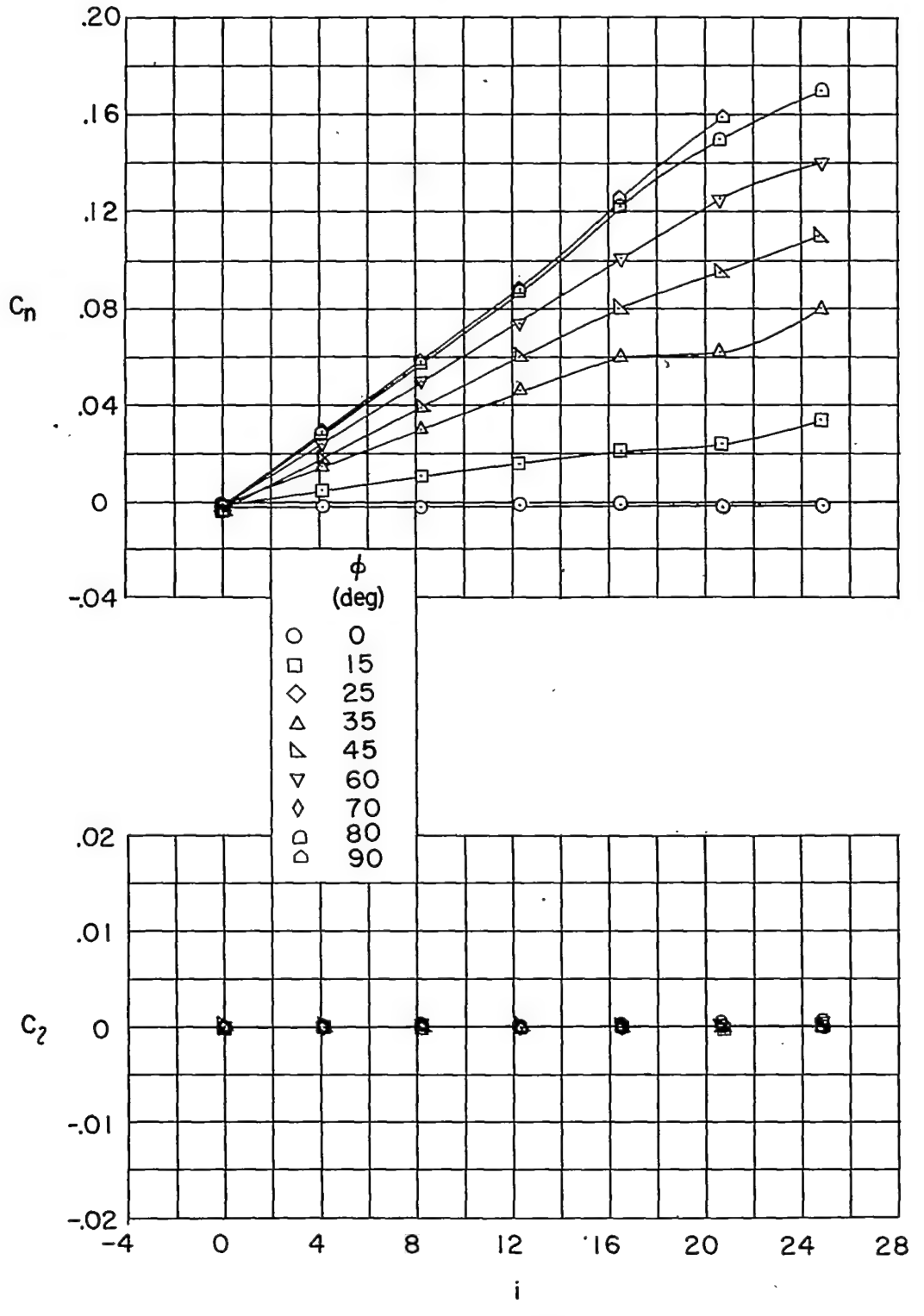

(a) Concluded.

Figure 4.- Continued.

[redacted]

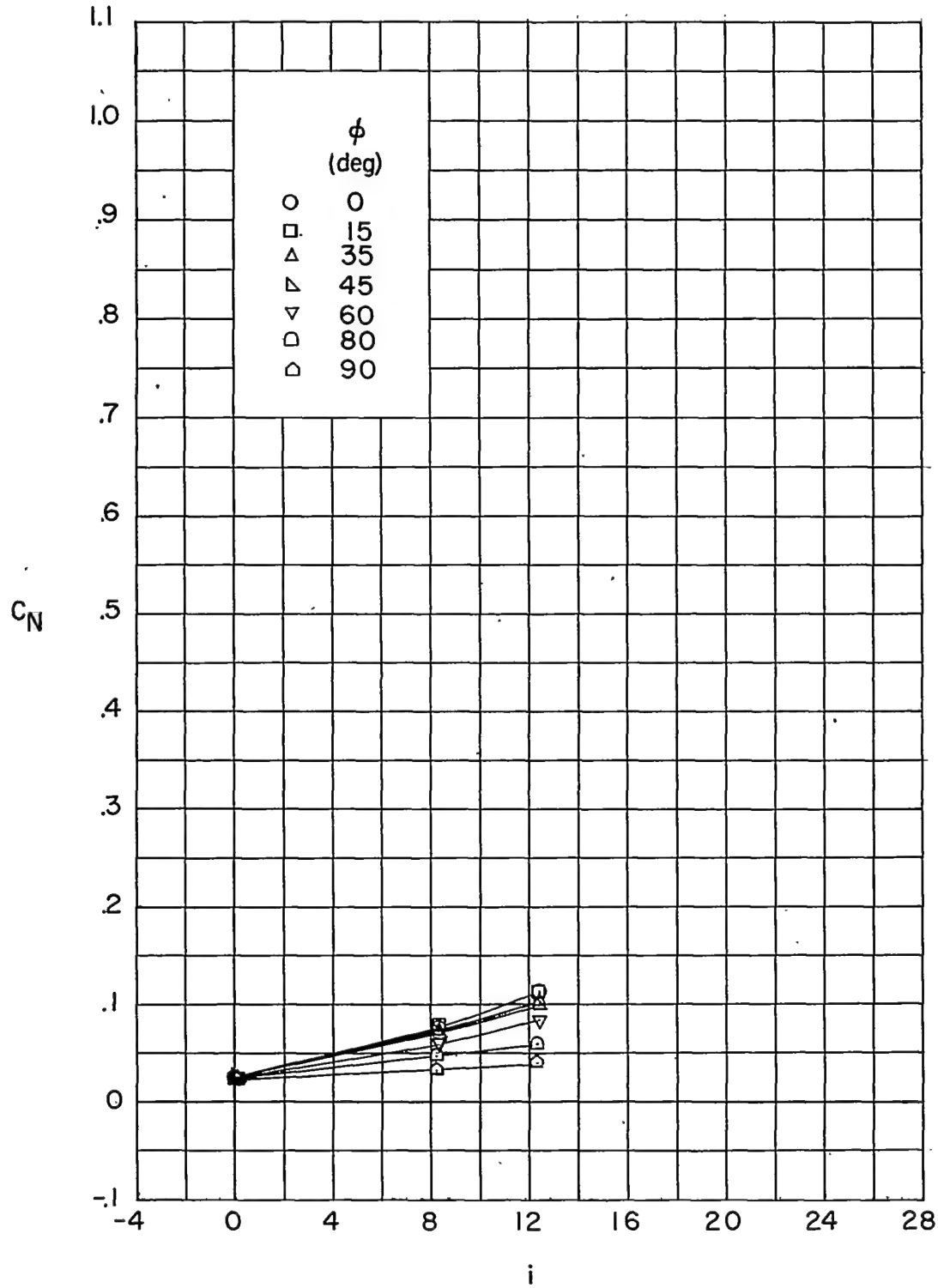

(b) $\delta_H = 8^\circ$.

Figure 4.- Continued.

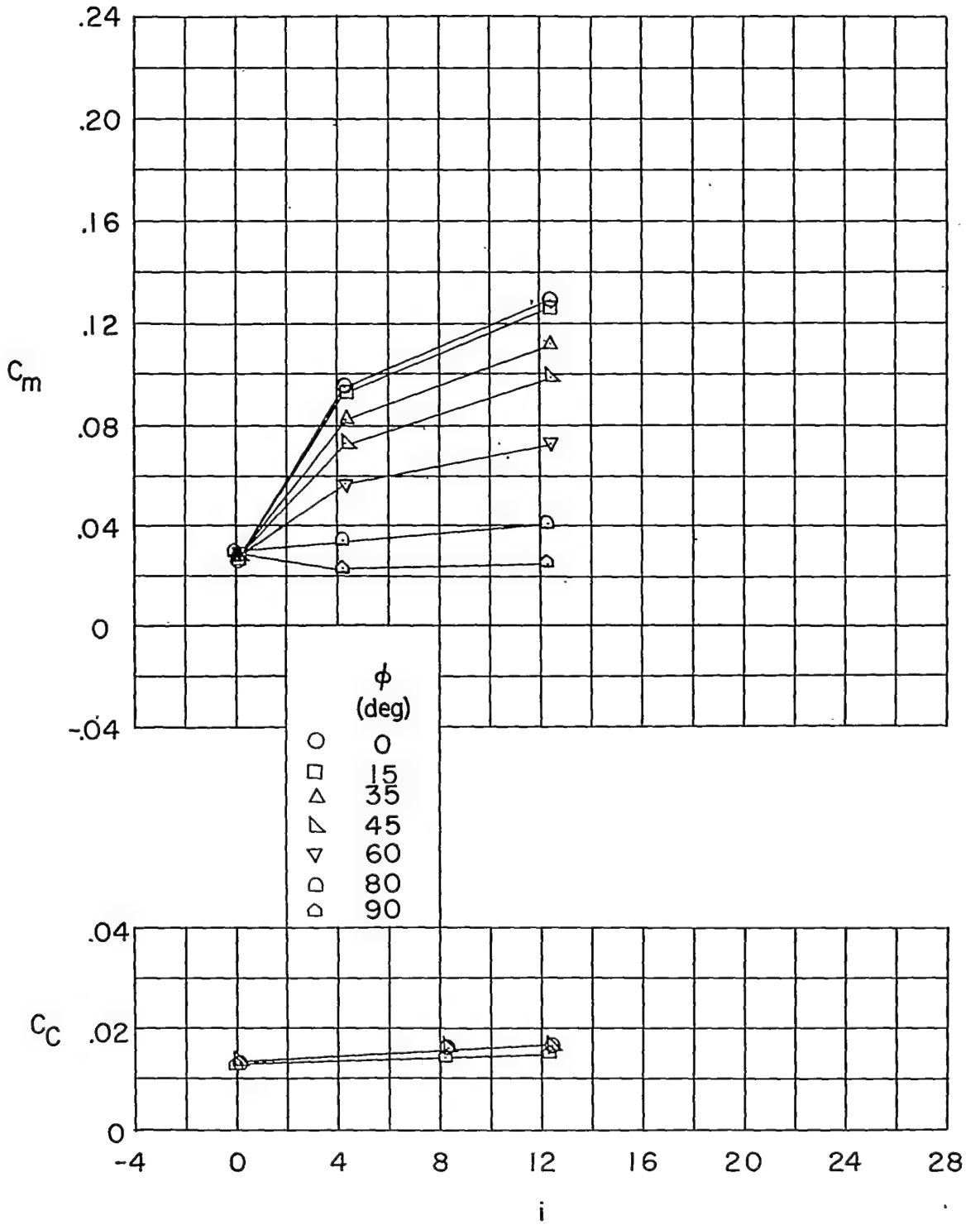

(b) Continued.

Figure 4.- Continued.

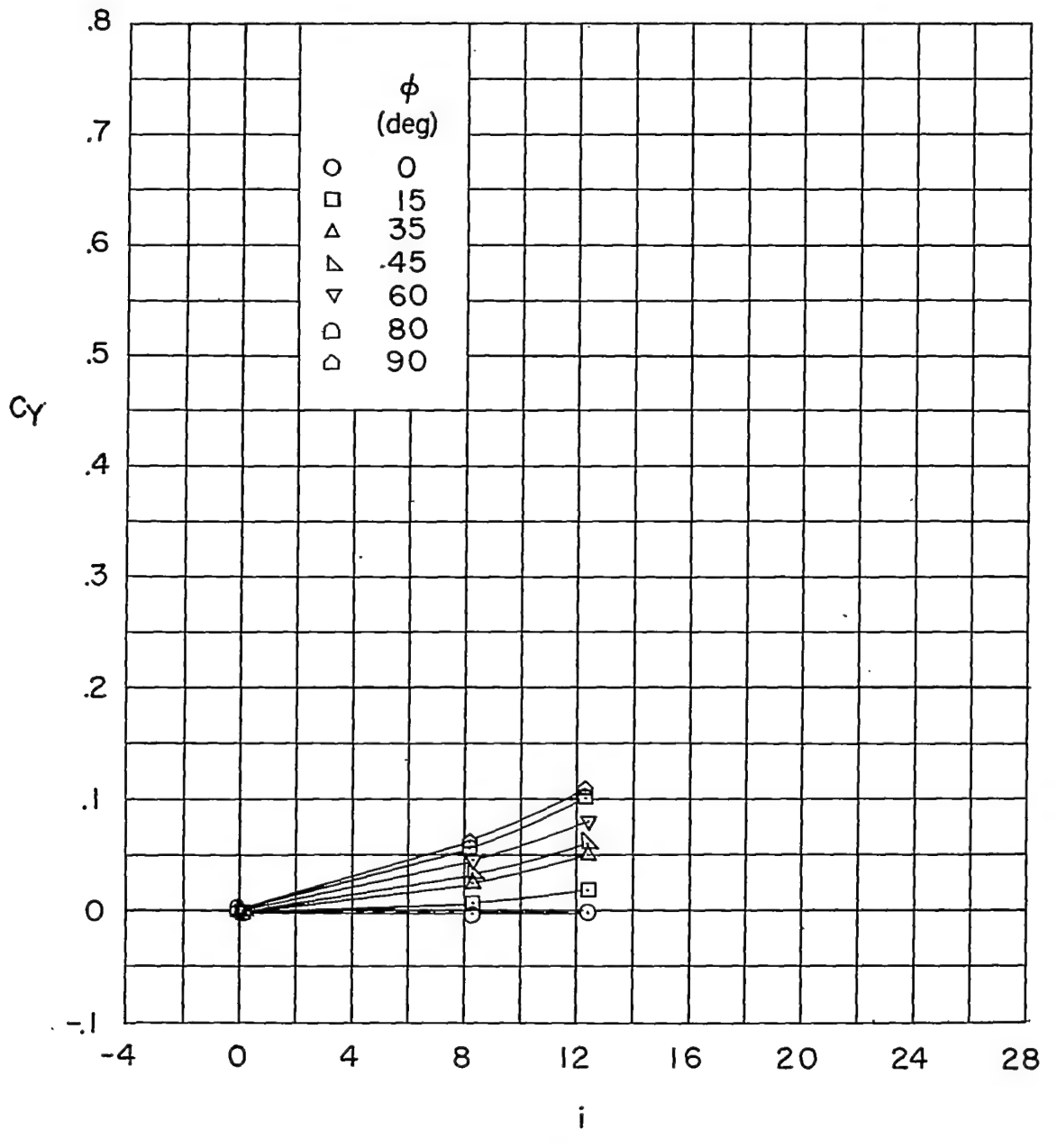

(p) Continued.

Figure 4.- Continued.

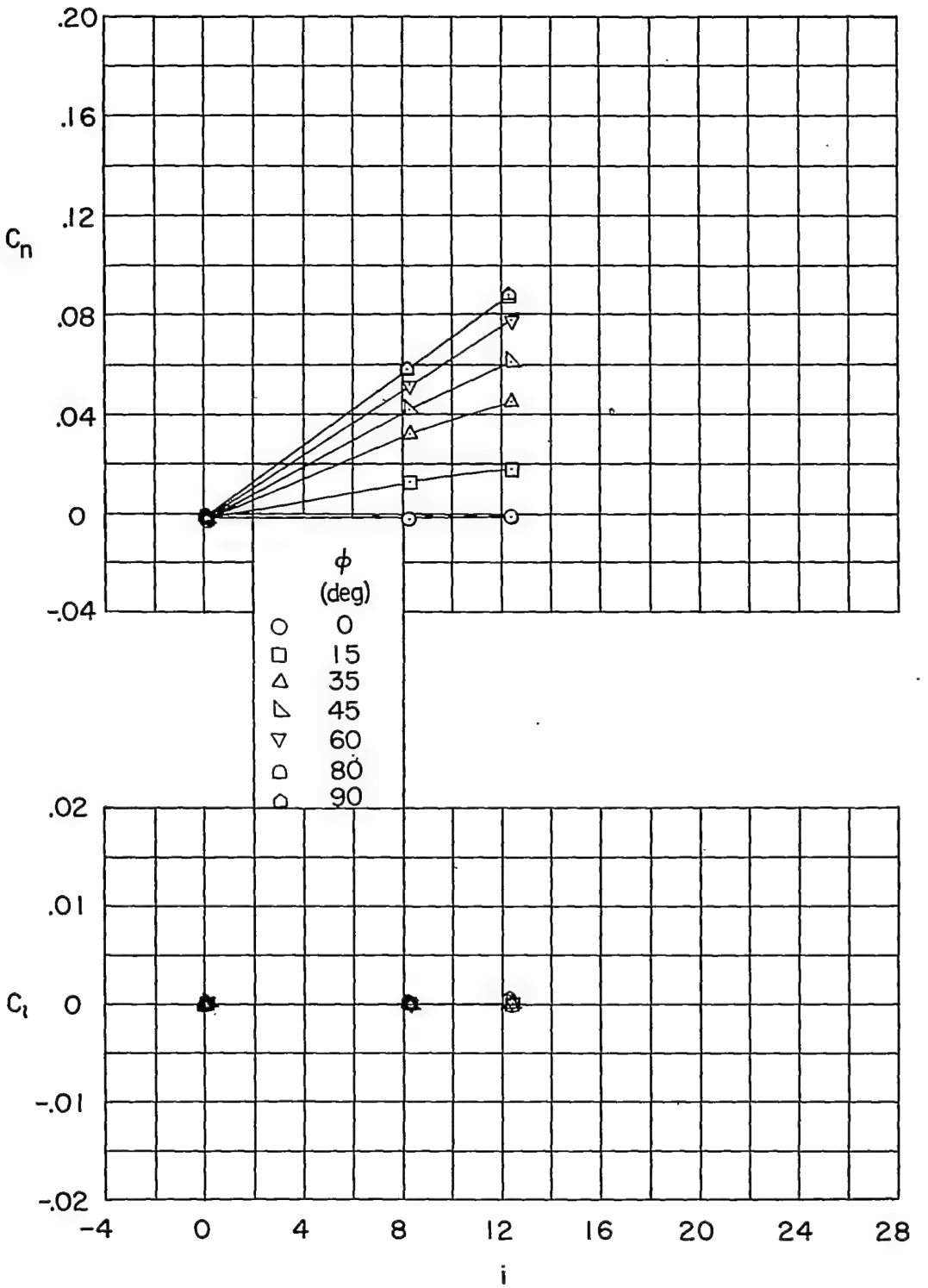

(b) Concluded.

Figure 4.- Continued.

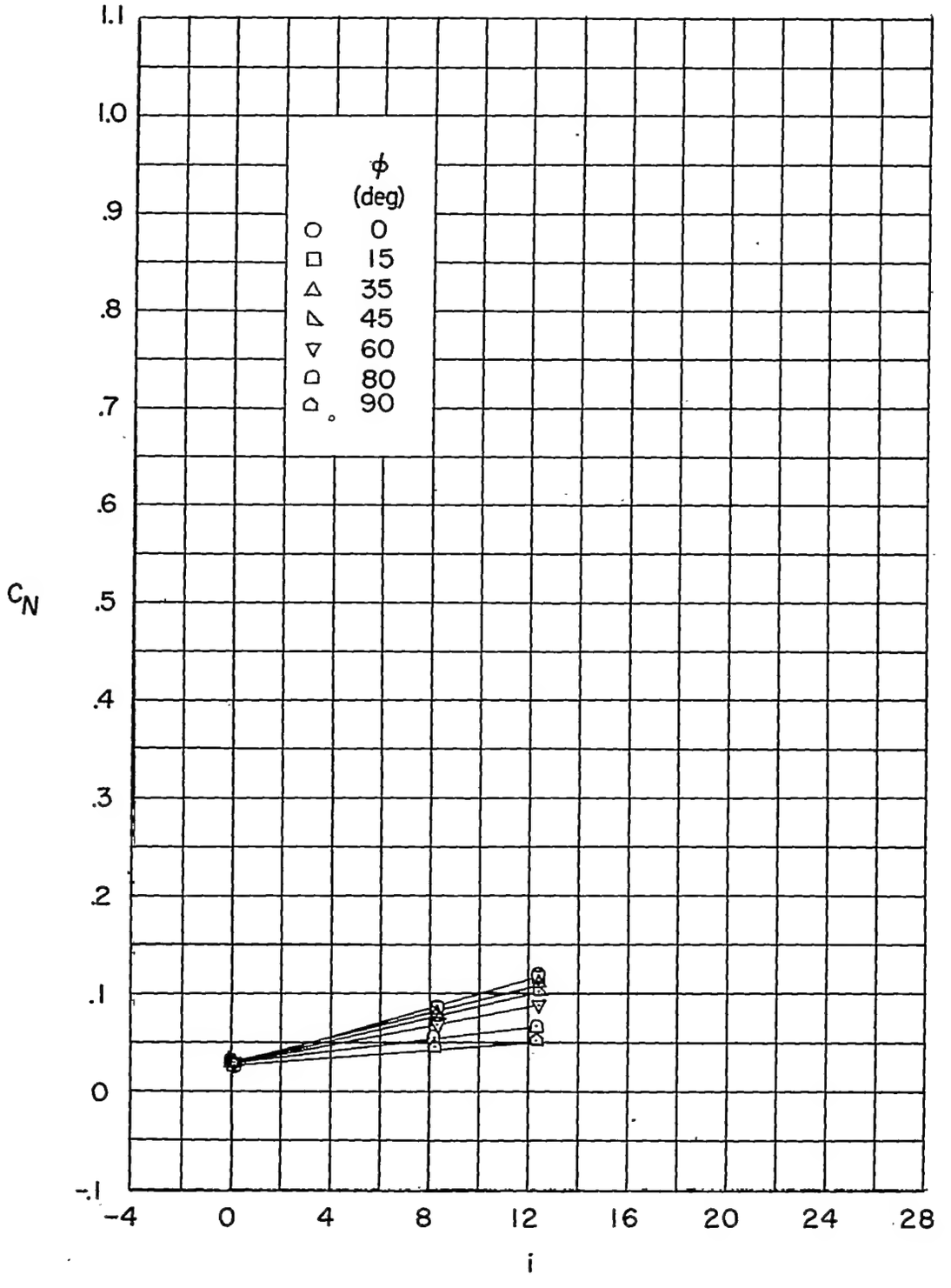

(c) $\delta_H = 12^\circ$.

Figure 4.- Continued.

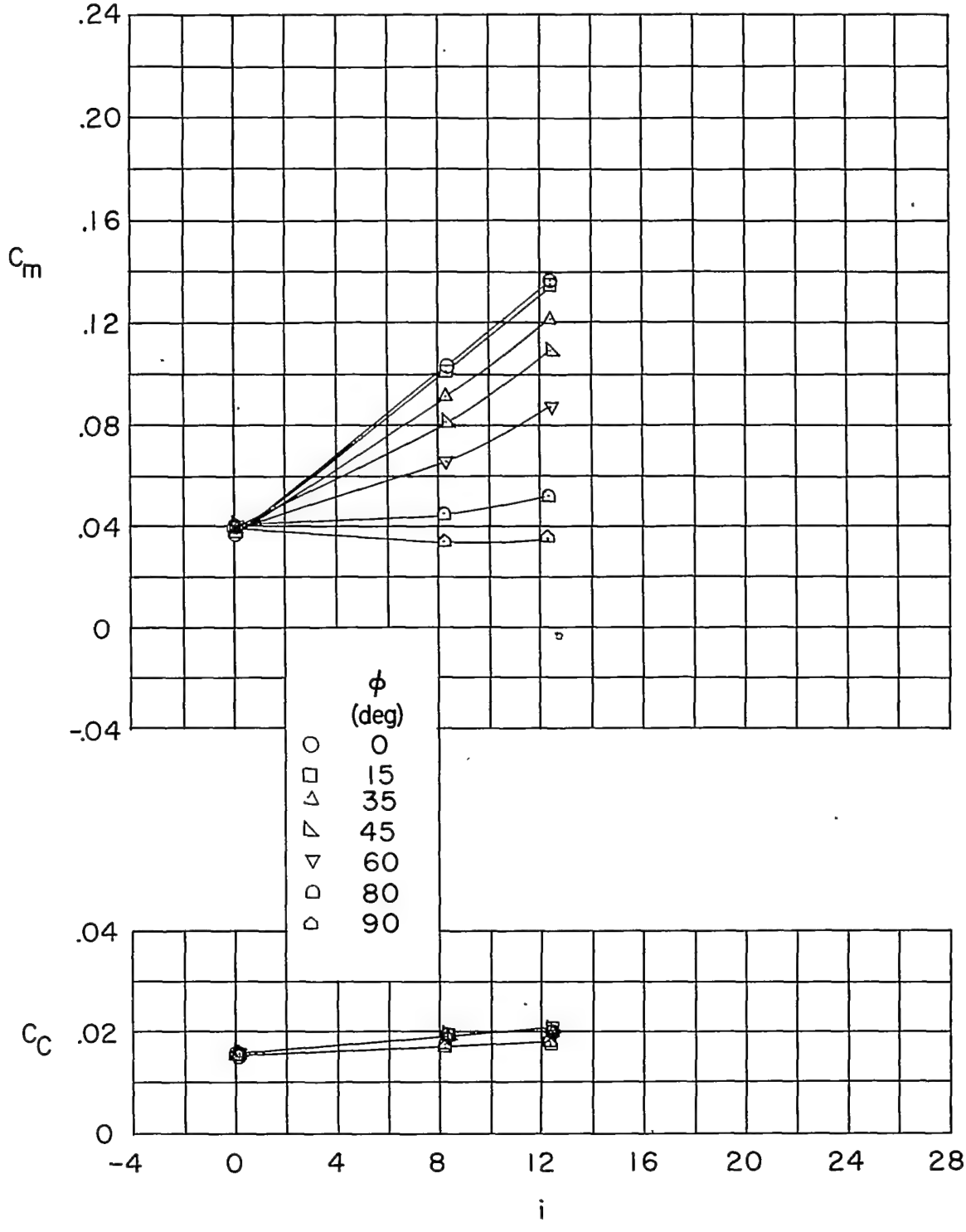

(c) Continued.

Figure 4.- Continued.

[redacted]

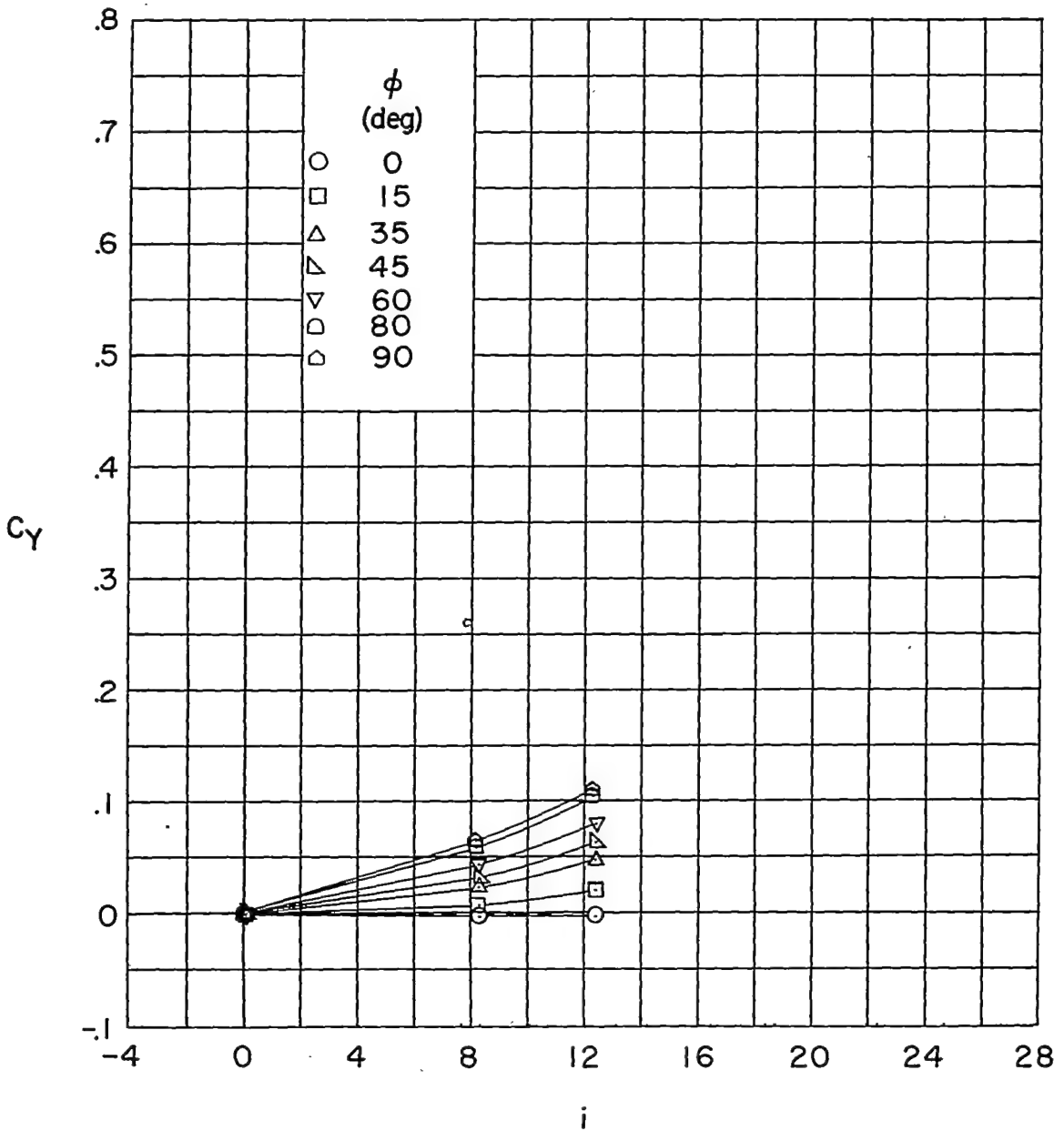

(c) Continued.

Figure 4.- Continued.

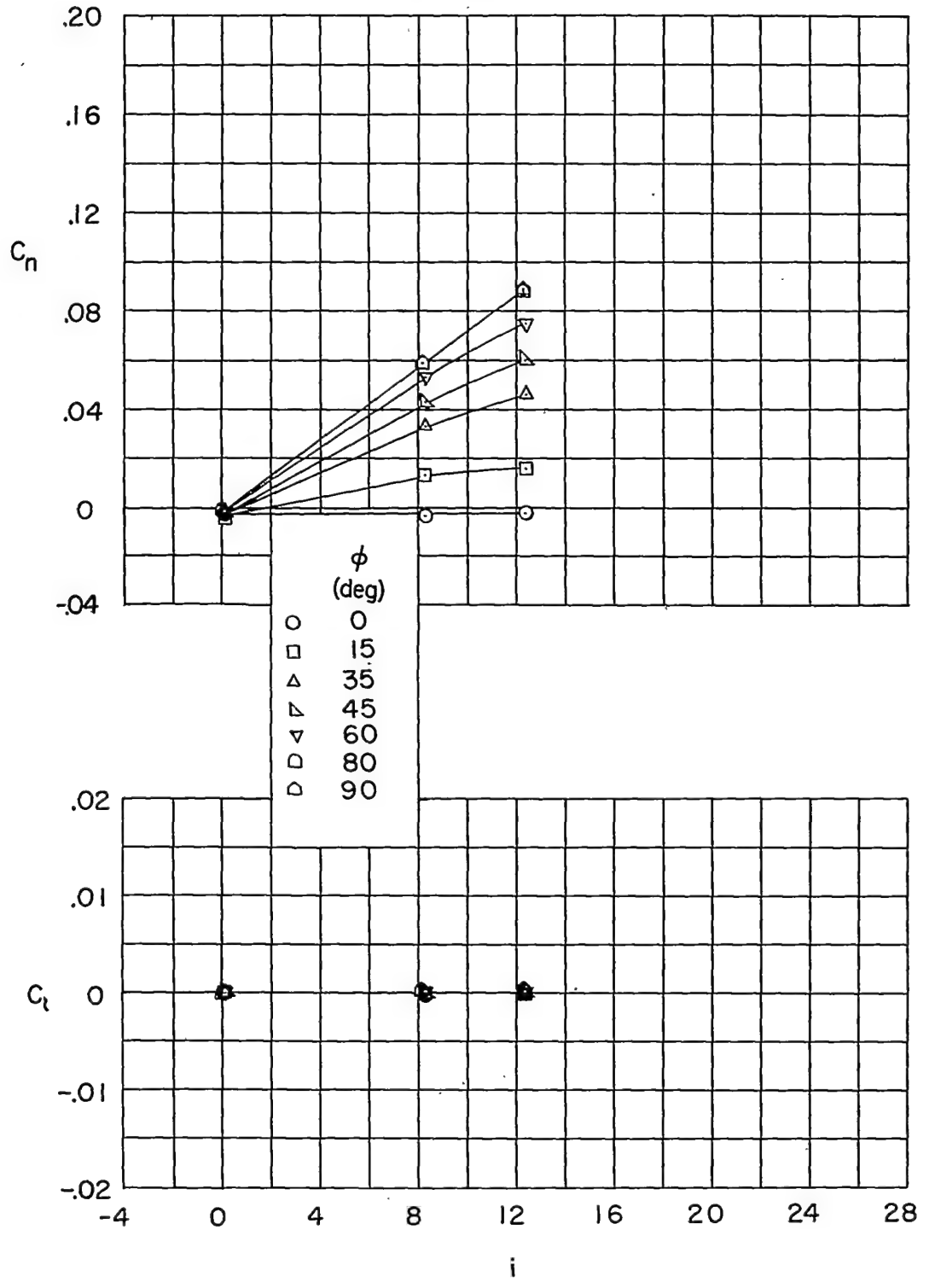

(c) Concluded.

Figure 4.- Concluded.

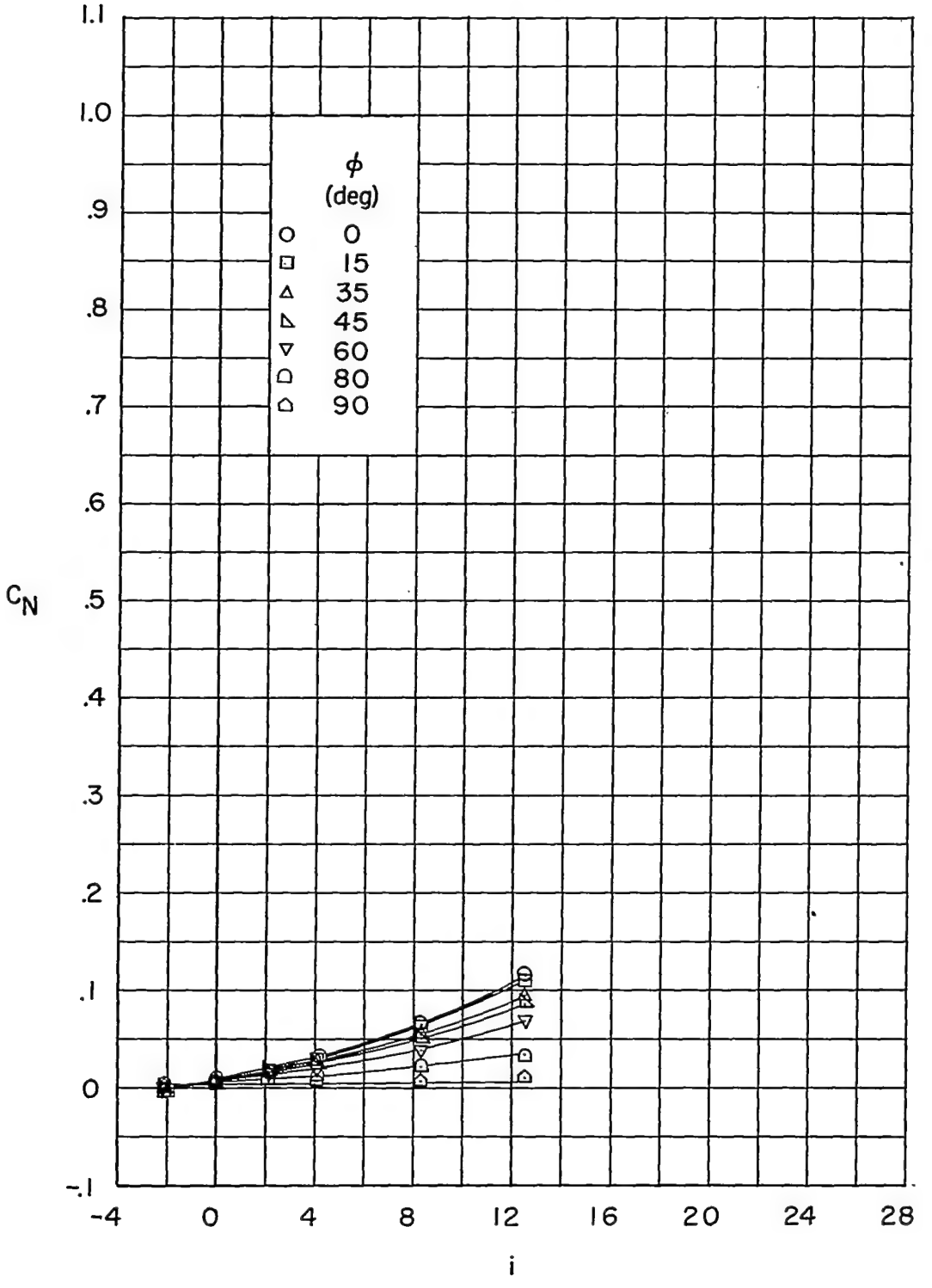

(a) $\delta_H = 0^o$.

Figure 5.- Body-canards. $l/d = 19.1$.

[redacted]

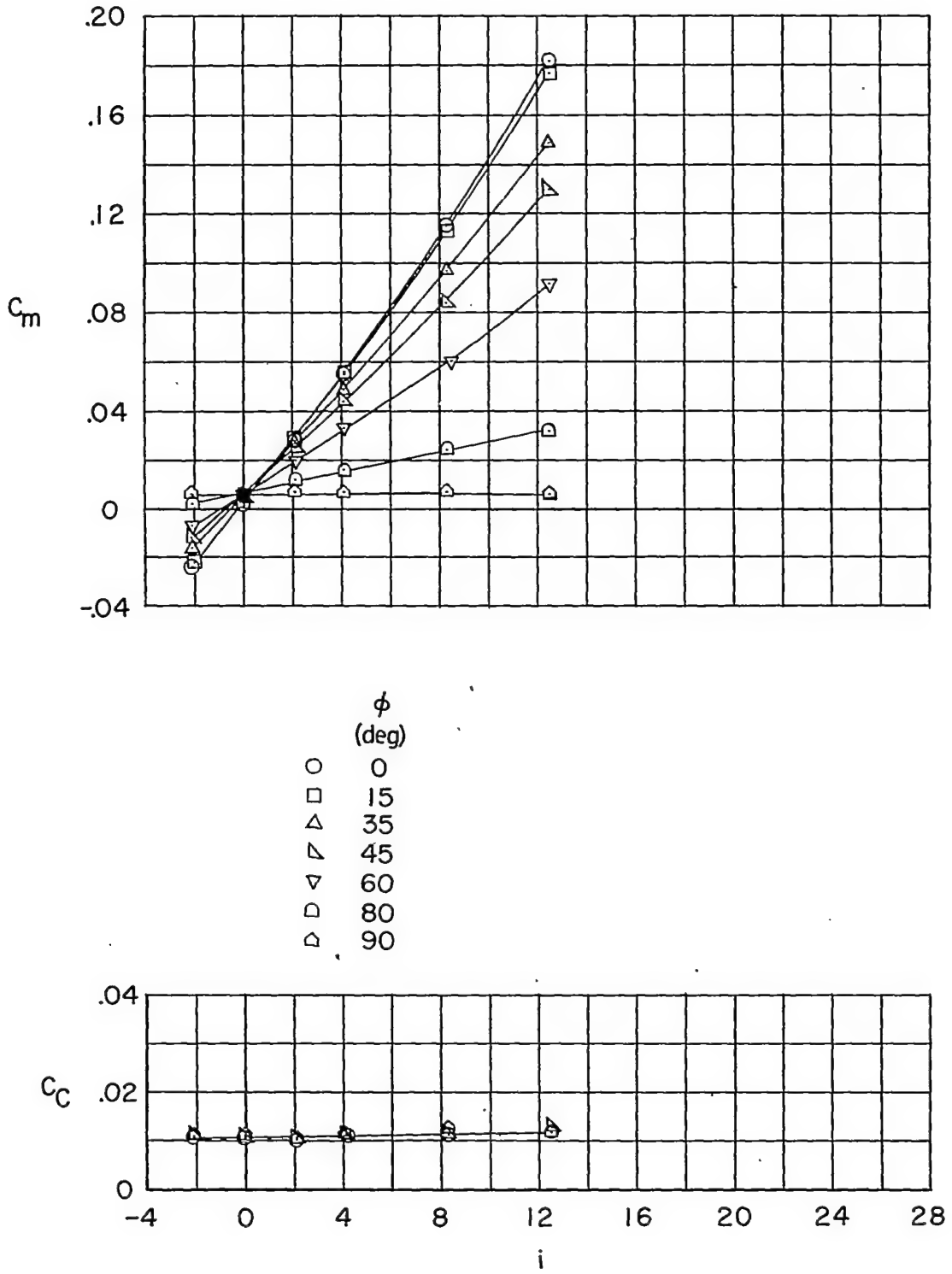

(a) Continued.

Figure 5.- Continued.

[redacted]

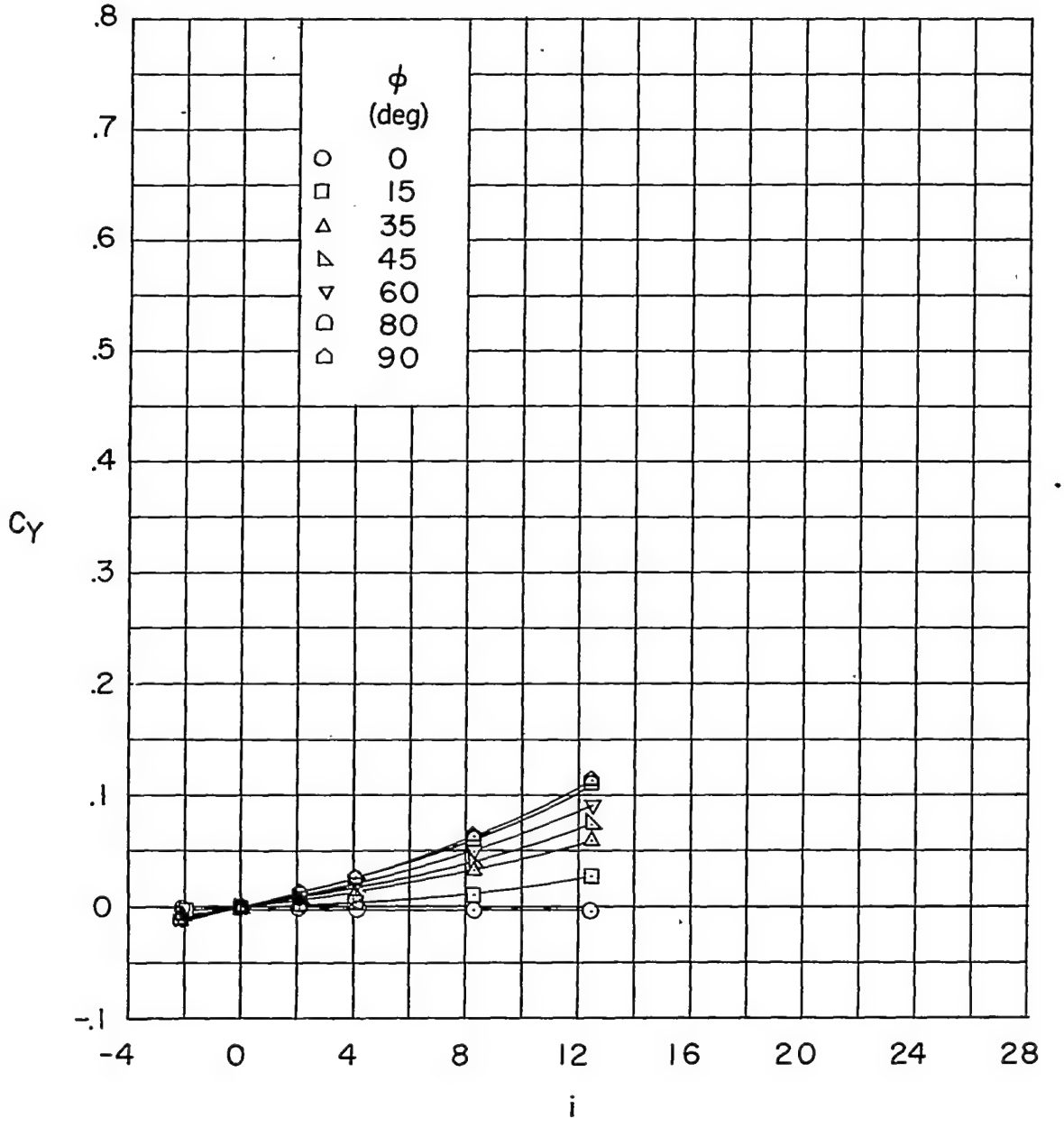

(a) Continued.

Figure 5.- Continued.

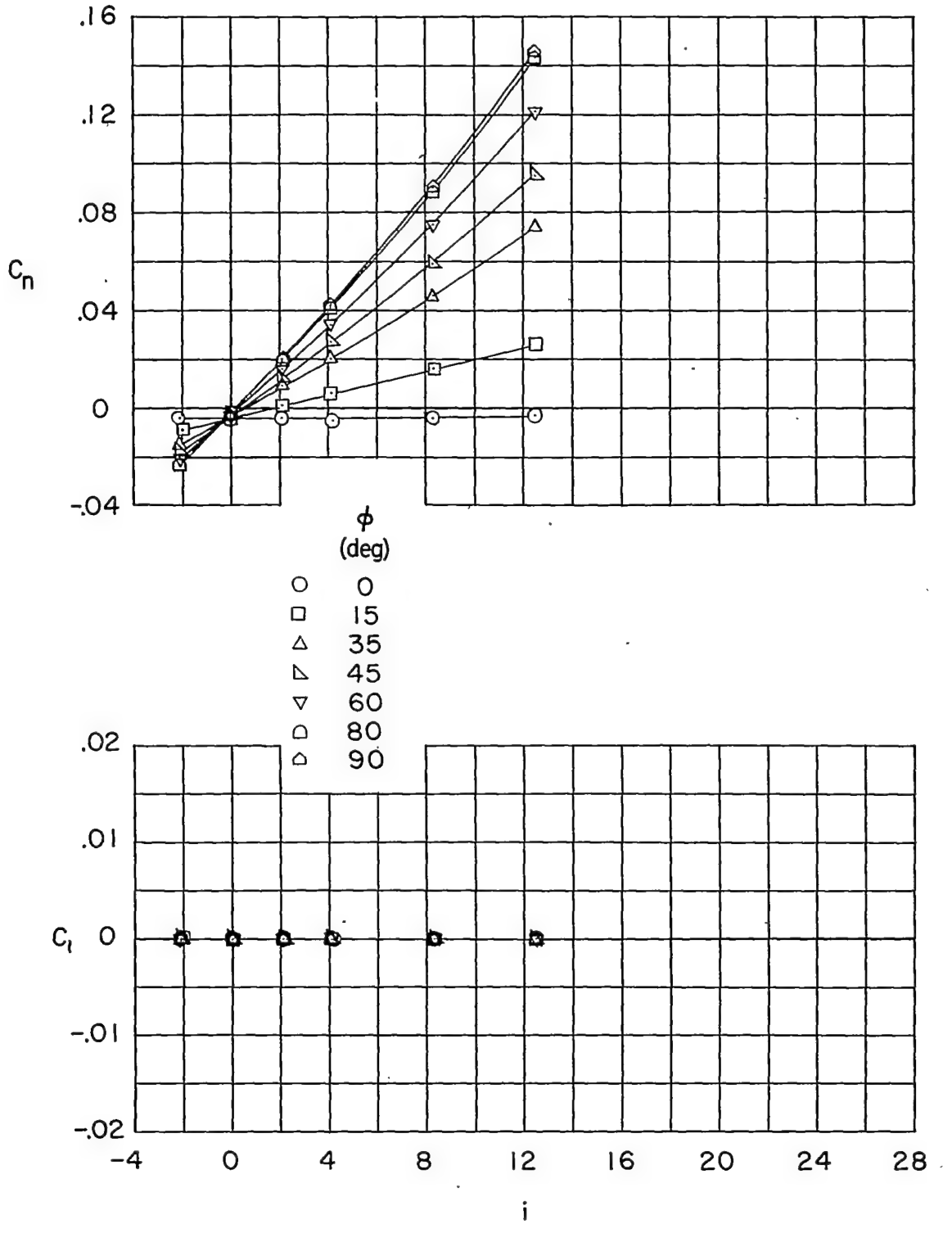

(a) Concluded.

Figure 5.- Continued.

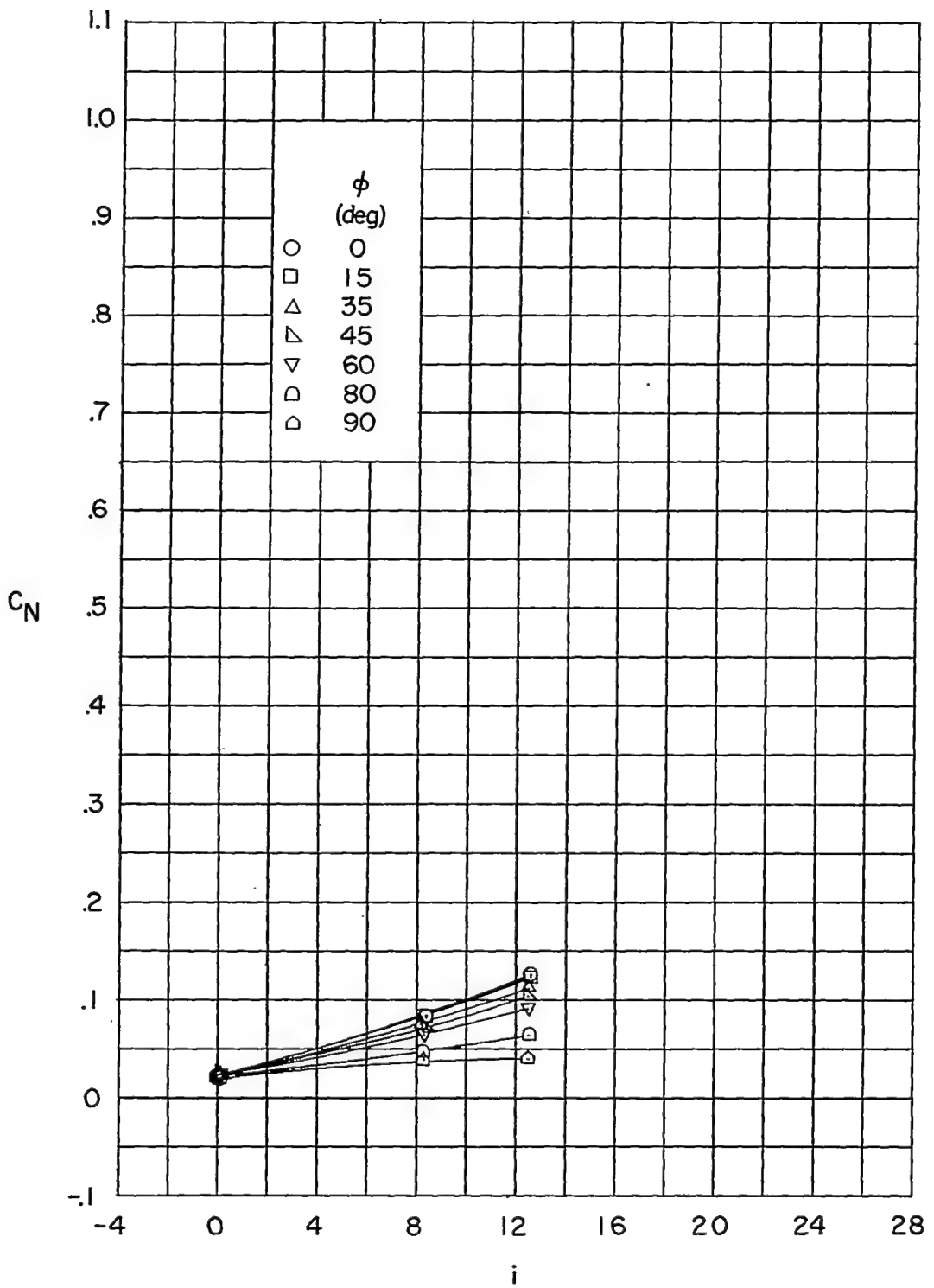

(b) $\delta_H = 8^\circ$.

Figure 5.- Continued.

[redacted]

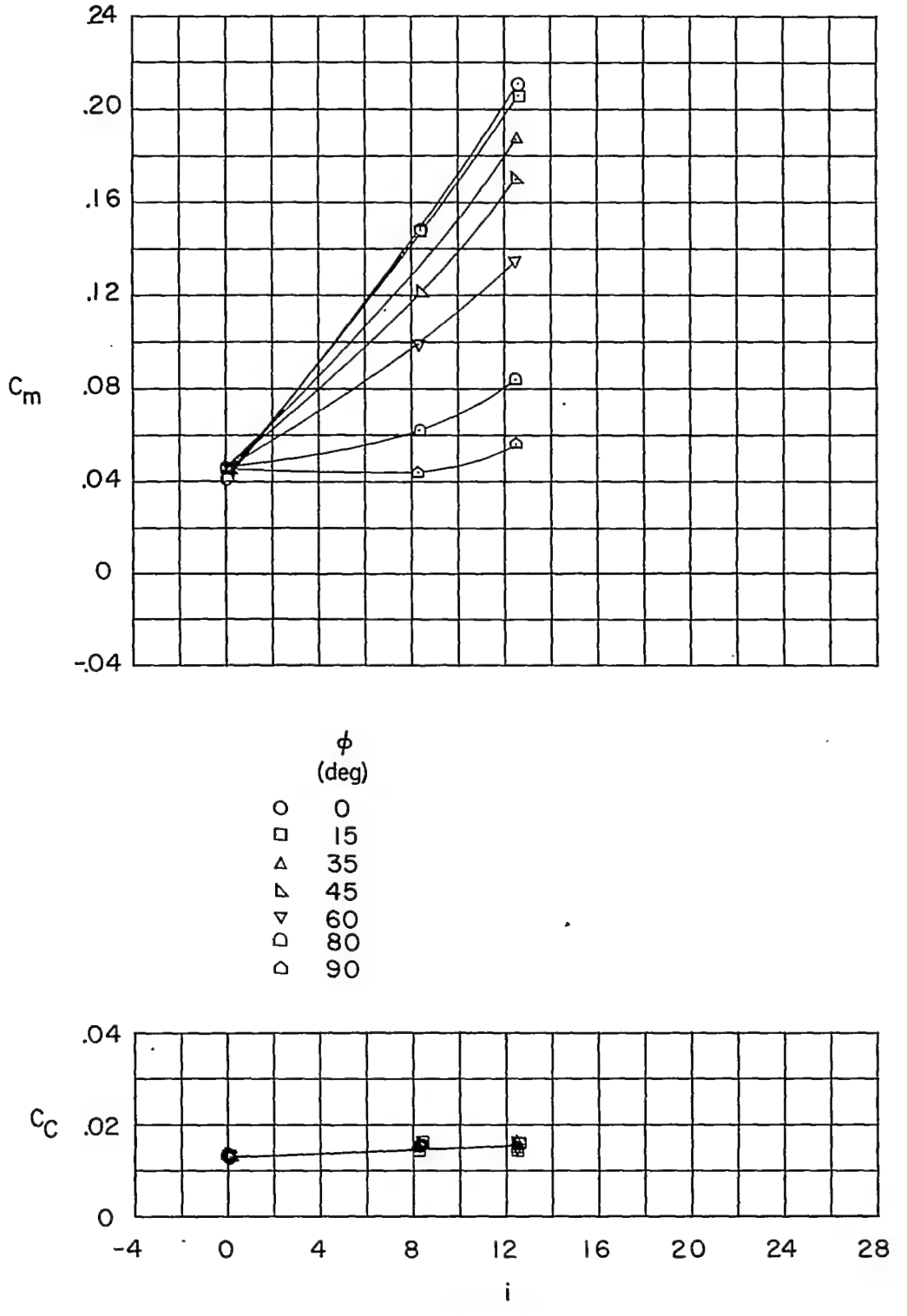

(b) Continued.

Figure 5.- Continued.

[redacted]

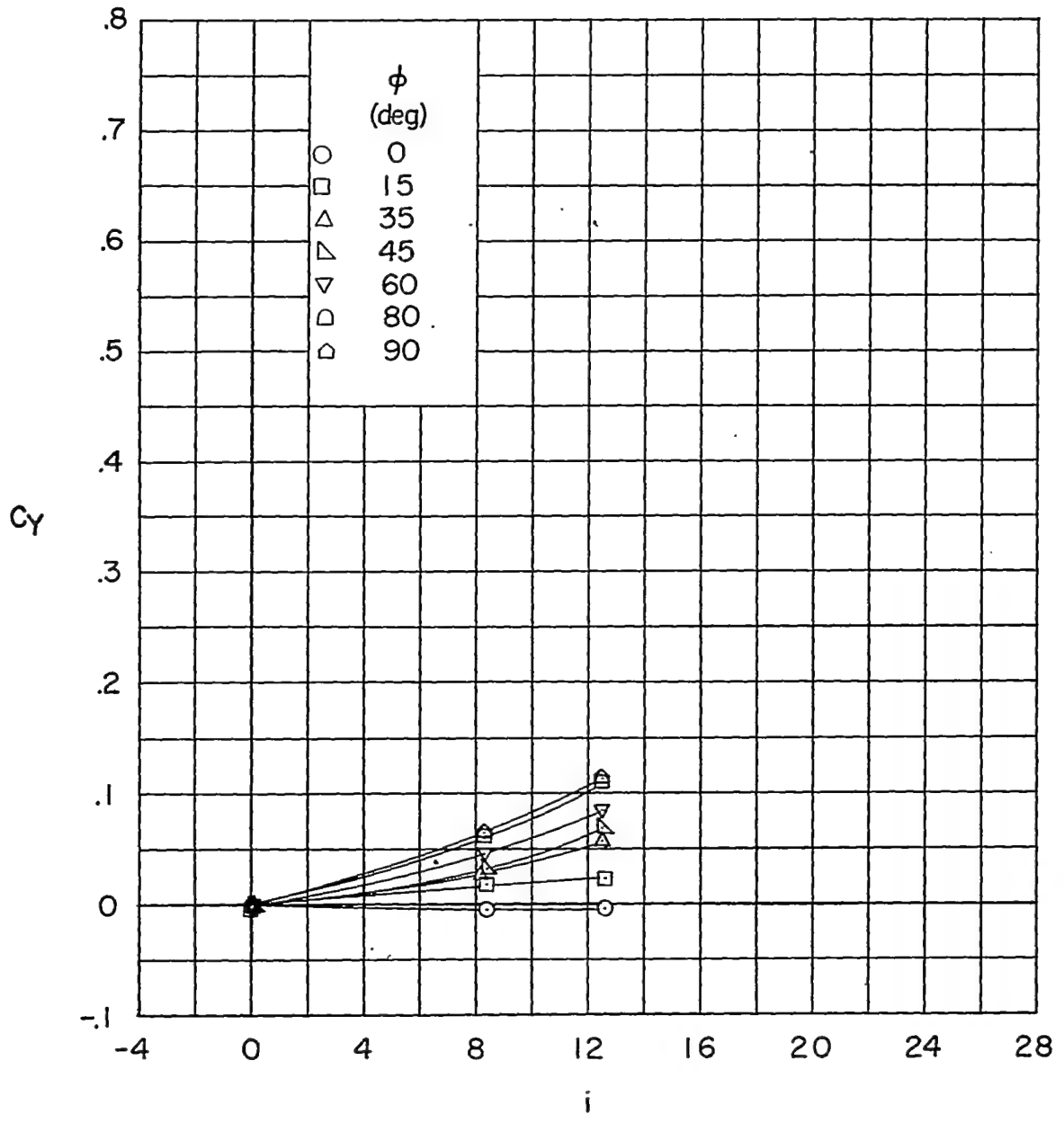

(b) Continued.

Figure 5.- Continued.

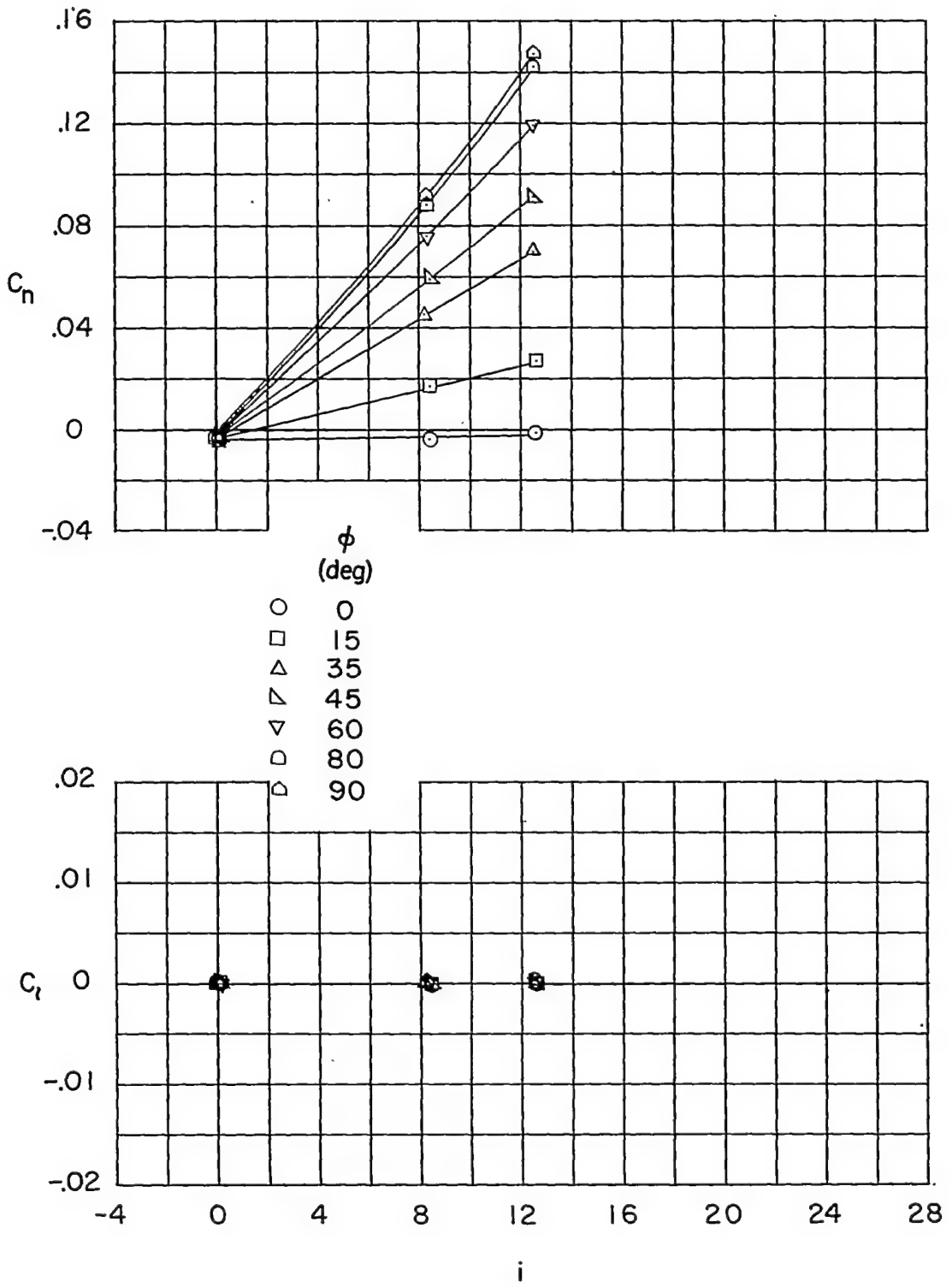

(b) Concluded.

Figure 5.- Continued.

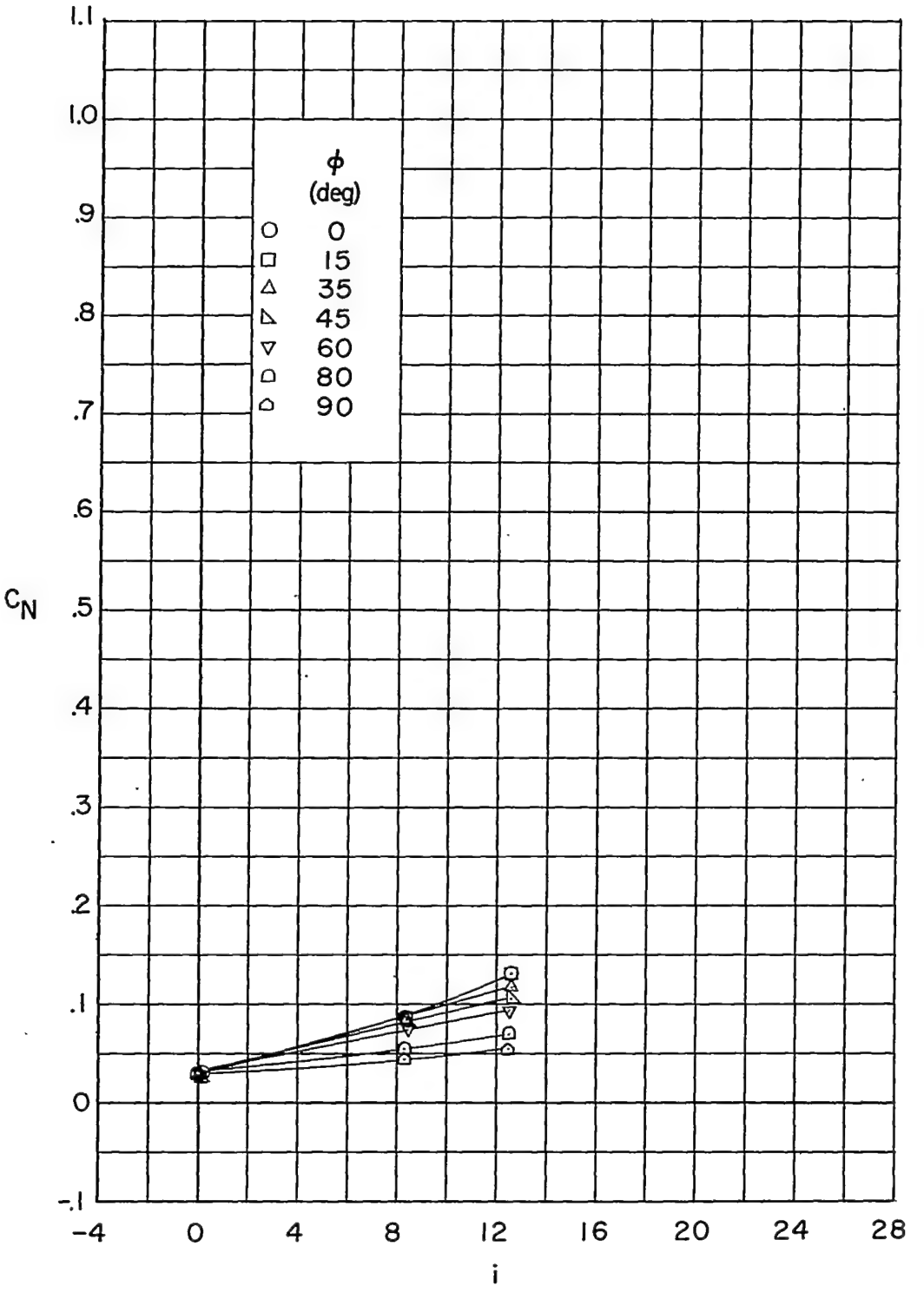

(c) $\delta_H = 12^\circ$.

Figure 5.- Continued.

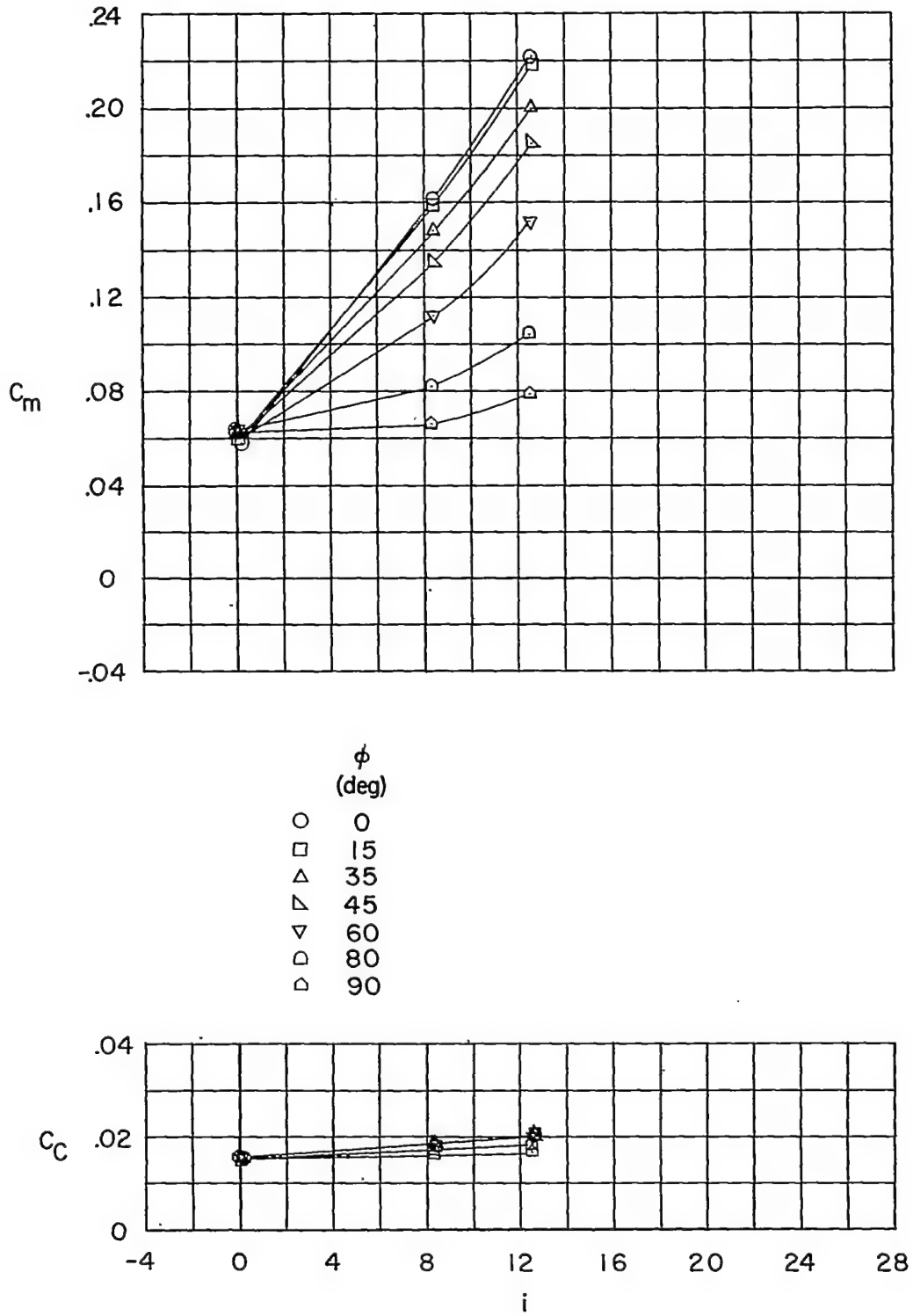

(c) Continued.

Figure 5.- Continued.

[redacted]

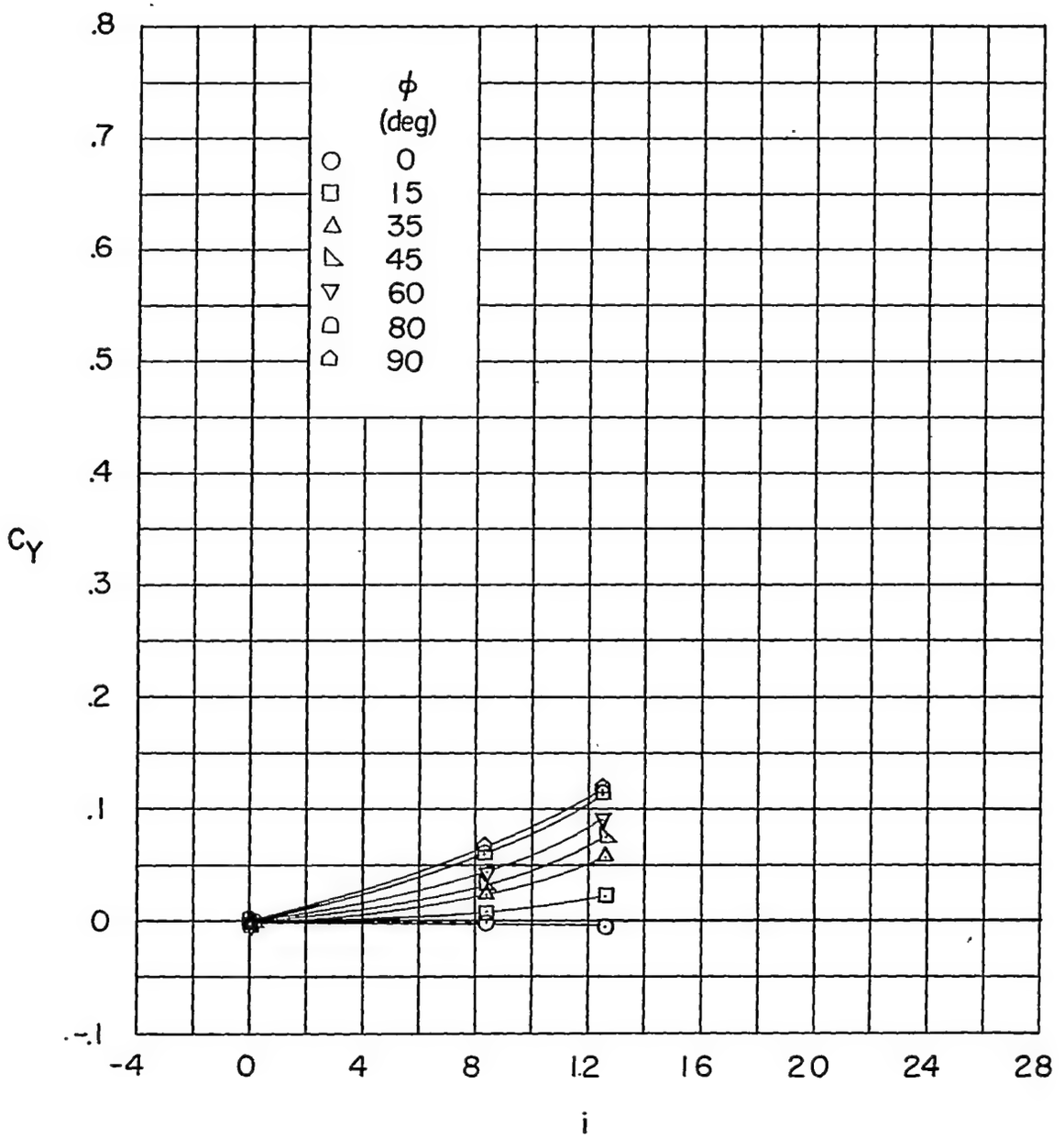

(c) Continued.

Figure 5.- Continued.

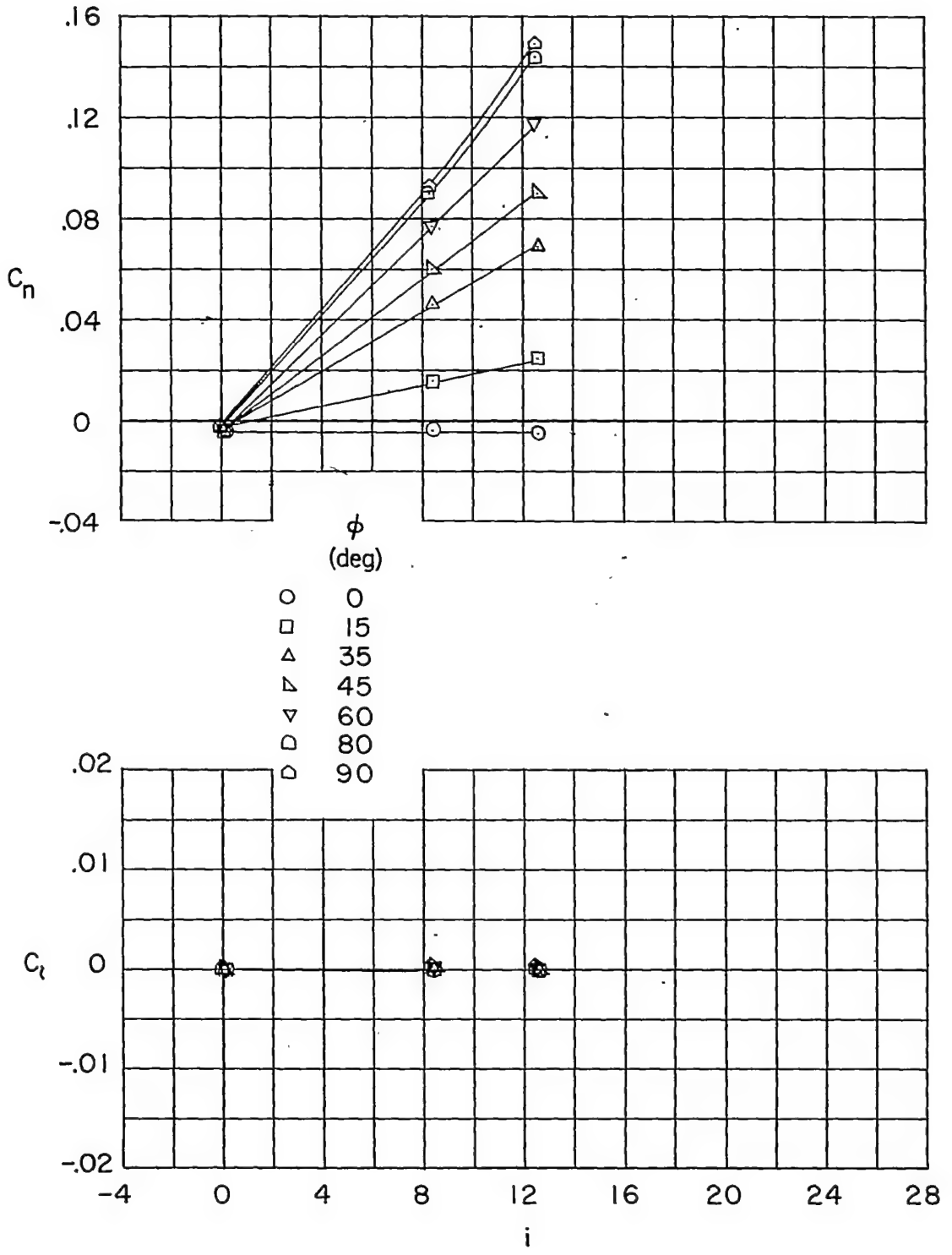

(c) Concluded.

Figure 5.- Concluded.

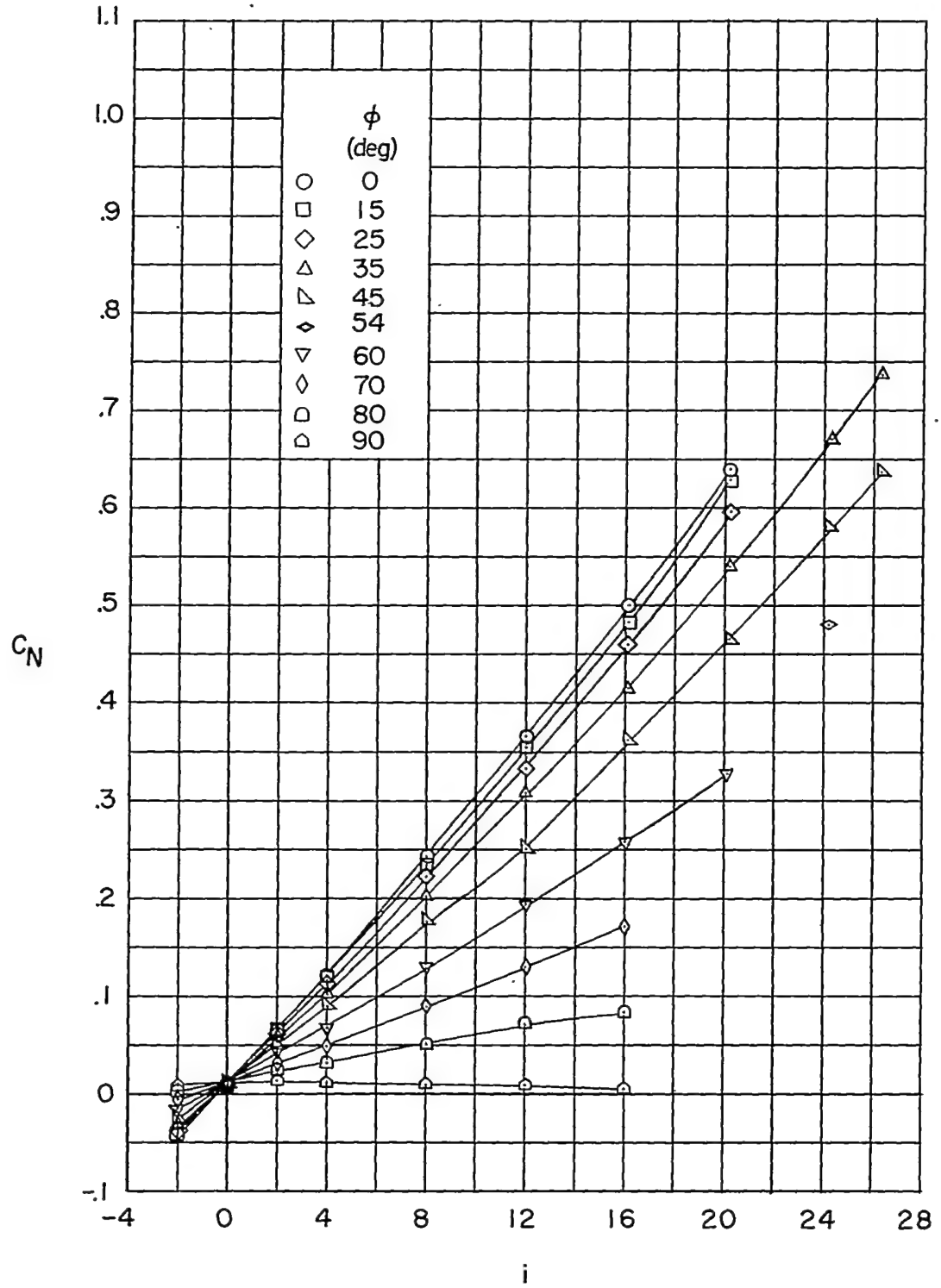

(a) Inline wings.

Figure 6.- Body-wing. $l/d = 15.7$.

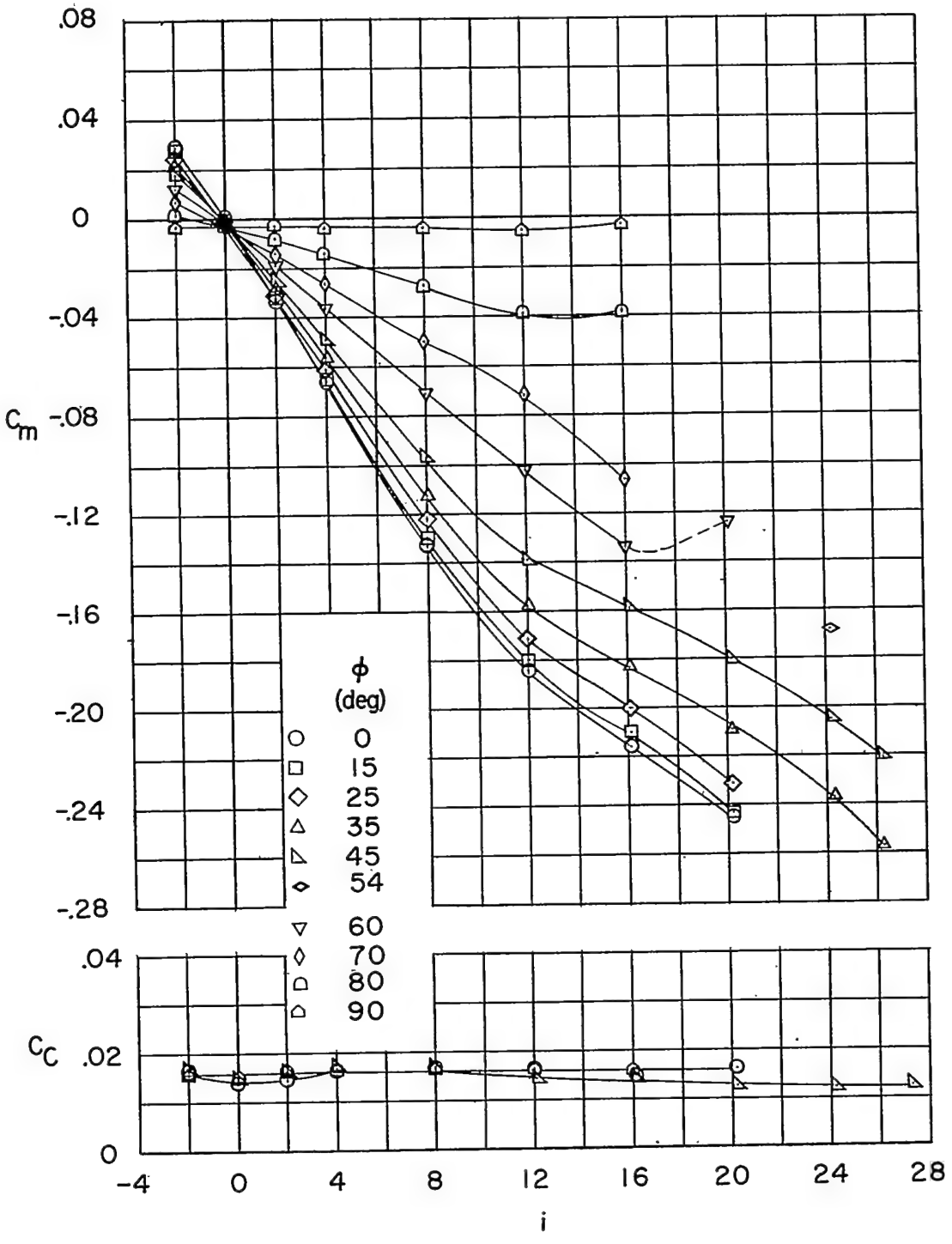

(a) Continued.

Figure 6.- Continued.

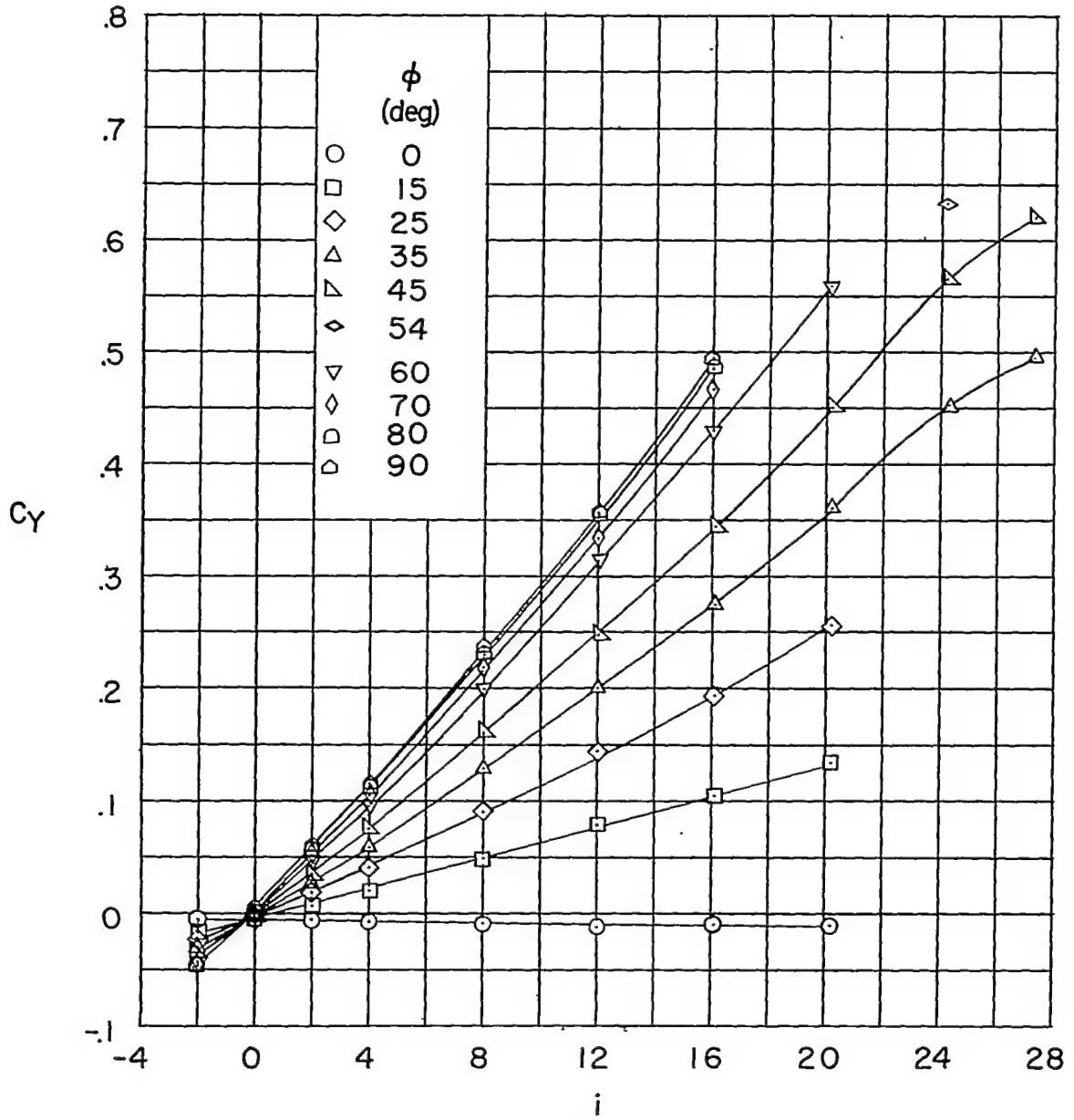

(a) Continued.

Figure 6.- Continued.

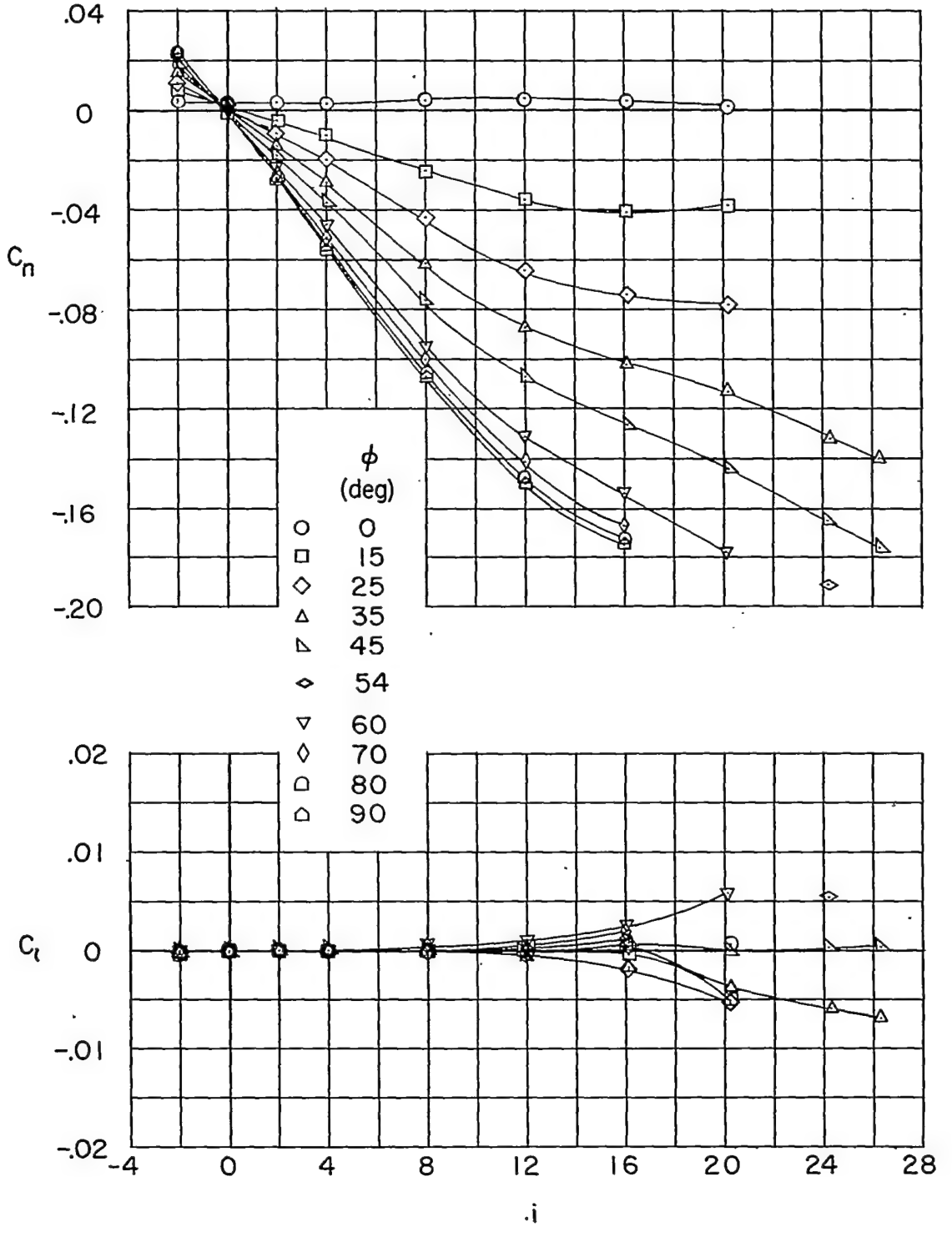

(a) Concluded.

Figure 6.- Continued.

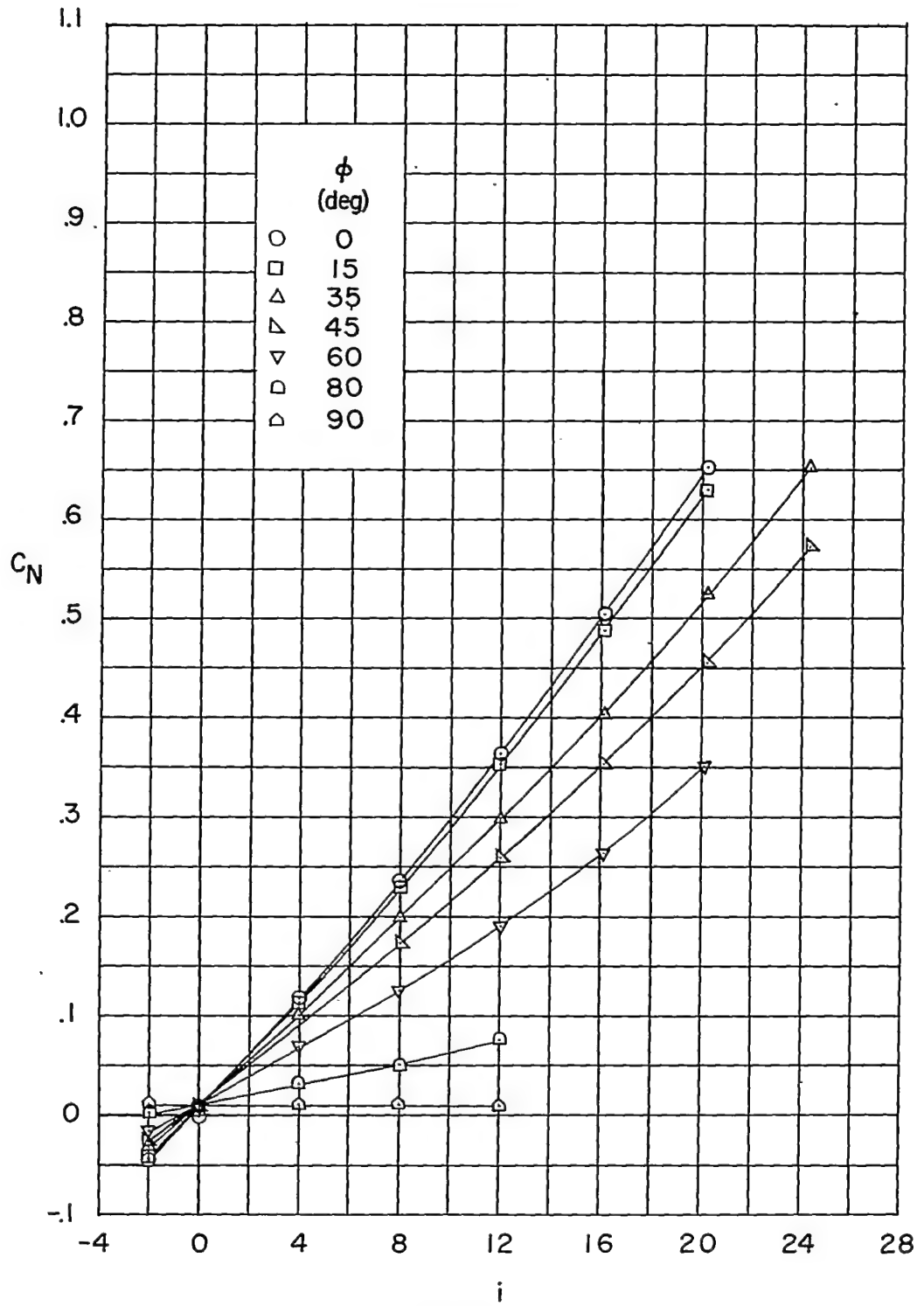

(b) Indexed wings.

Figure 6.- Continued.

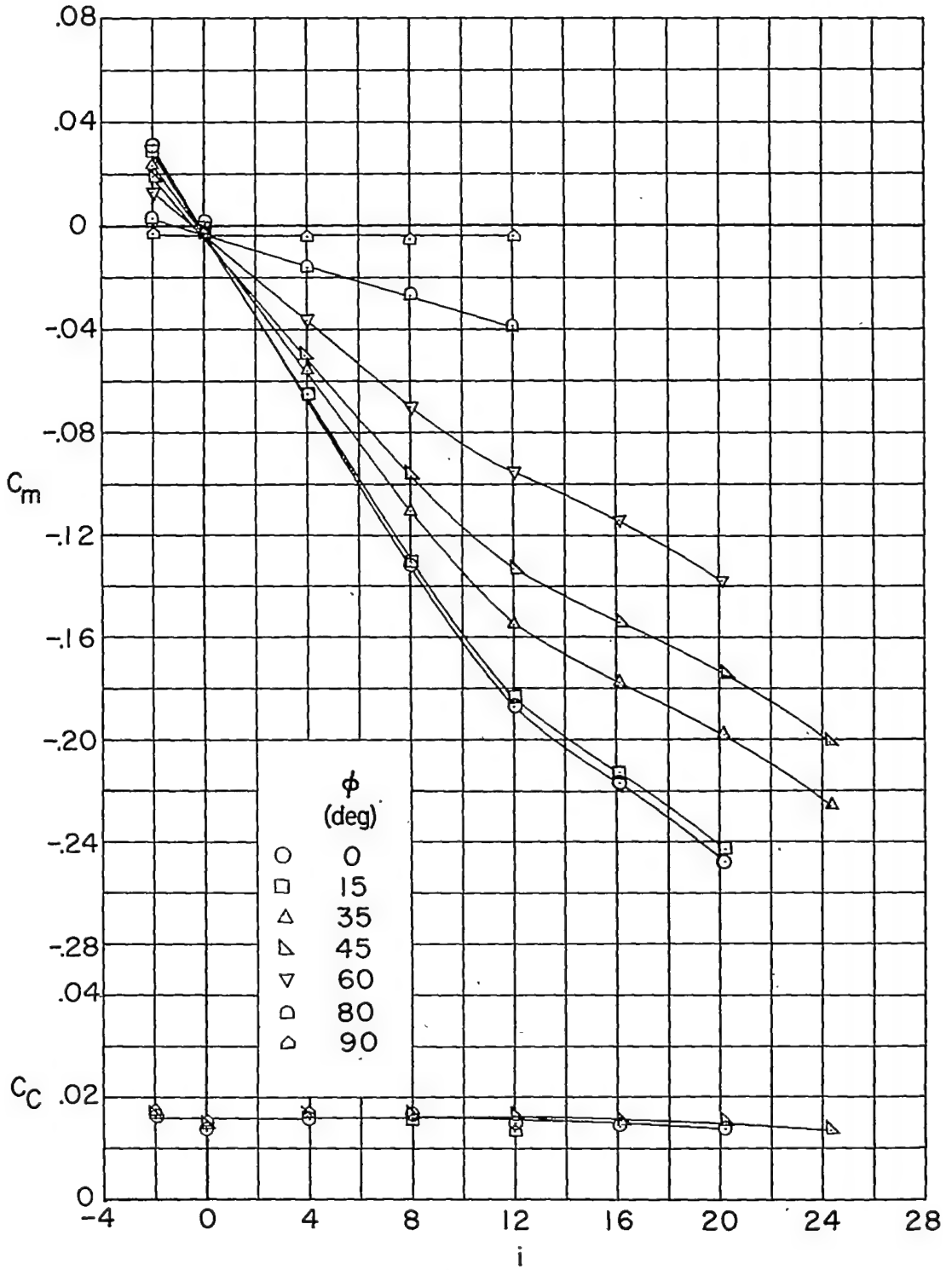

(b) Continued.

Figure 6.- Continued.

[redacted]

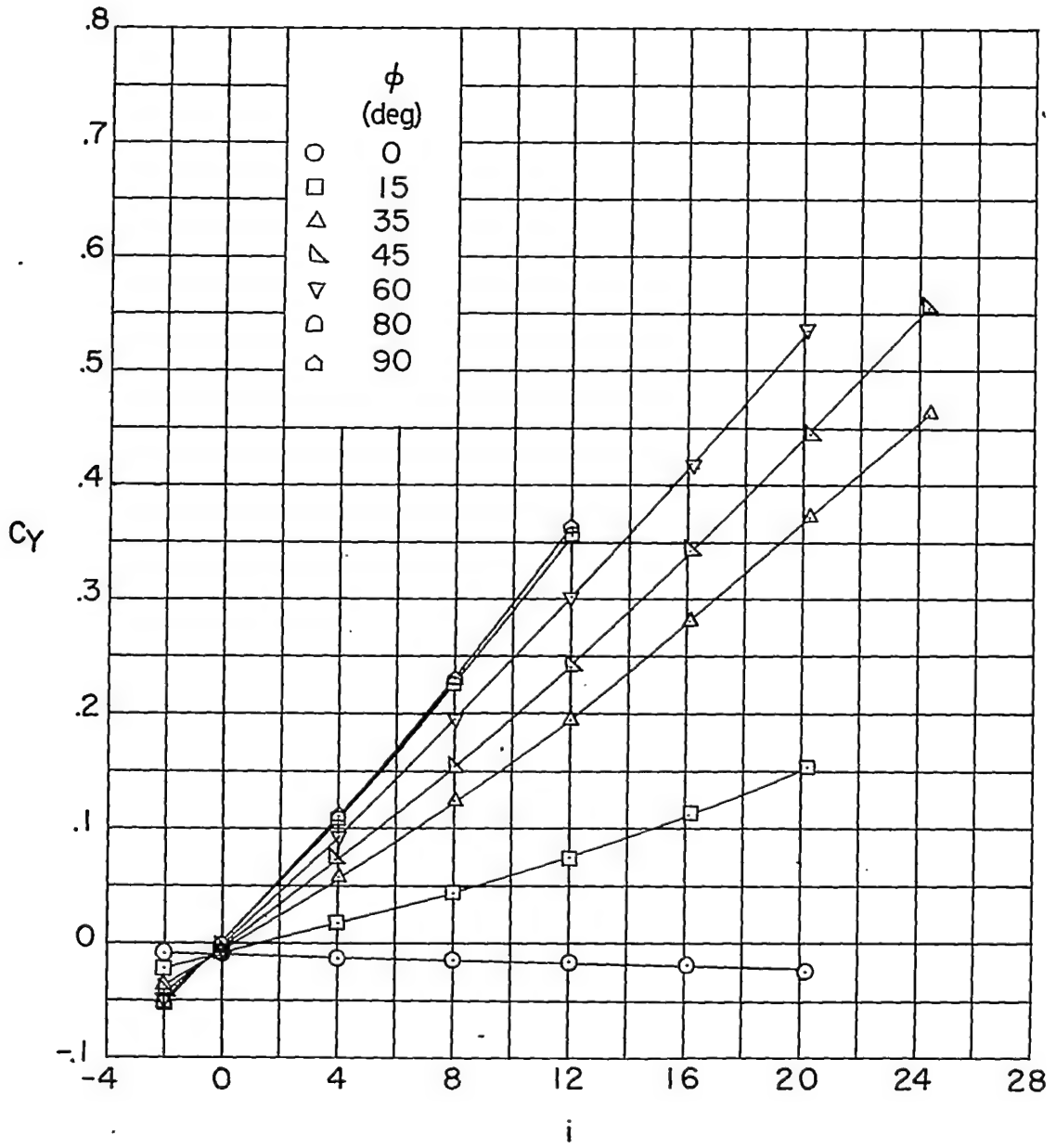

(b) Continued.

Figure 6.- Continued.

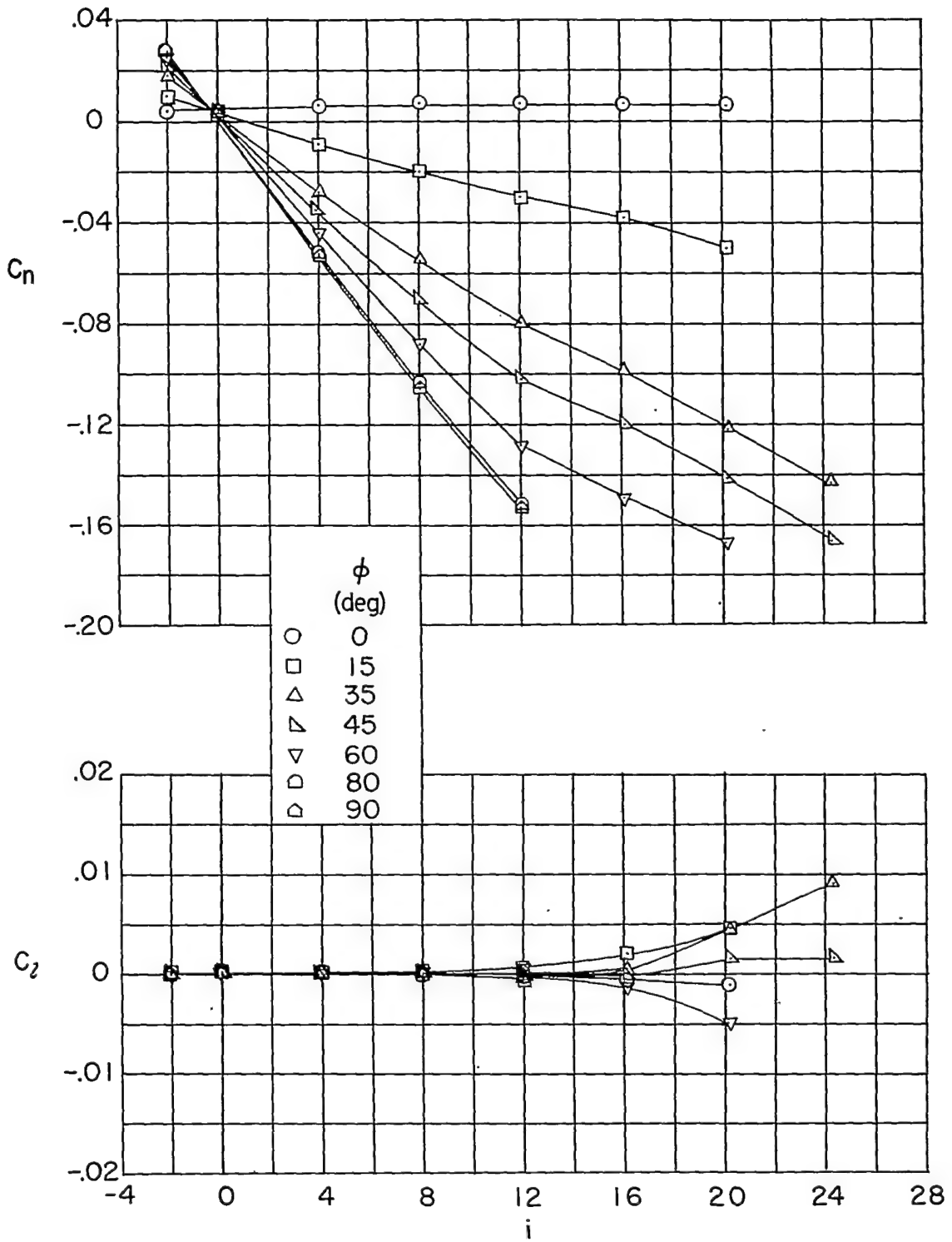

(b) Concluded.

Figure 6.- Concluded.

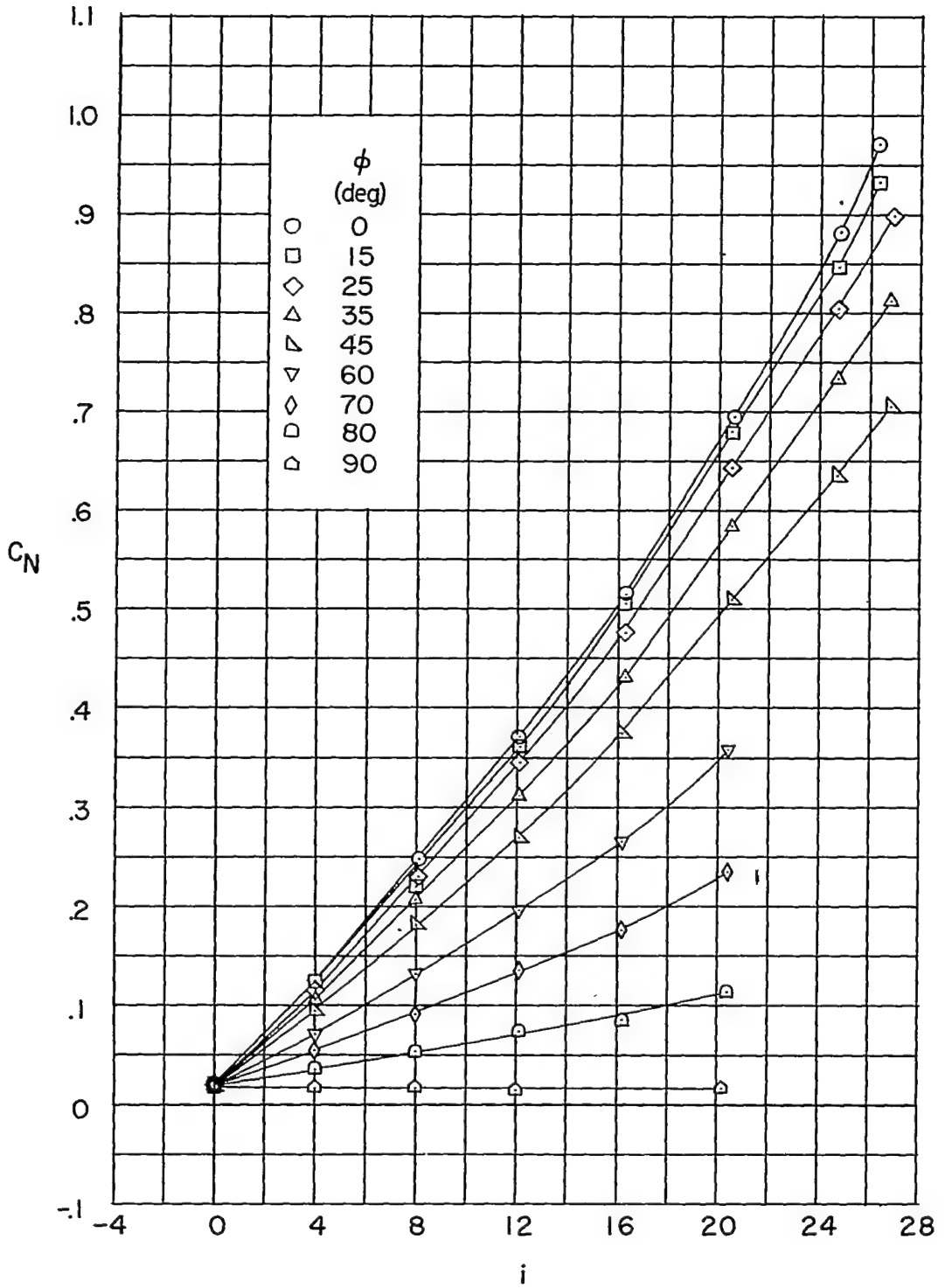

(a) Inline wings.

Figure 7.- Body-wings. $l/d = 19.1$.

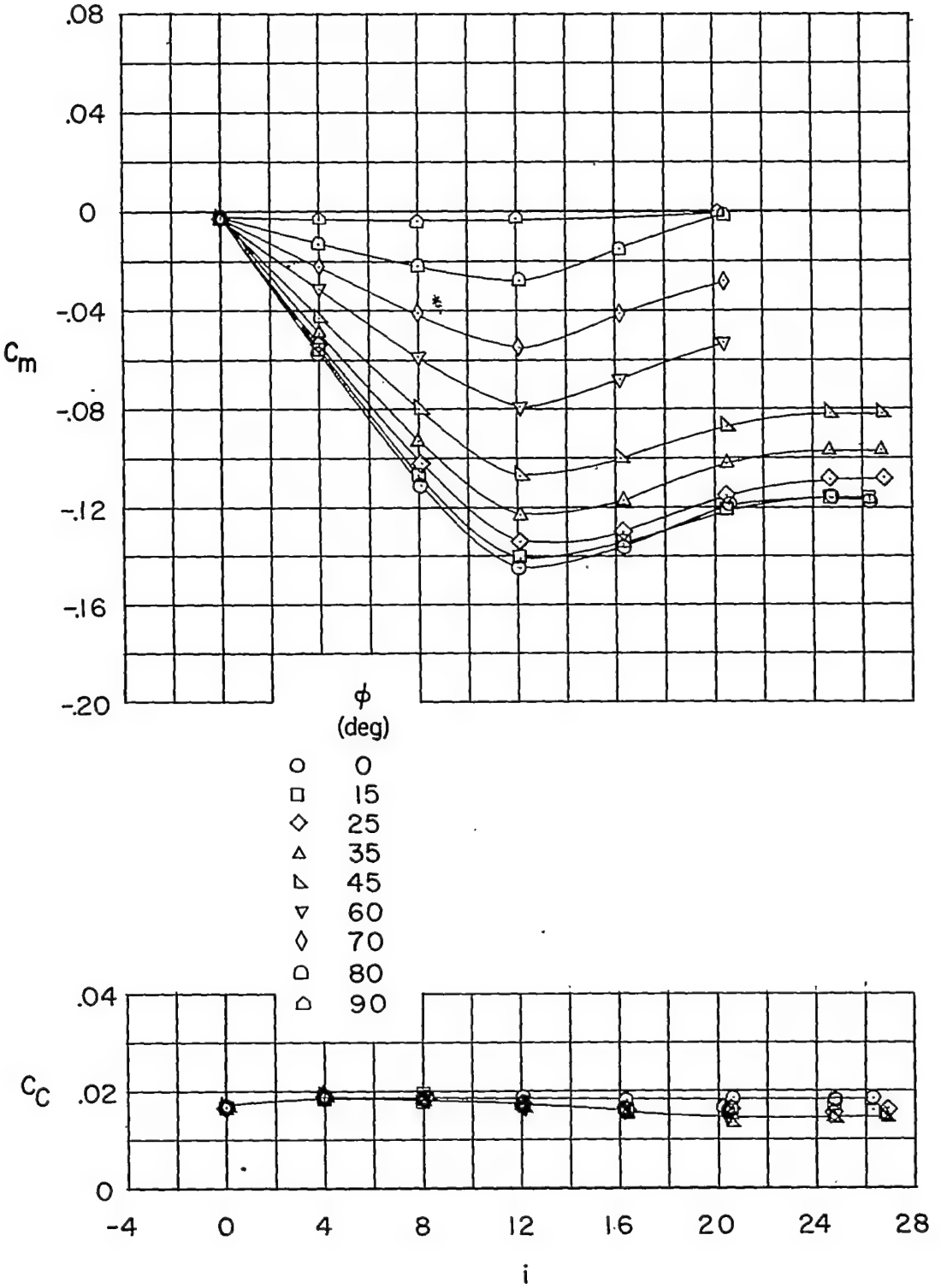

(a) Continued.

Figure 7.- Continued.

[redacted]

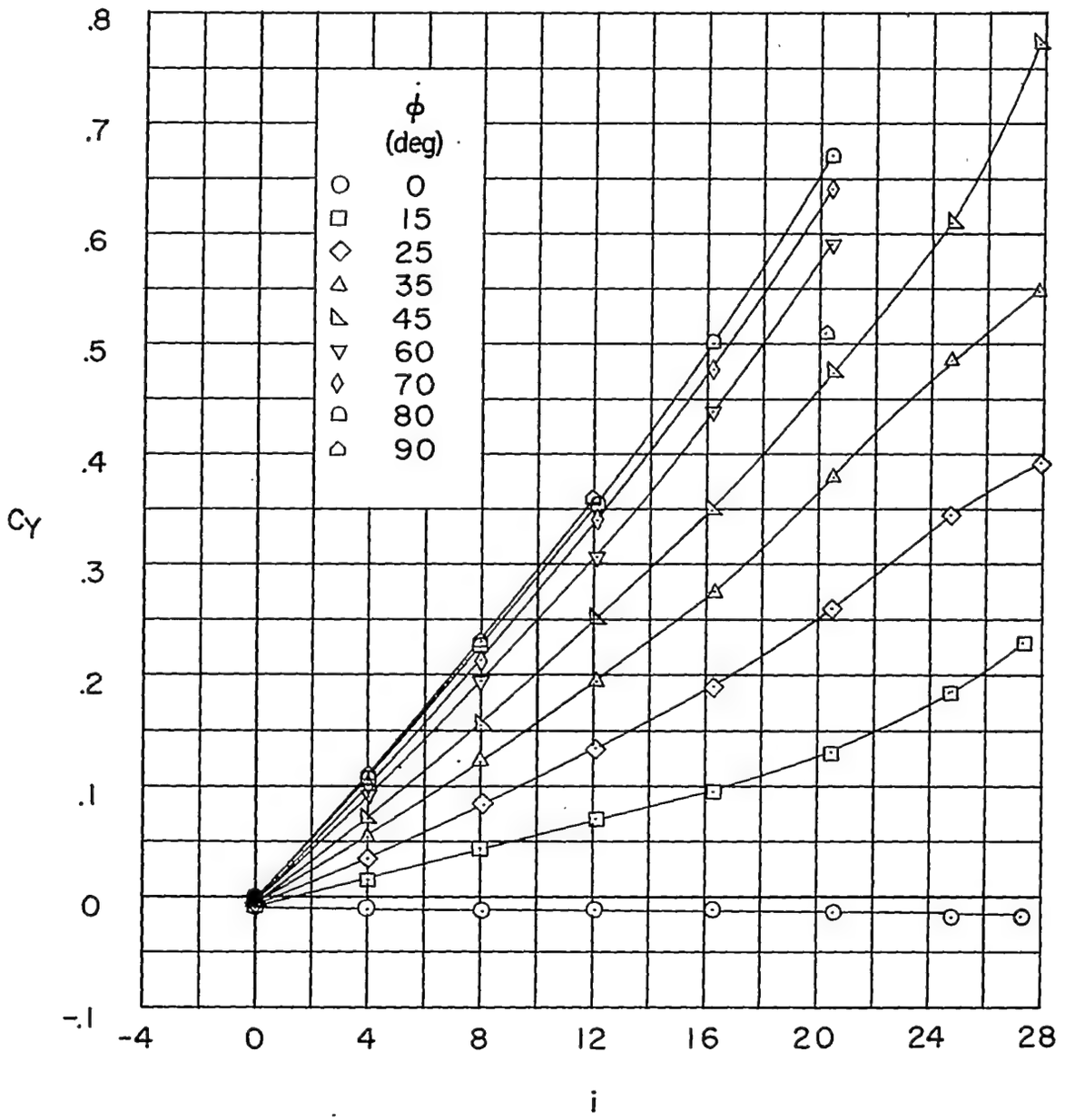

(a) Continued.

Figure 7.- Continued.

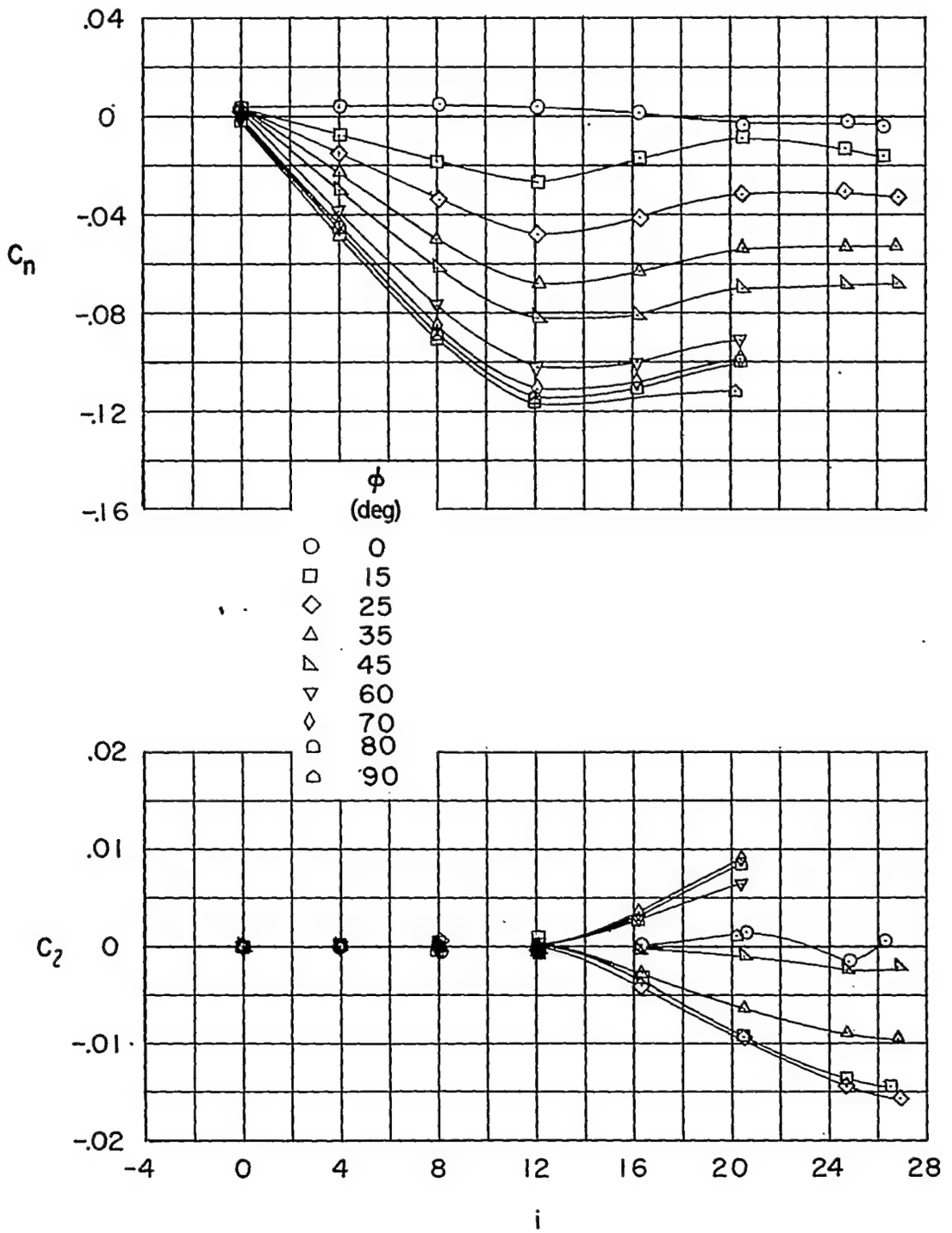

(a) Concluded.

Figure 7.- Continued.

[redacted]

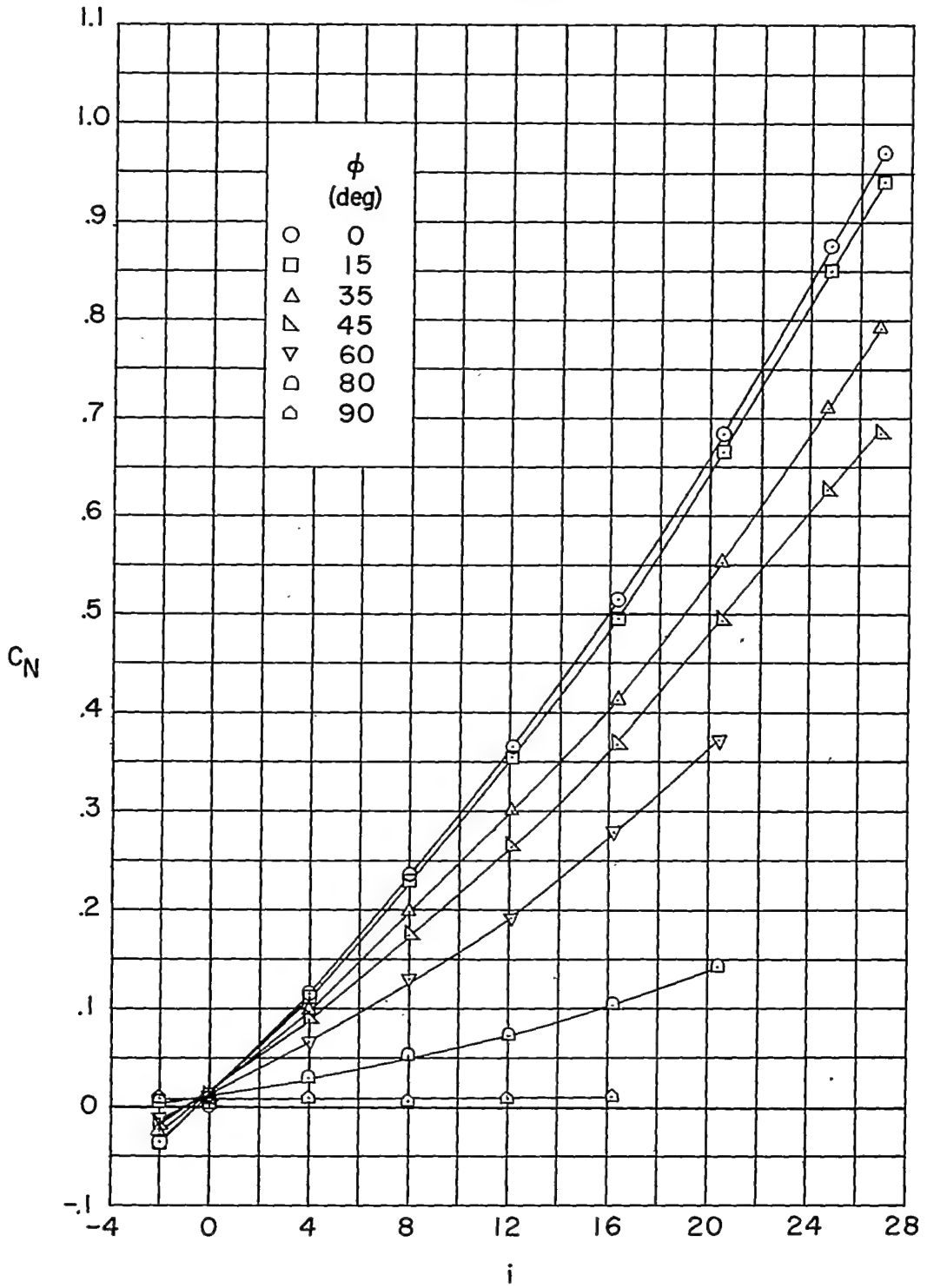

(b) Indexed wings.

Figure 7.- Continued.

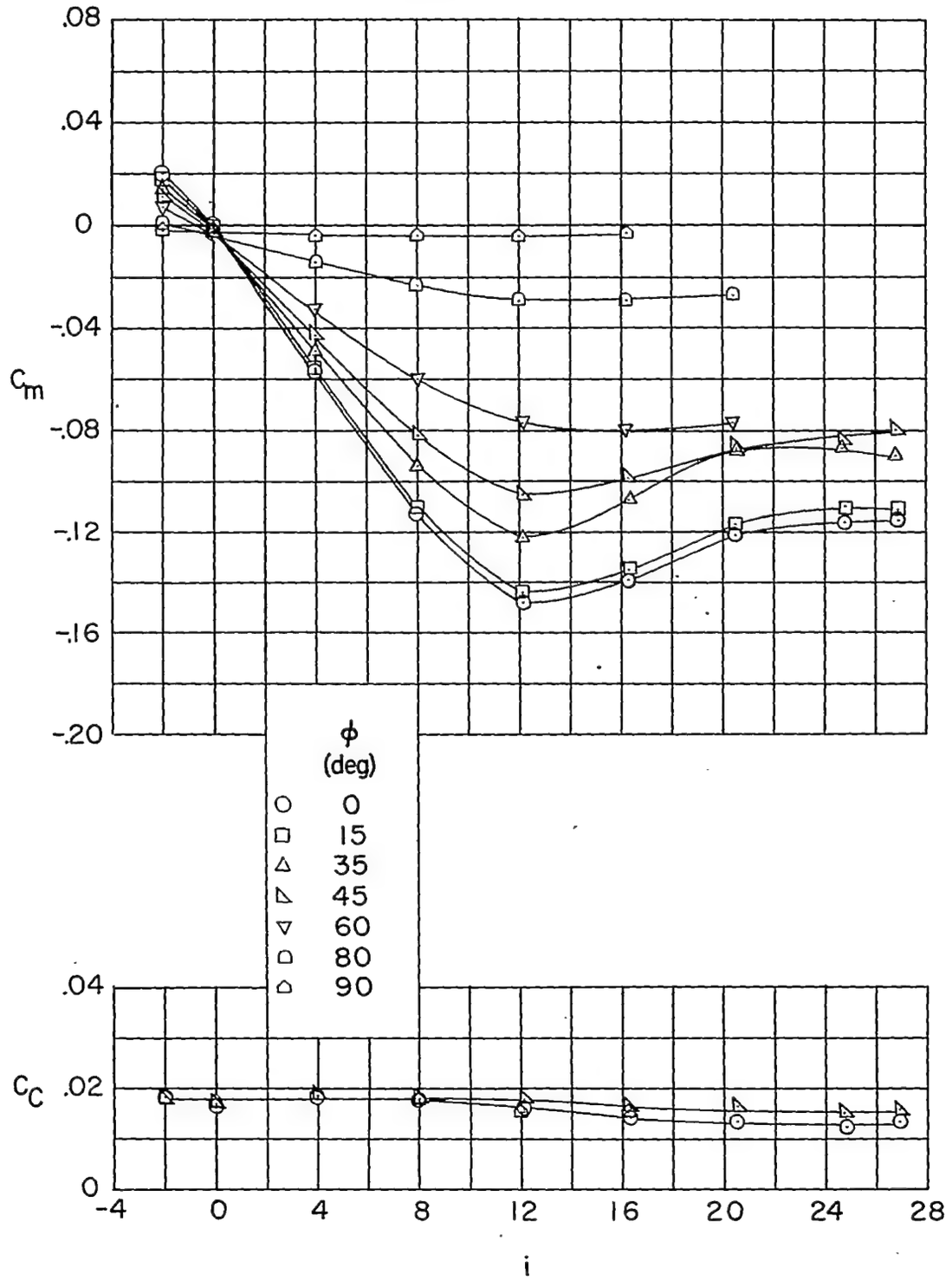

(b) Continued.

Figure 7.- Continued.

[redacted]

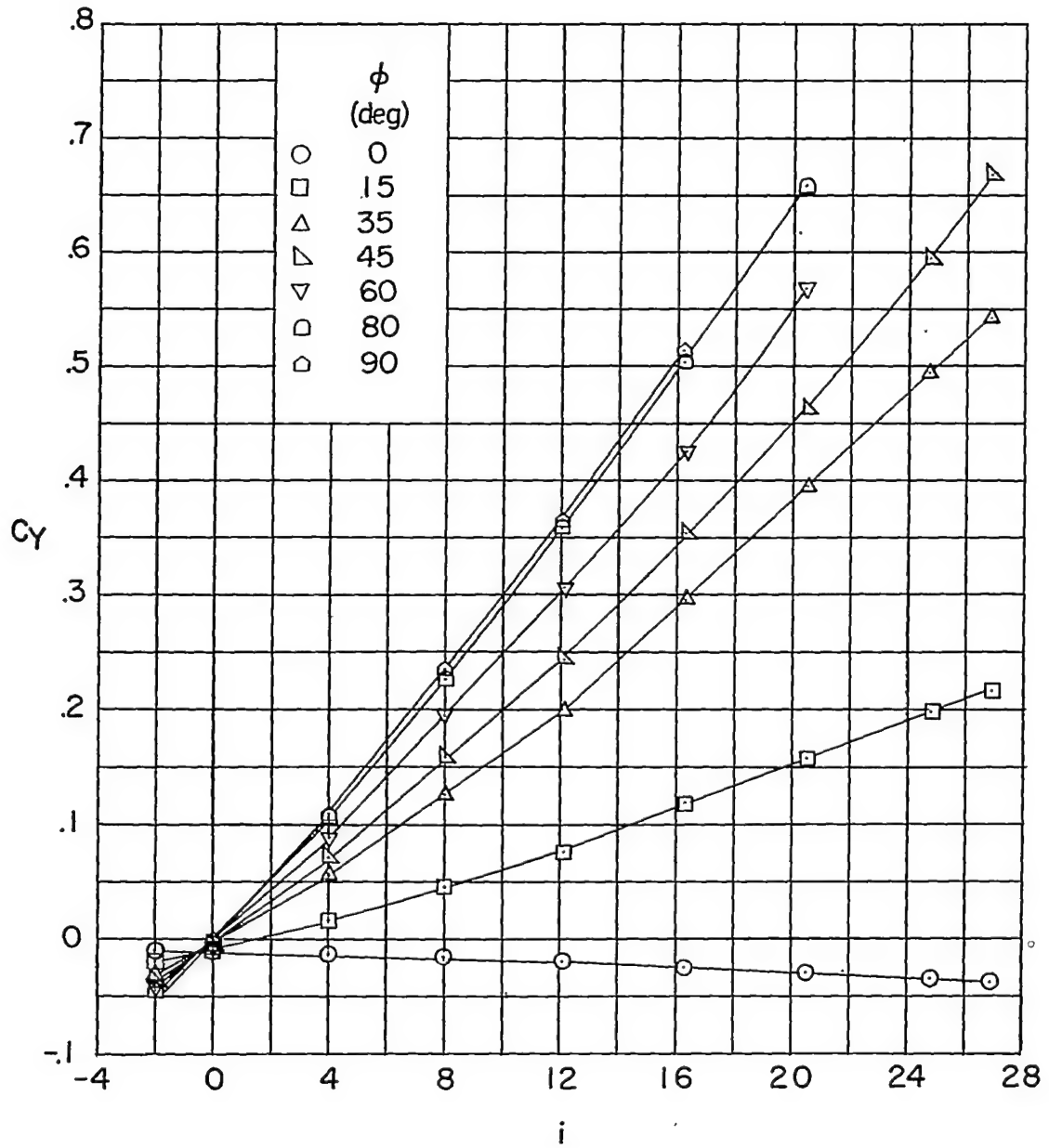

(b) Continued.

Figure 7.- Continued.

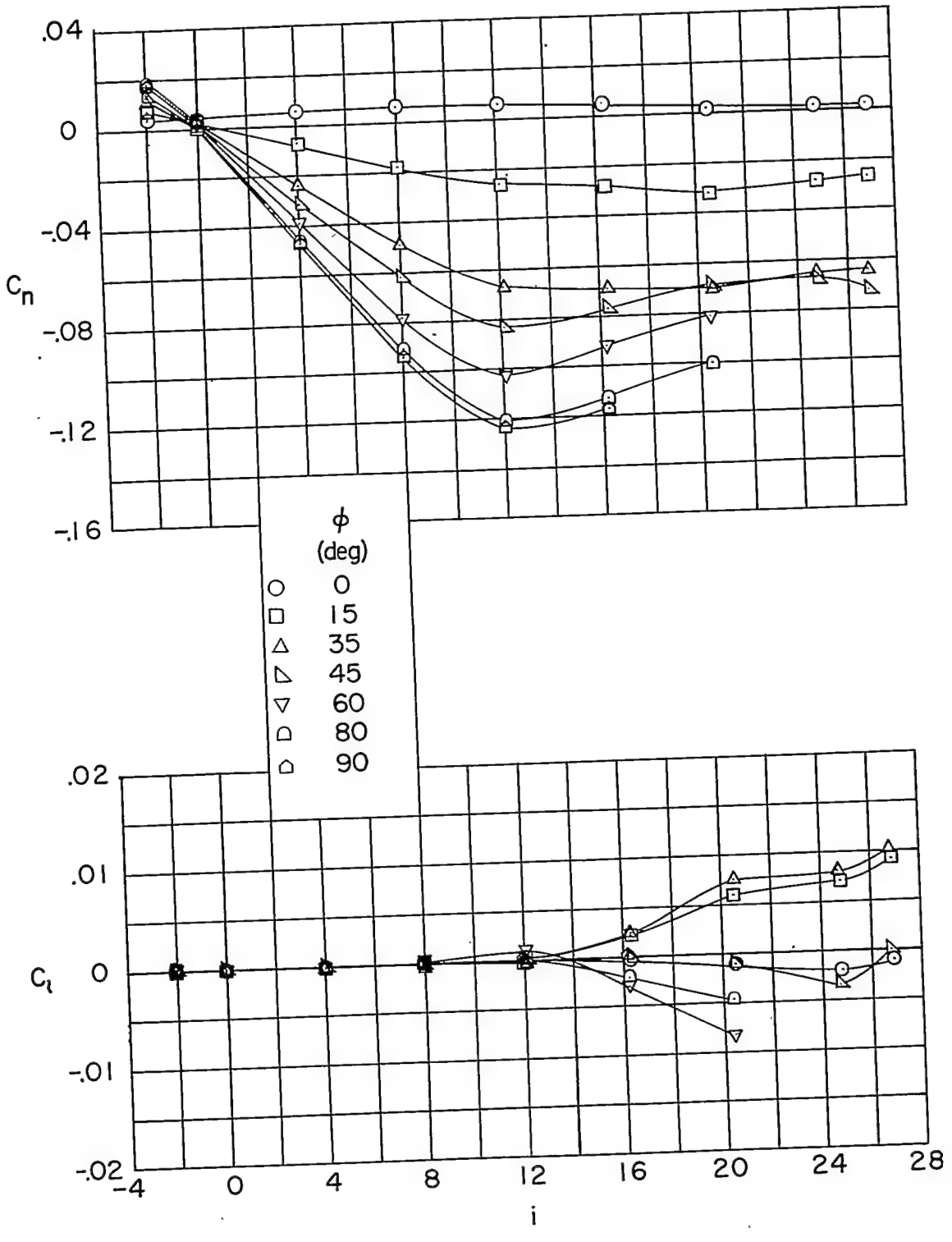

(b) Concluded.

Figure 7.- Concluded.

[redacted]

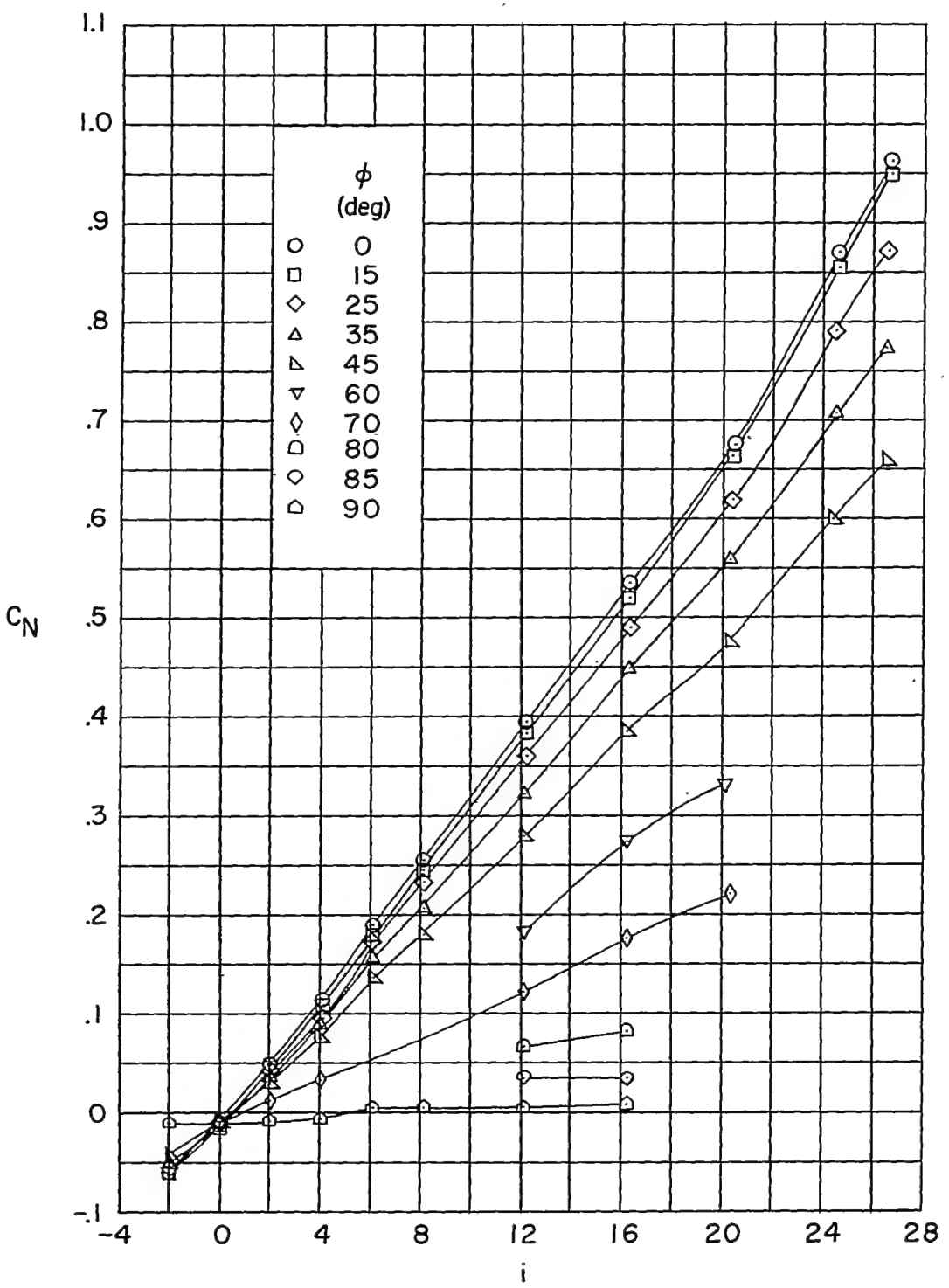

(a) $\delta_H = 0.$

Figure 8.- Body-wing-canard. $l/d = 15.7$; inline wings.

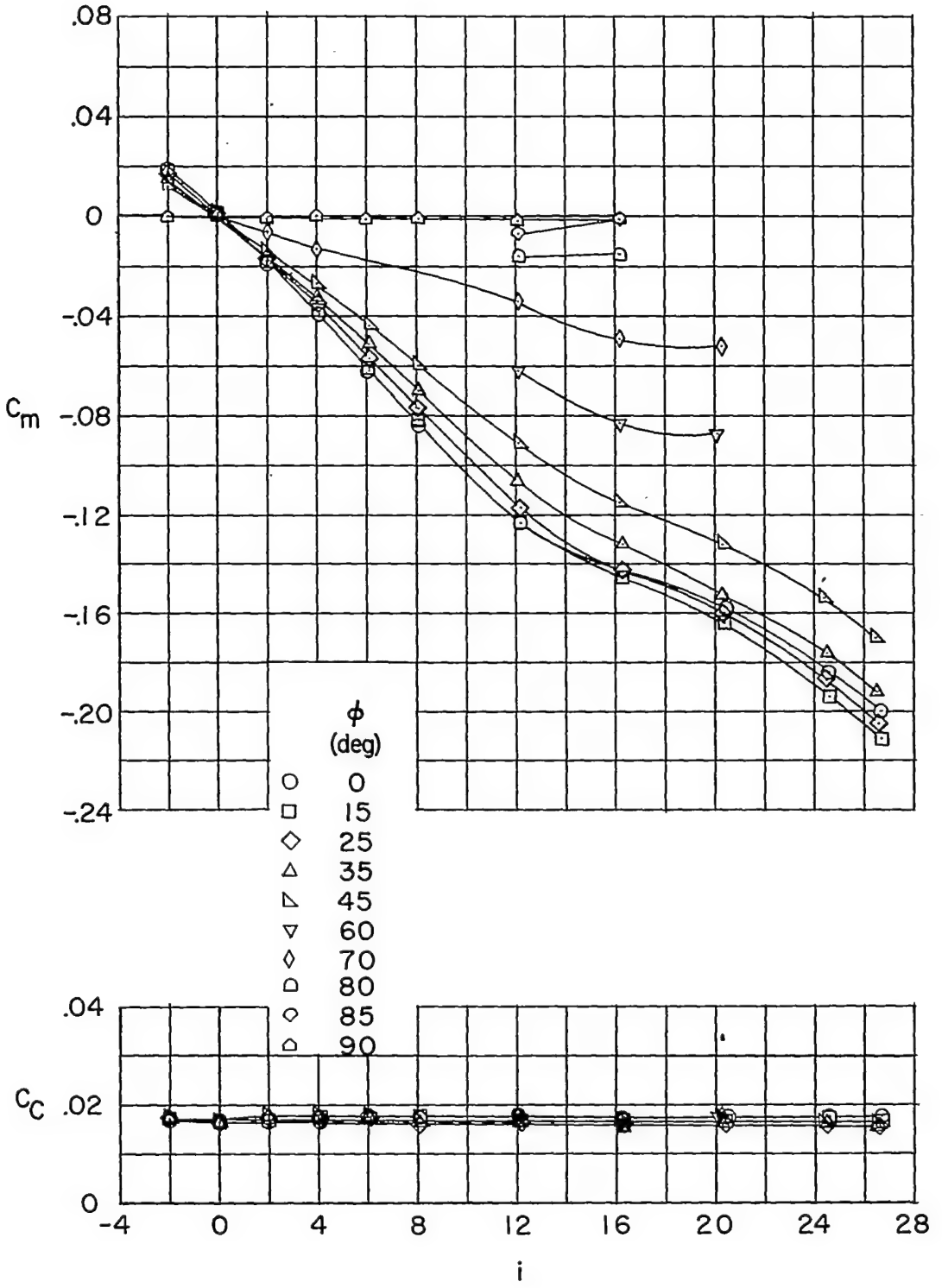

(a) Continued.

Figure 8.- Continued.

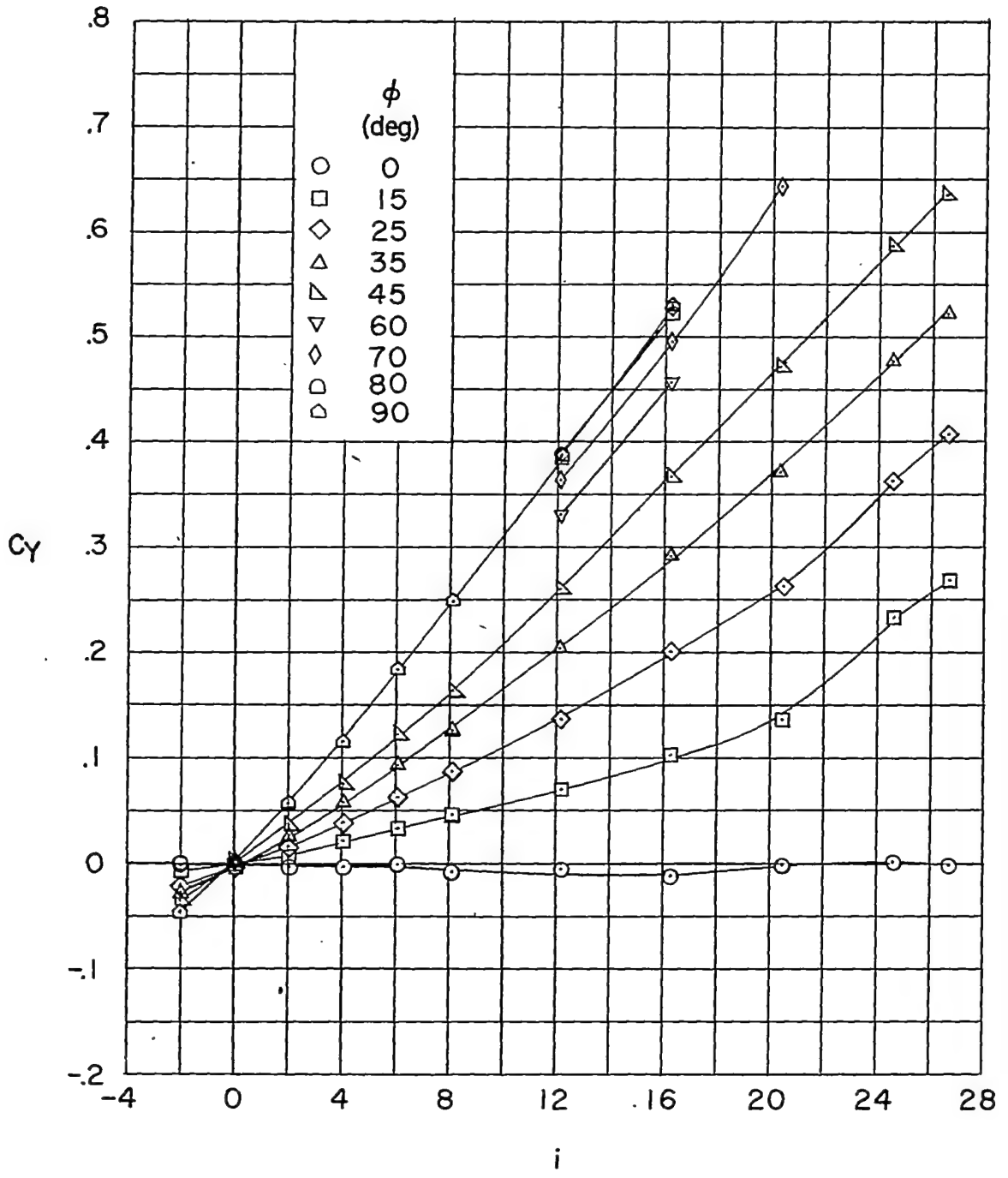

(a) Continued.

Figure 8.- Continued.

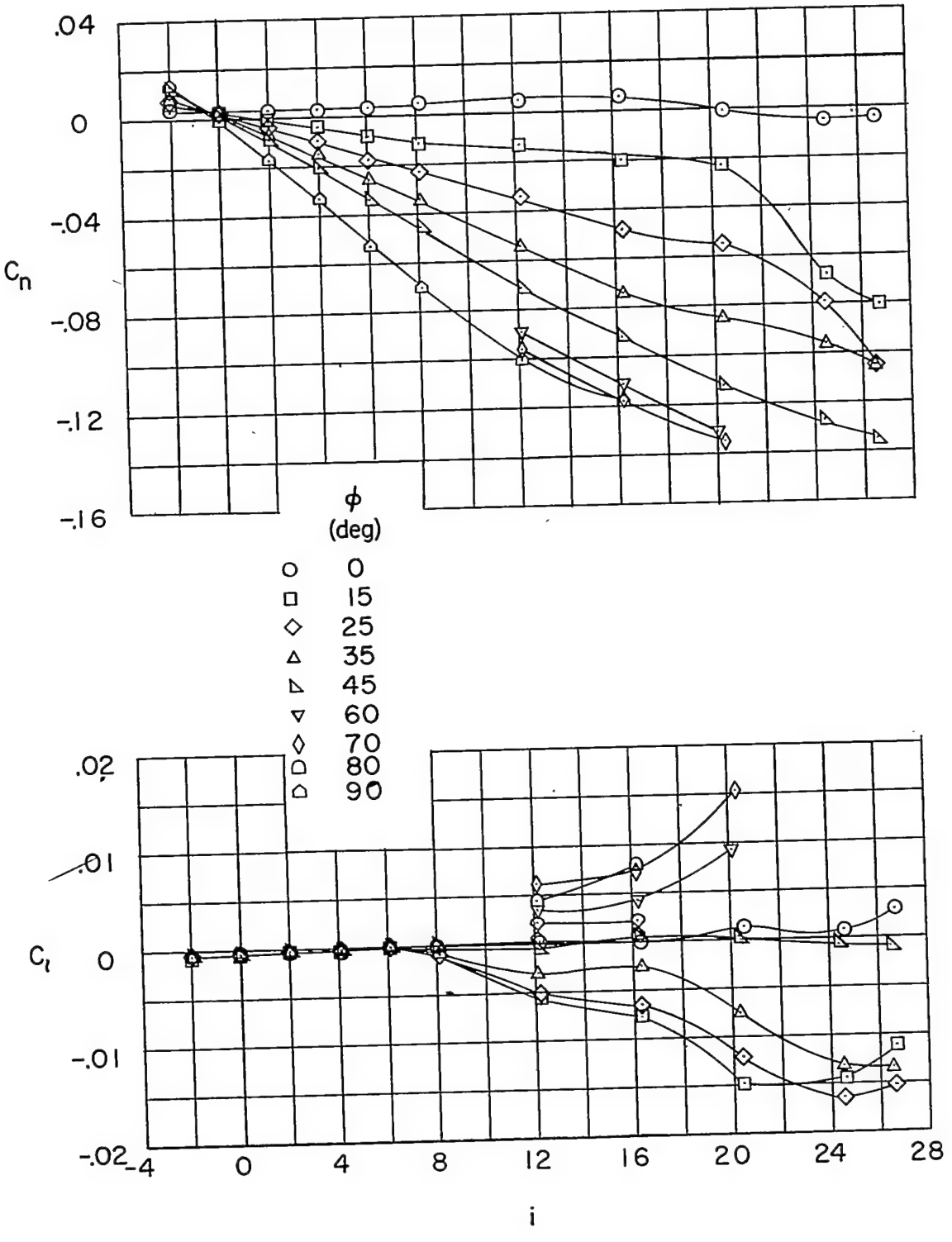

(a) Concluded.

Figure 8.- Continued.

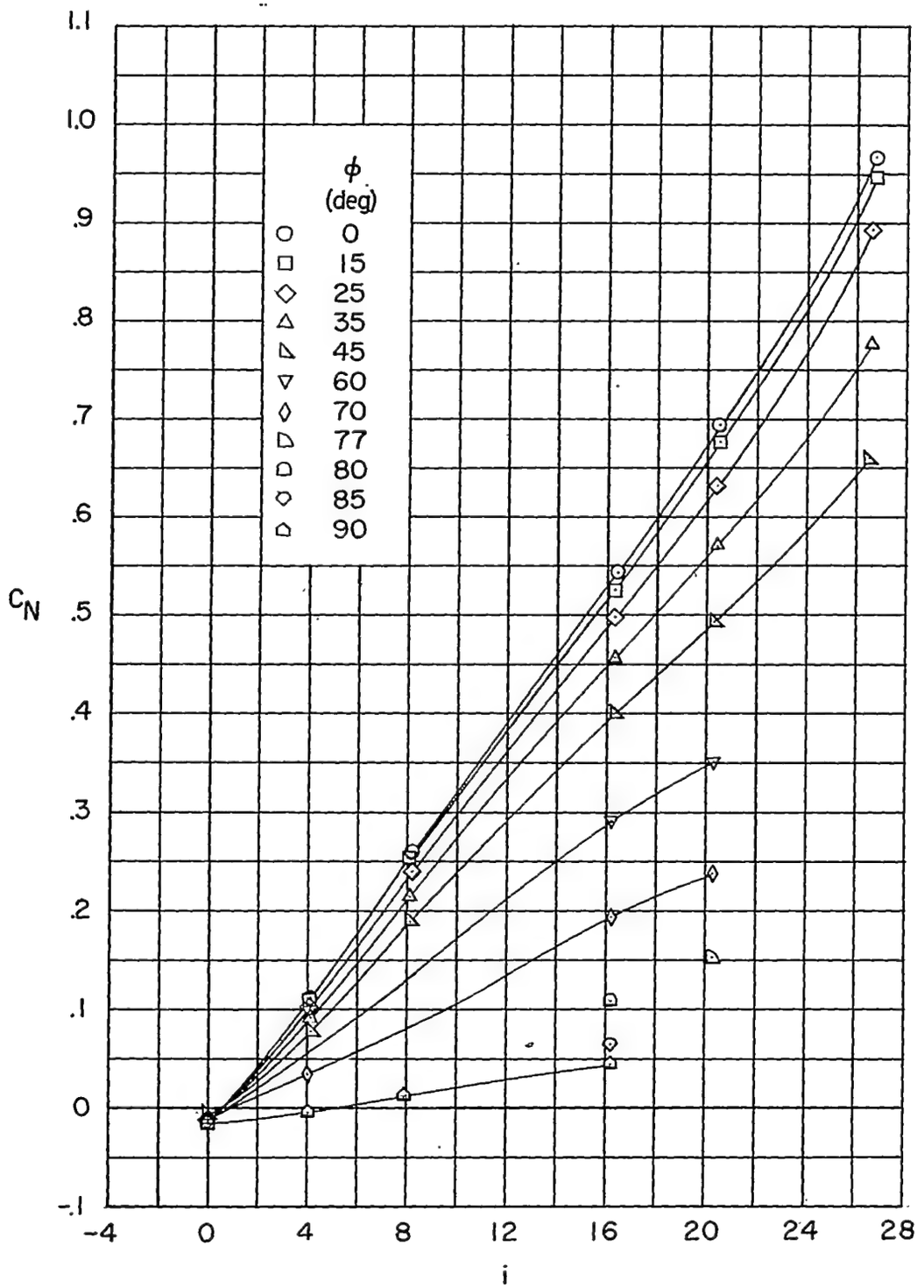

(b) $\delta_H = 4^\circ$.

Figure 8.- Continued.

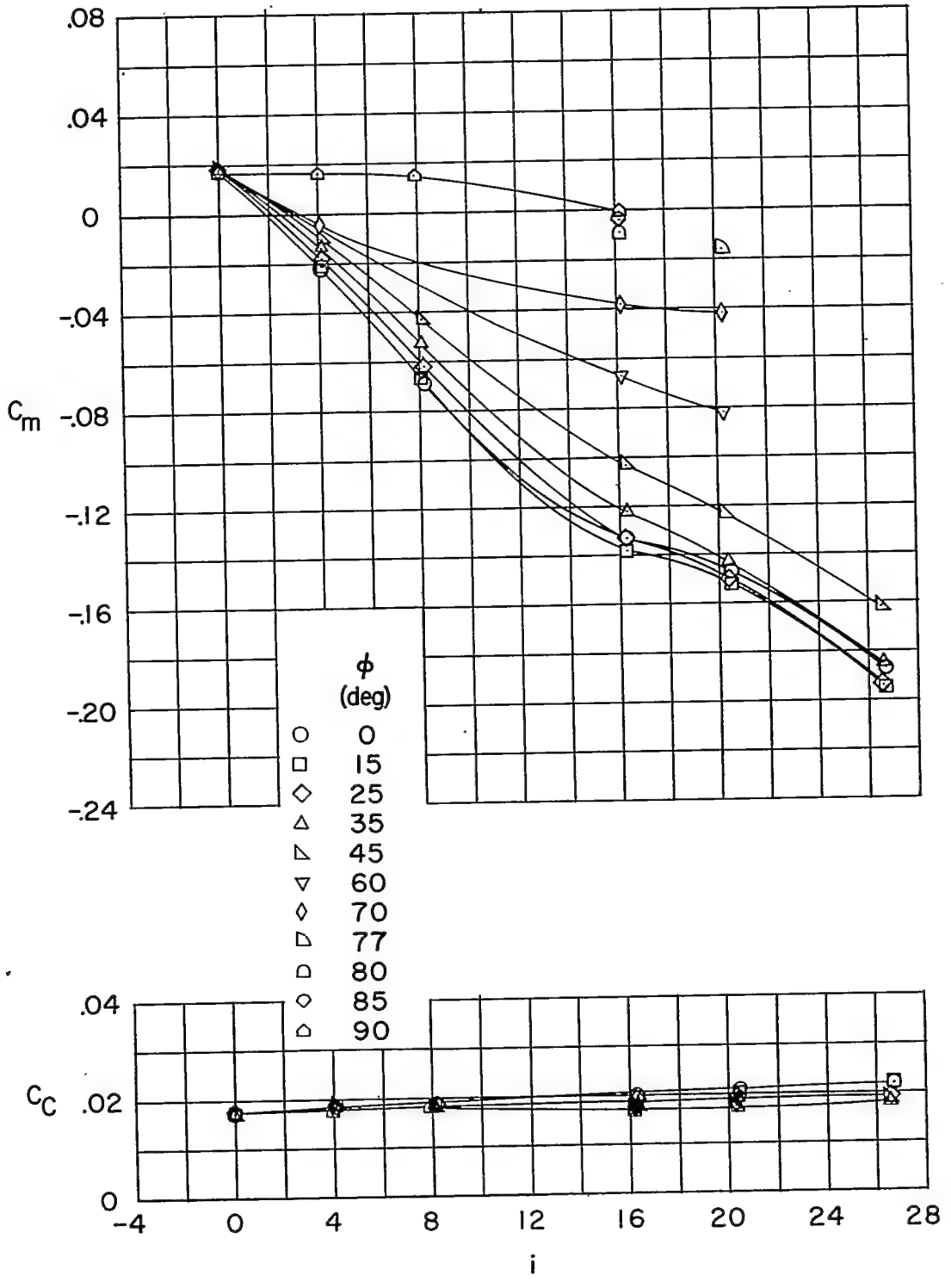

(b) Continued.

Figure 8.- Continued.

[redacted]

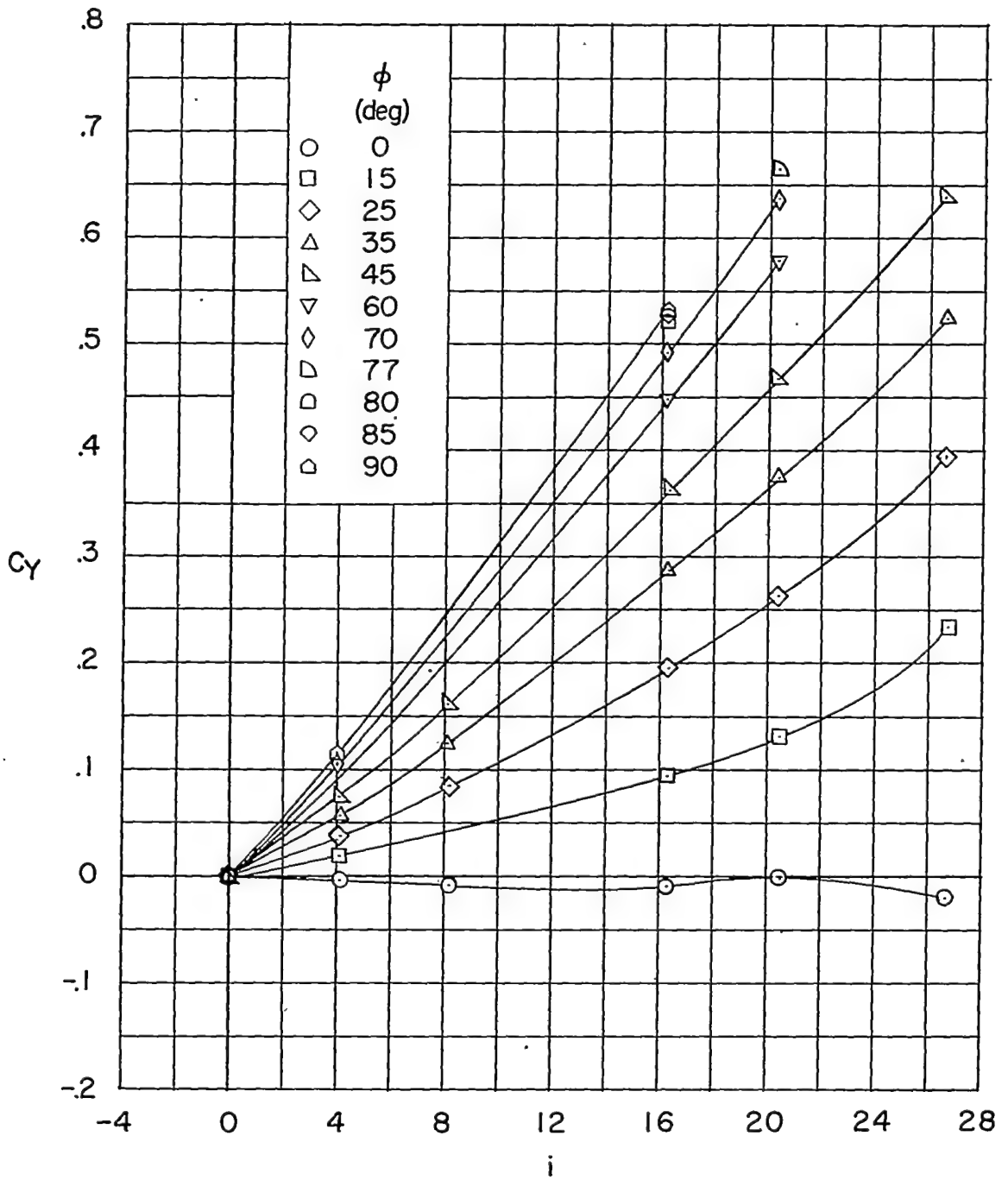

(b) Continued.

Figure 8.- Continued.

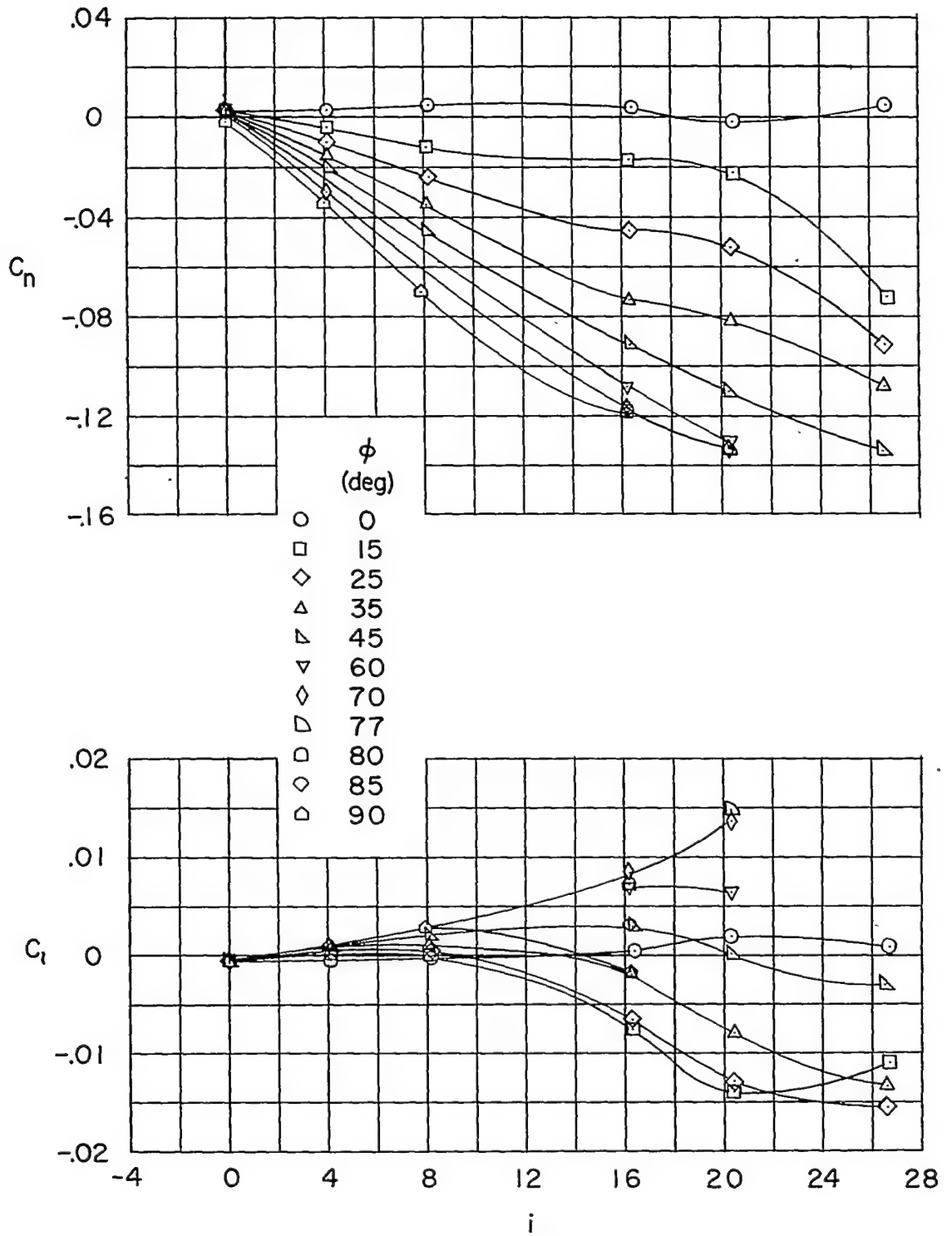

(b) Concluded.

Figure 8.- Continued.

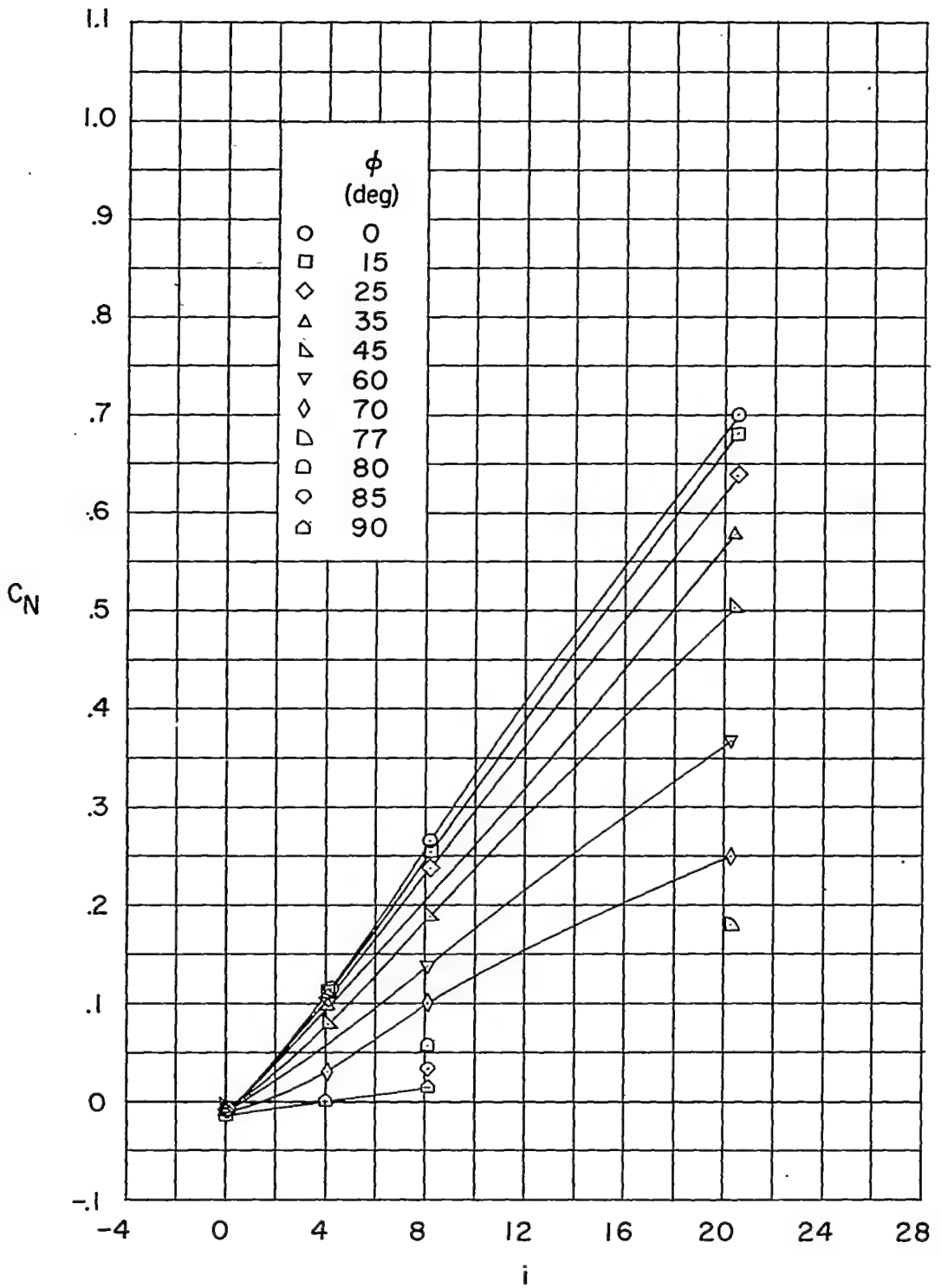

(c) $\delta_H = 8^\circ$.

Figure 8.- Continued.

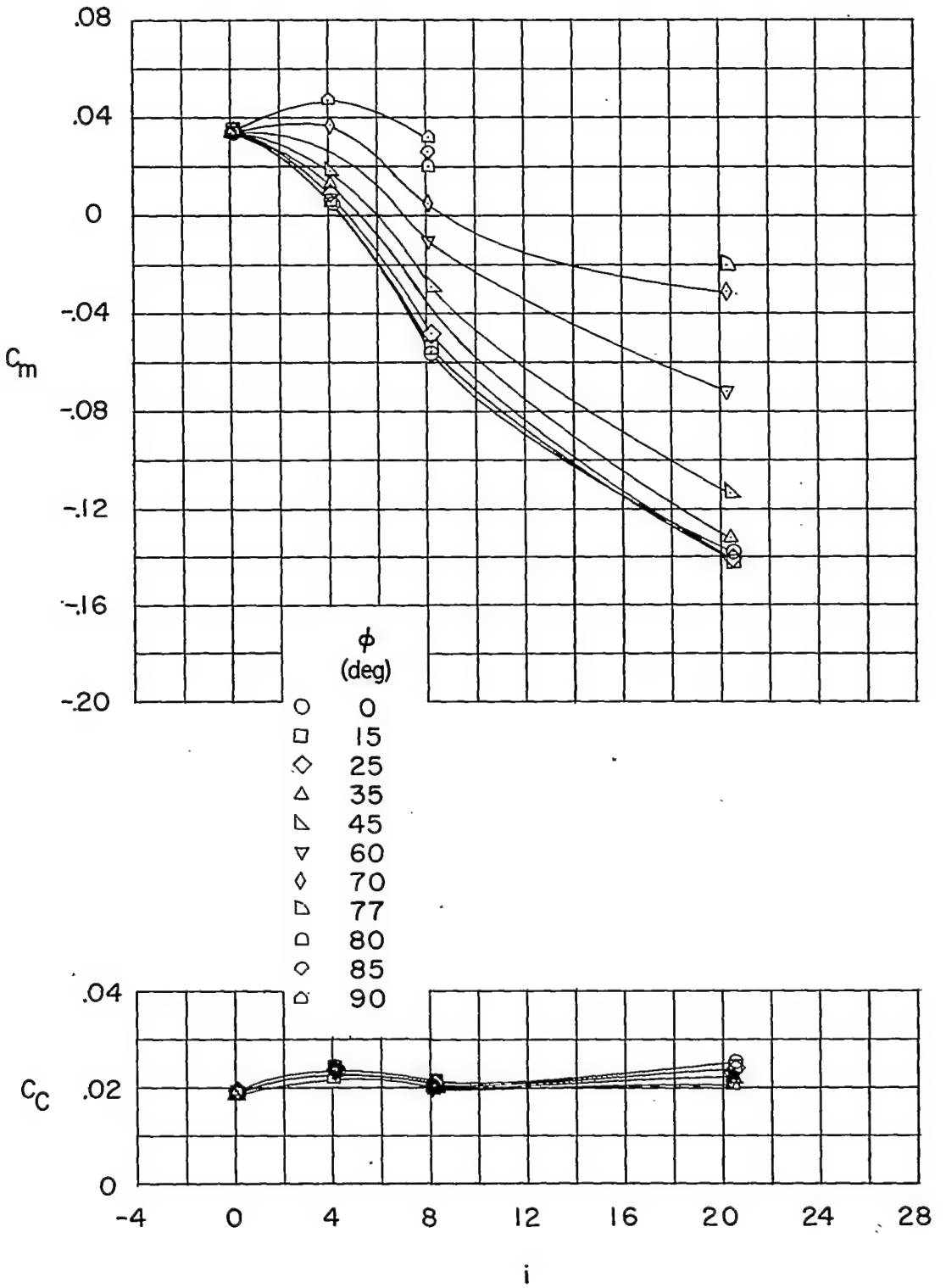

(c) Continued.

Figure 8.- Continued.

[redacted]

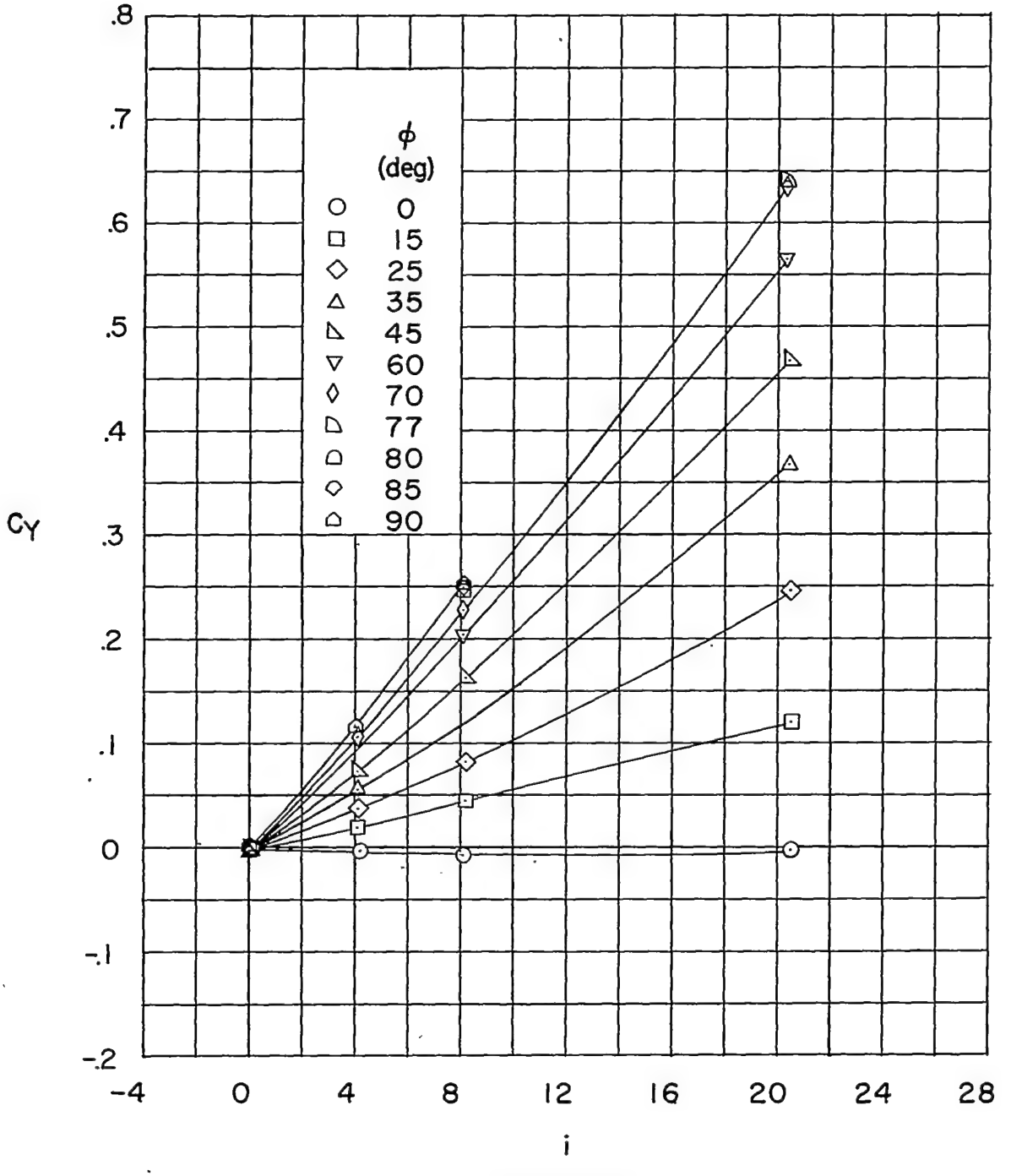

(c) Continued.

Figure 8.- Continued.

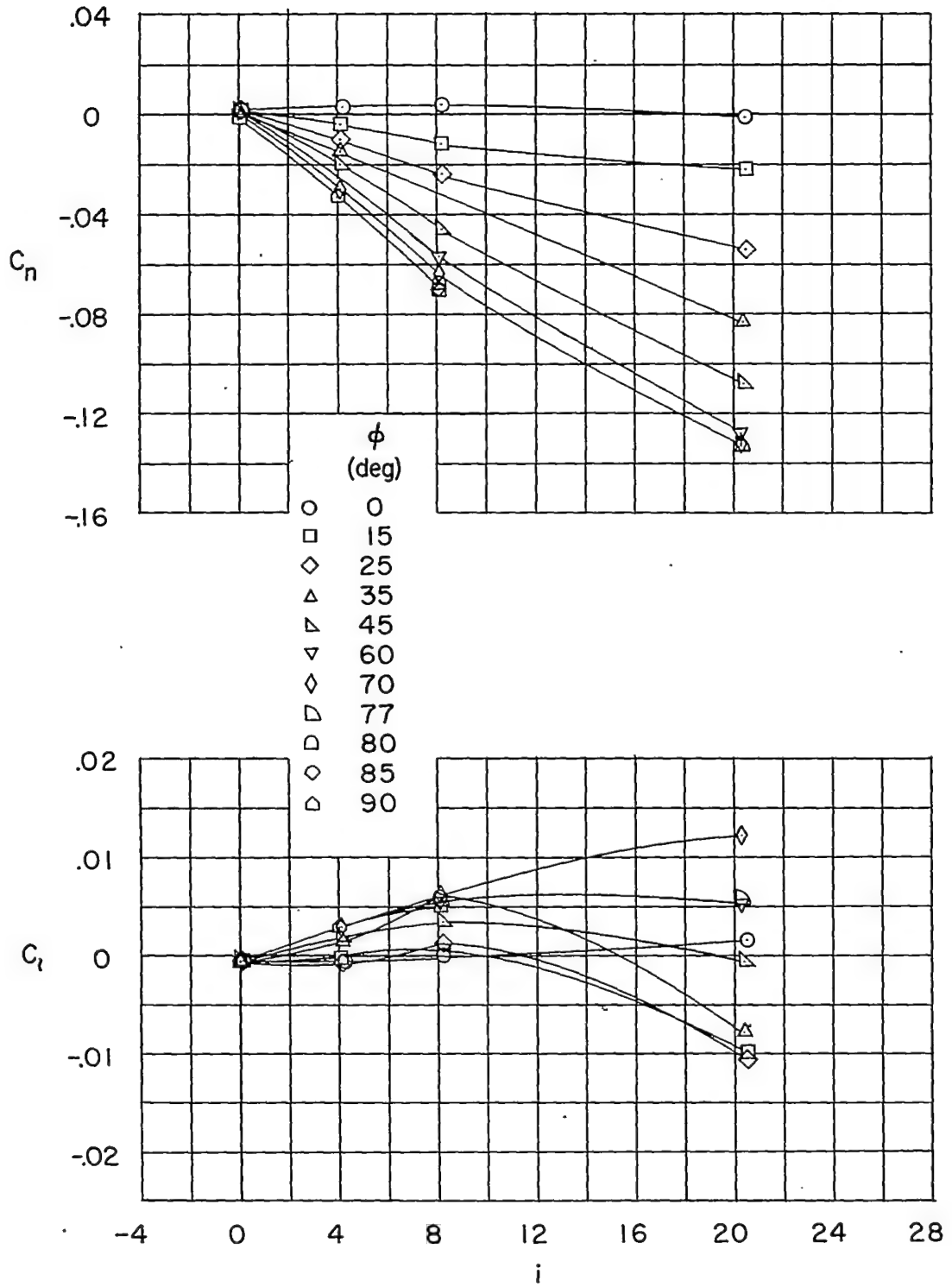

(c) Concluded.

Figure 8.- Continued.

[redacted]

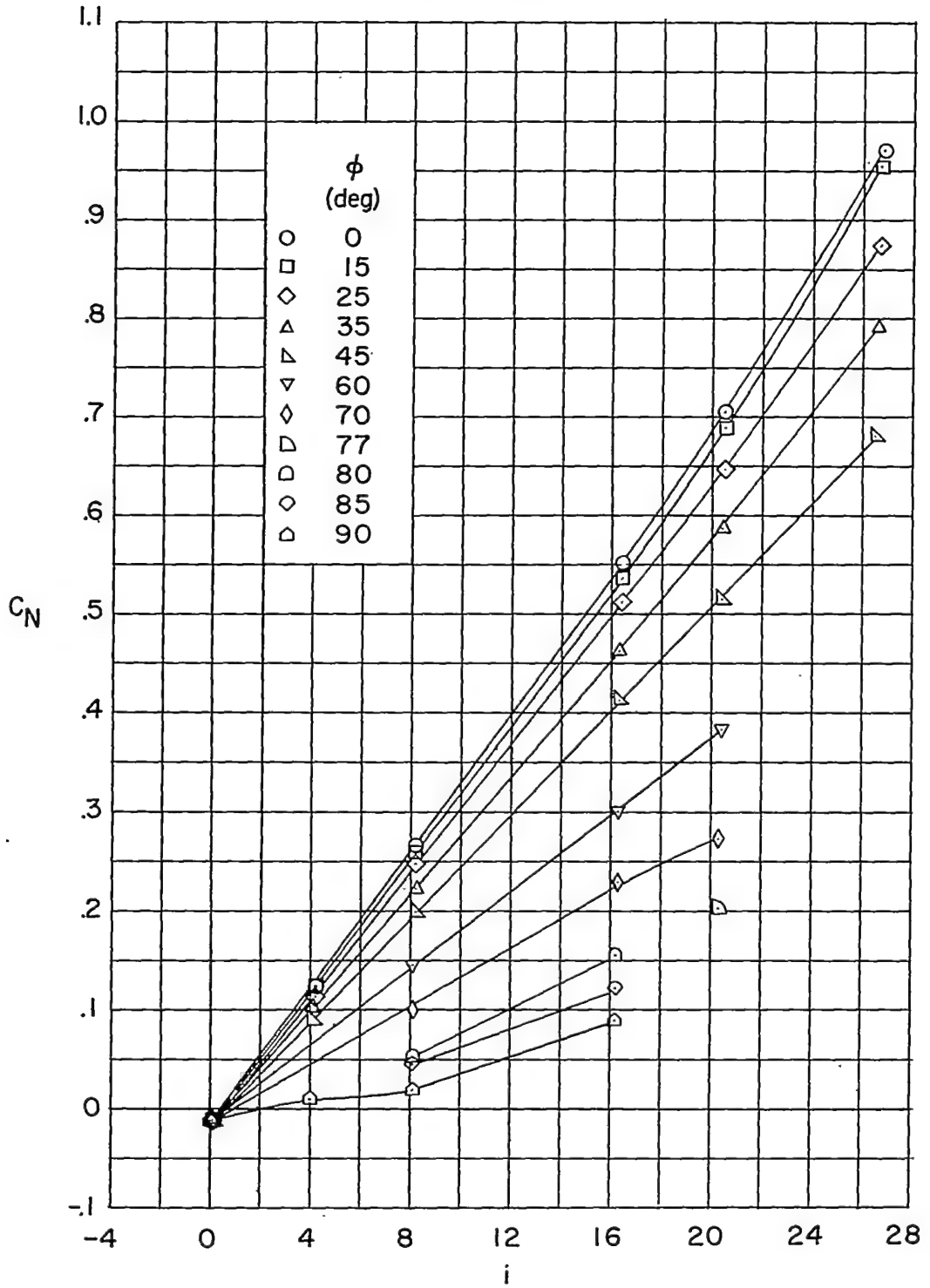

(d) $\delta_H = 12.$

Figure 8.- Continued.

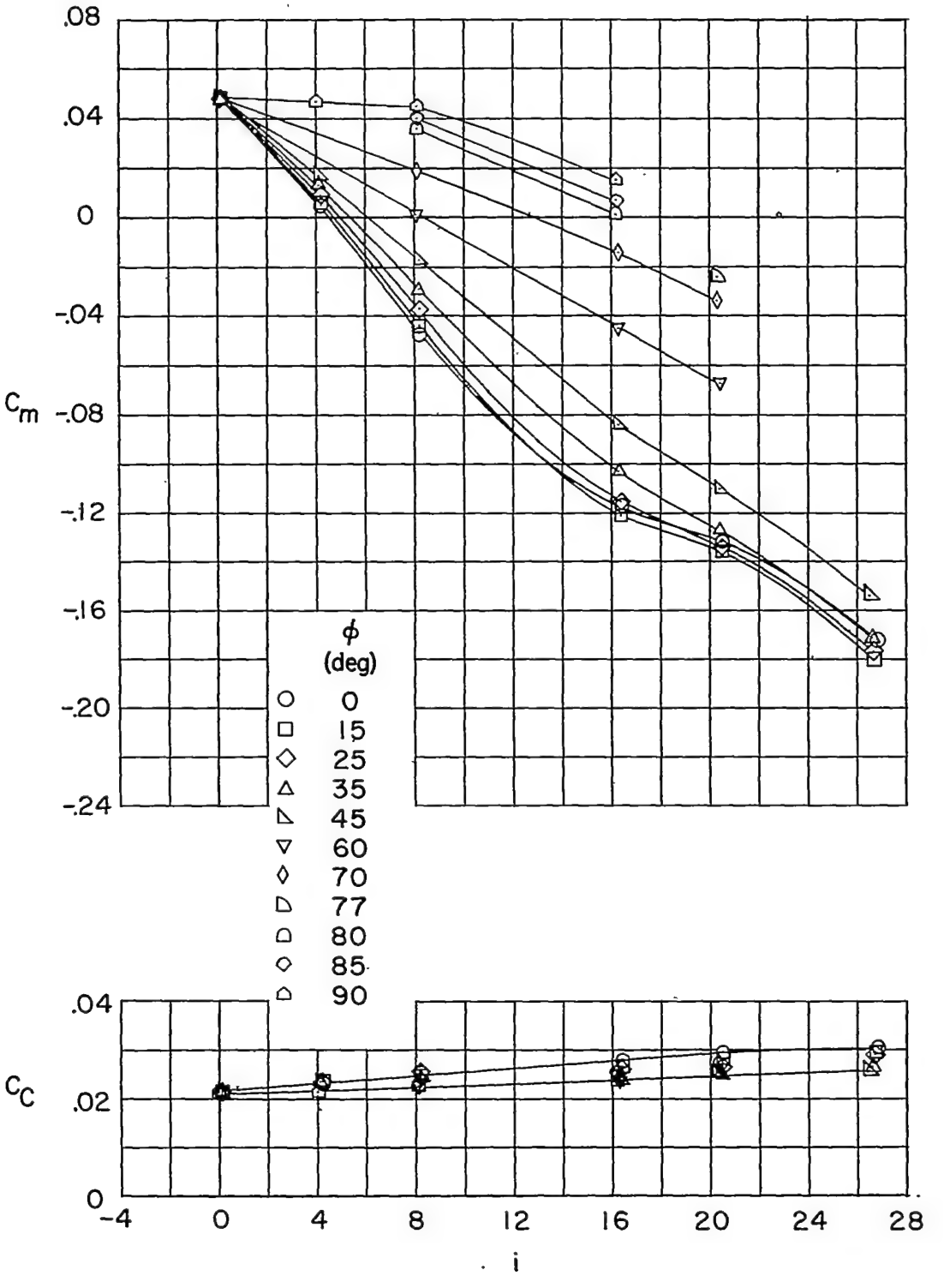

(d) Continued.

Figure 8.- Continued.

[redacted]

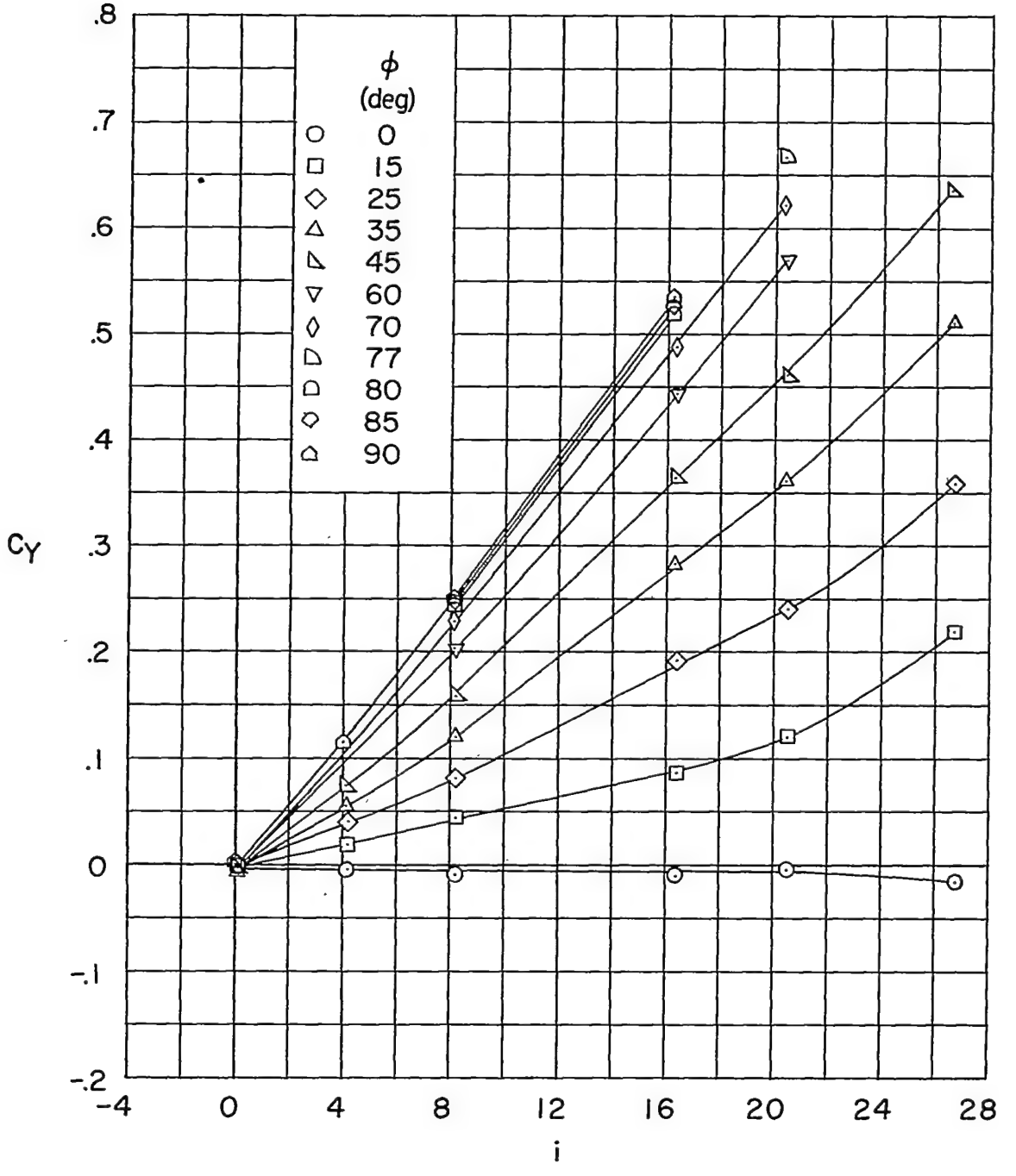

(d) Continued.

Figure 8.- Continued.

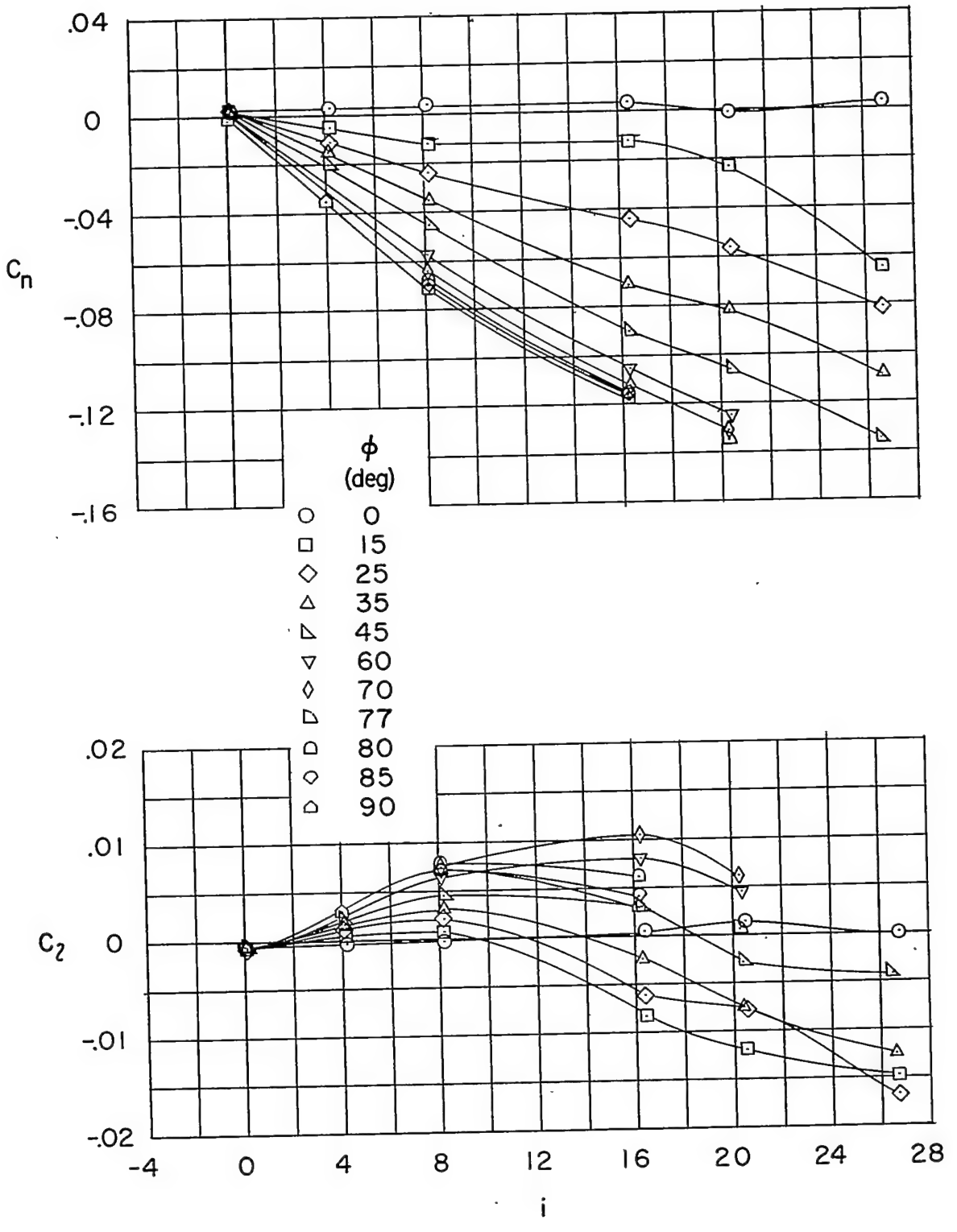

(d) Concluded.

Figure 8.- Continued.

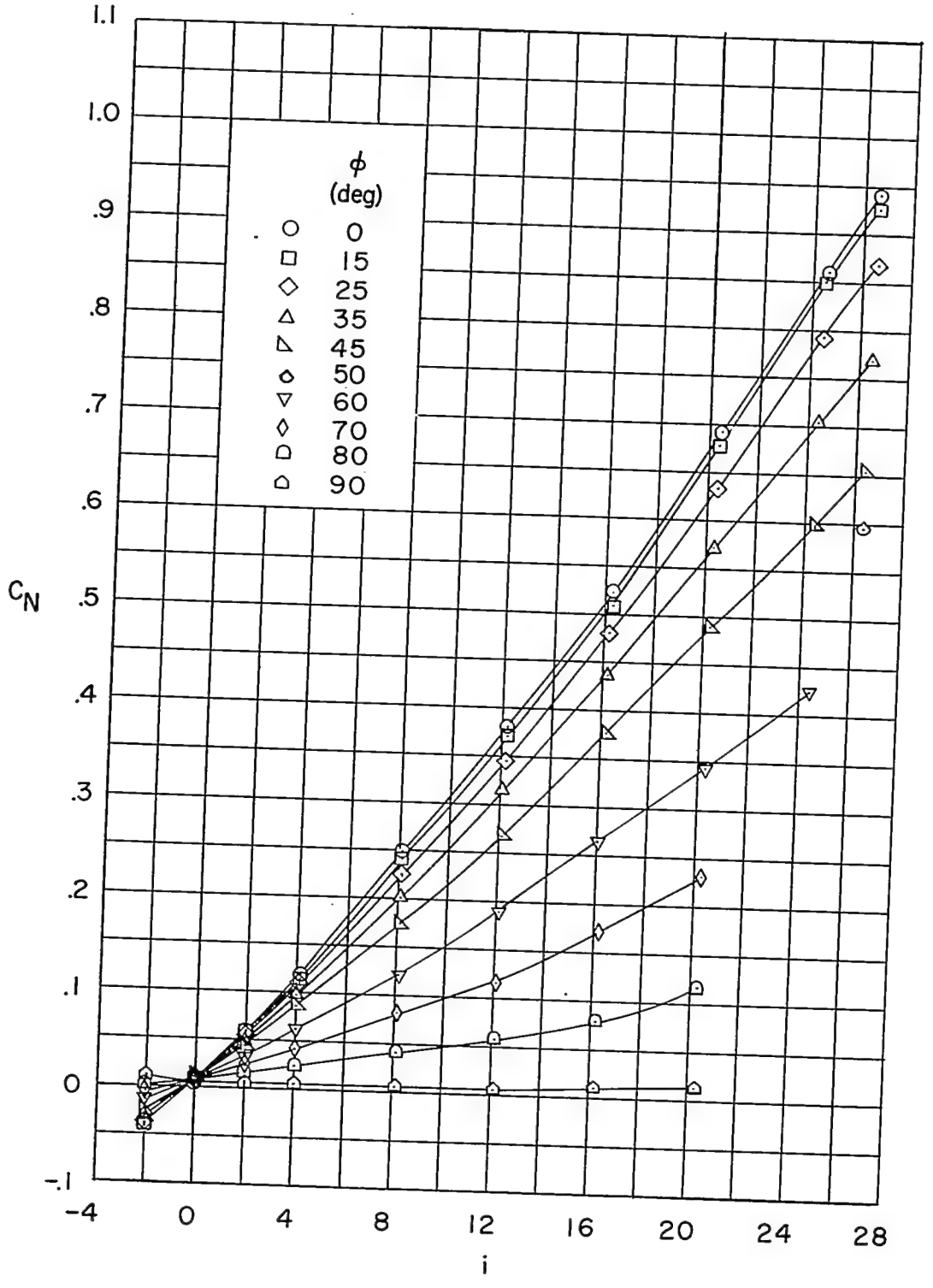

(e) $\delta_a = \pm 10^\circ$.

Figure 8.- Continued.

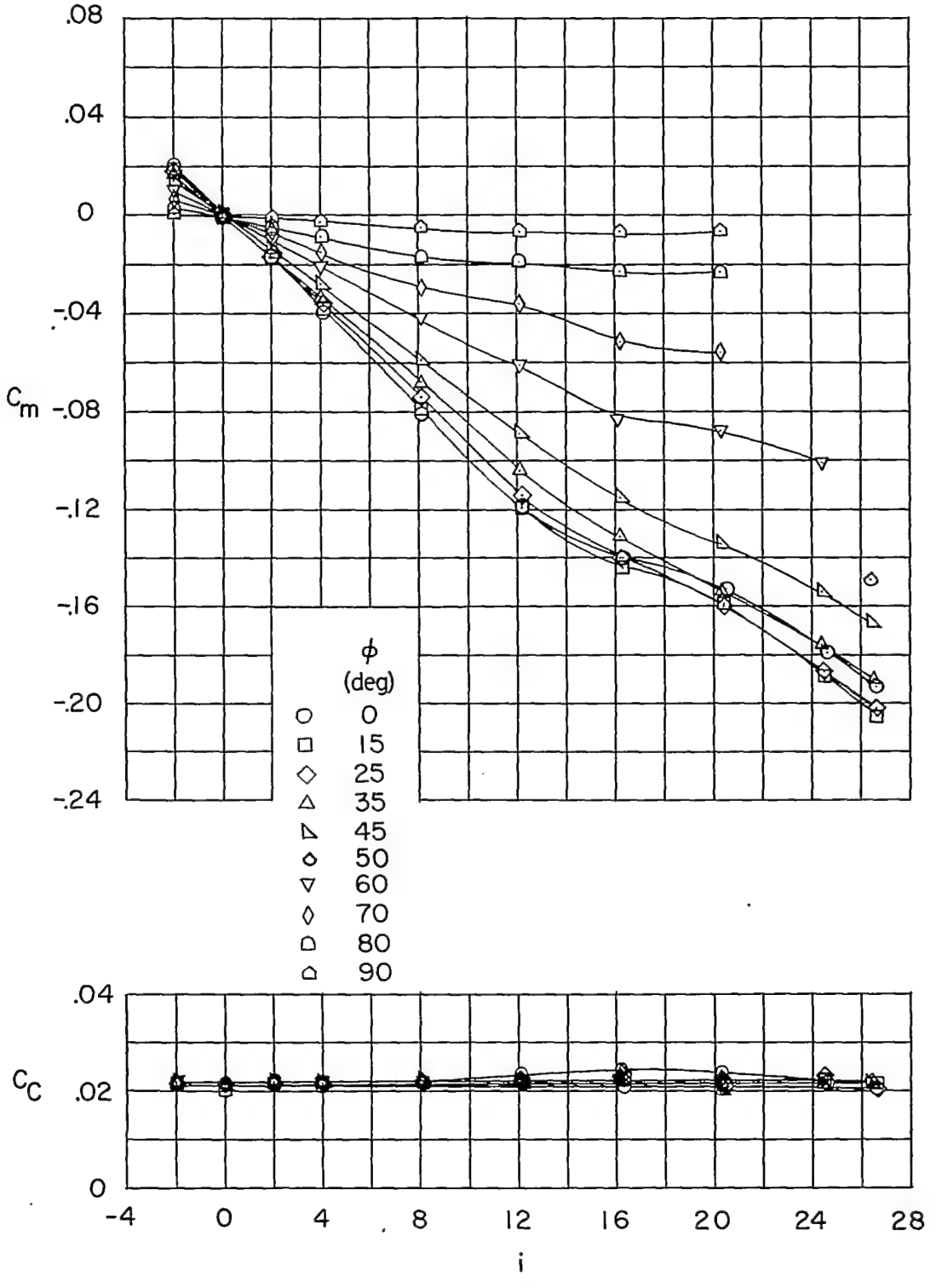

(e) Continued.

Figure 8.- Continued.

[redacted]

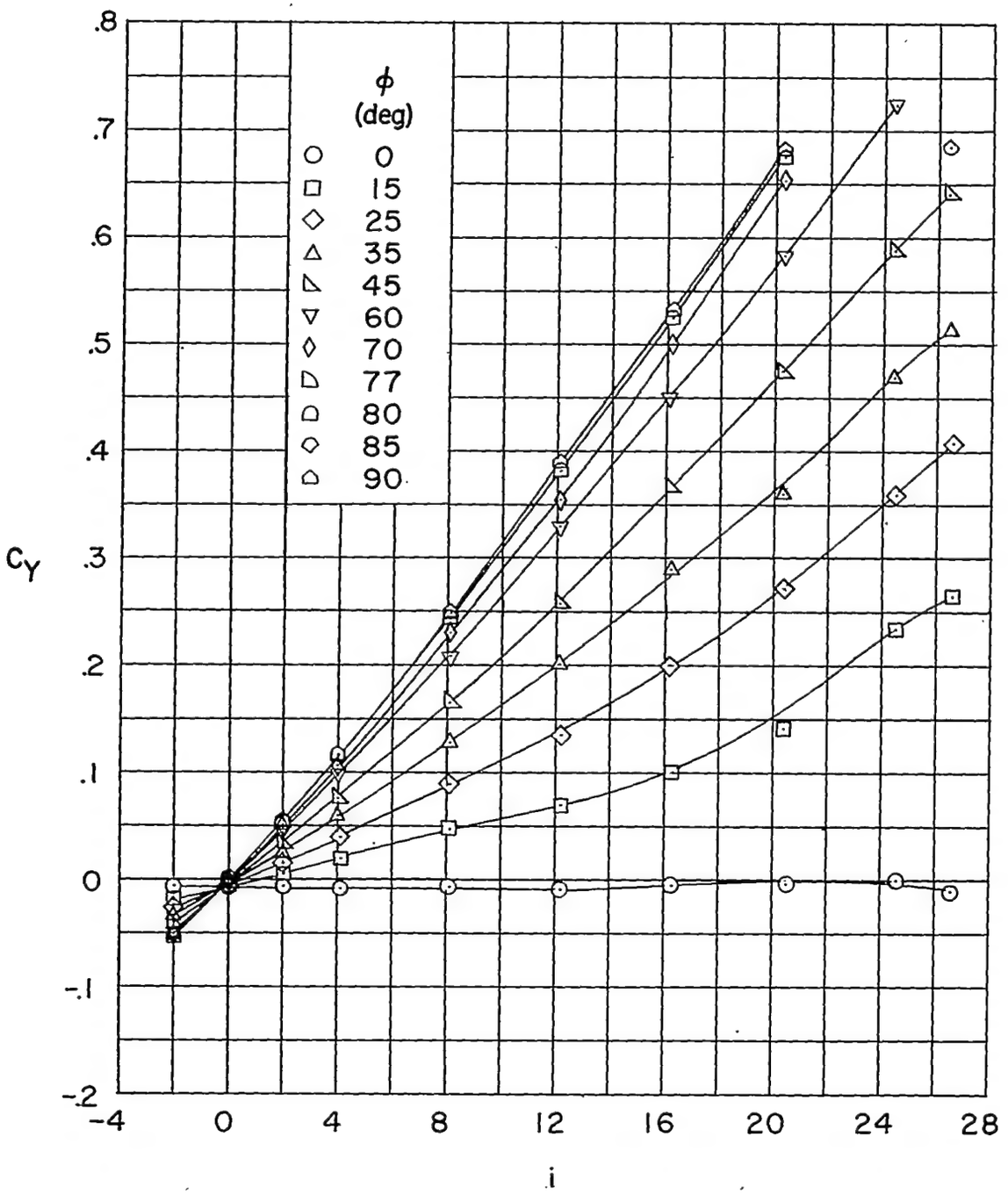

(e) Continued.

Figure 8.- Continued.

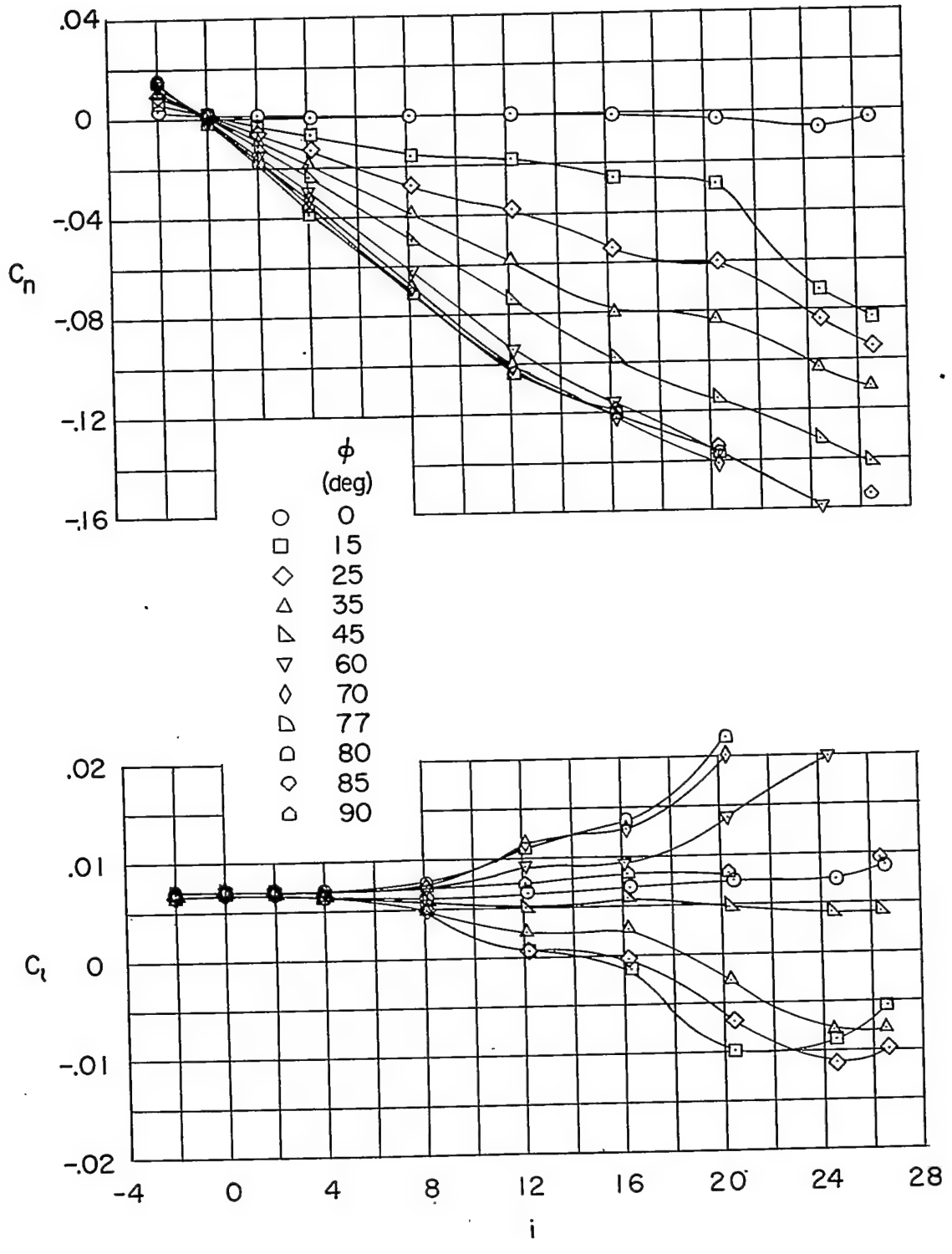

(e) Concluded.

Figure 8.- Concluded.

[redacted]

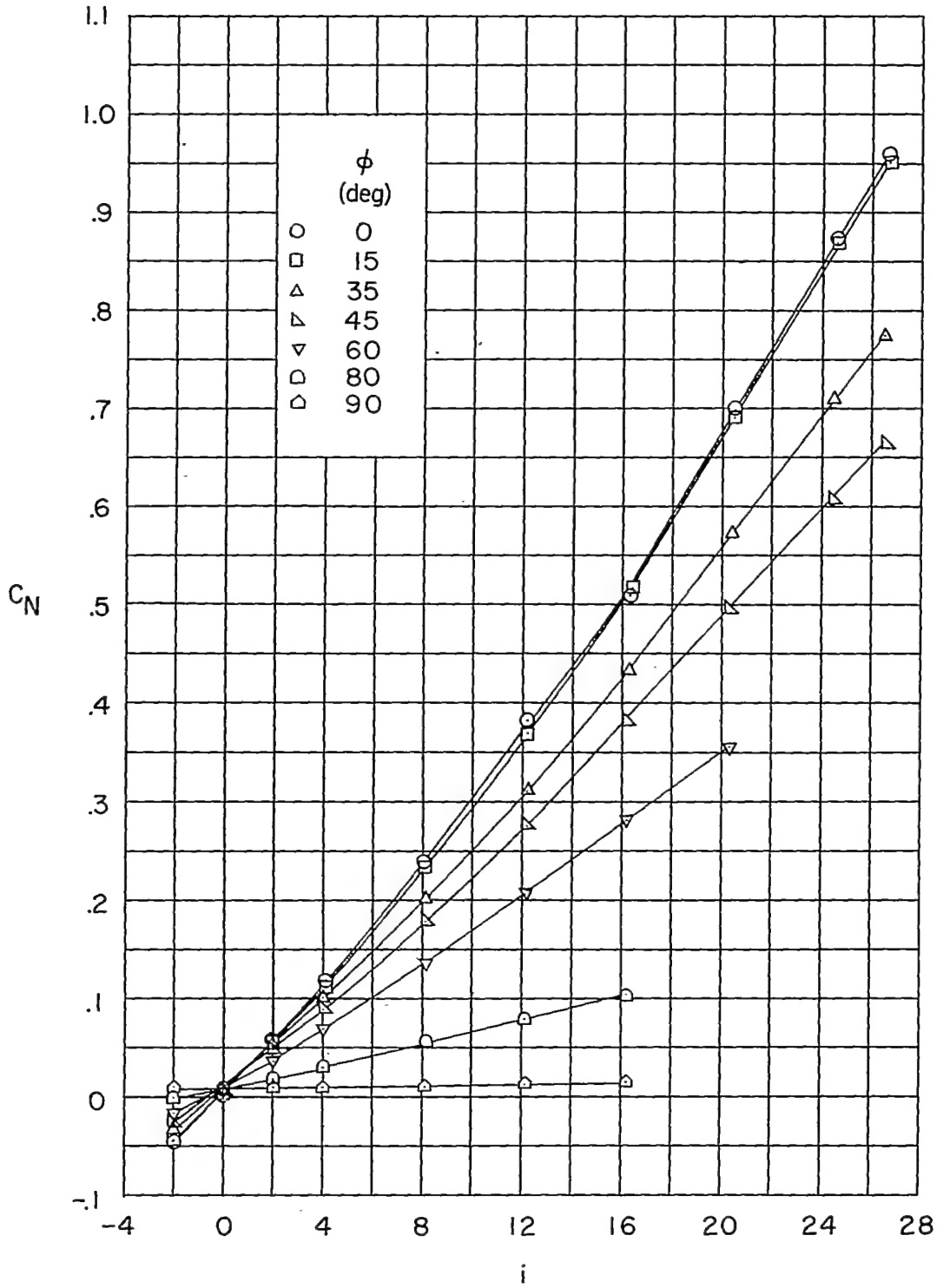

(a) $\delta_H = 0^o$.

Figure 9.- Body-wing-canard. $l/d = 15.7$; indexed wings.

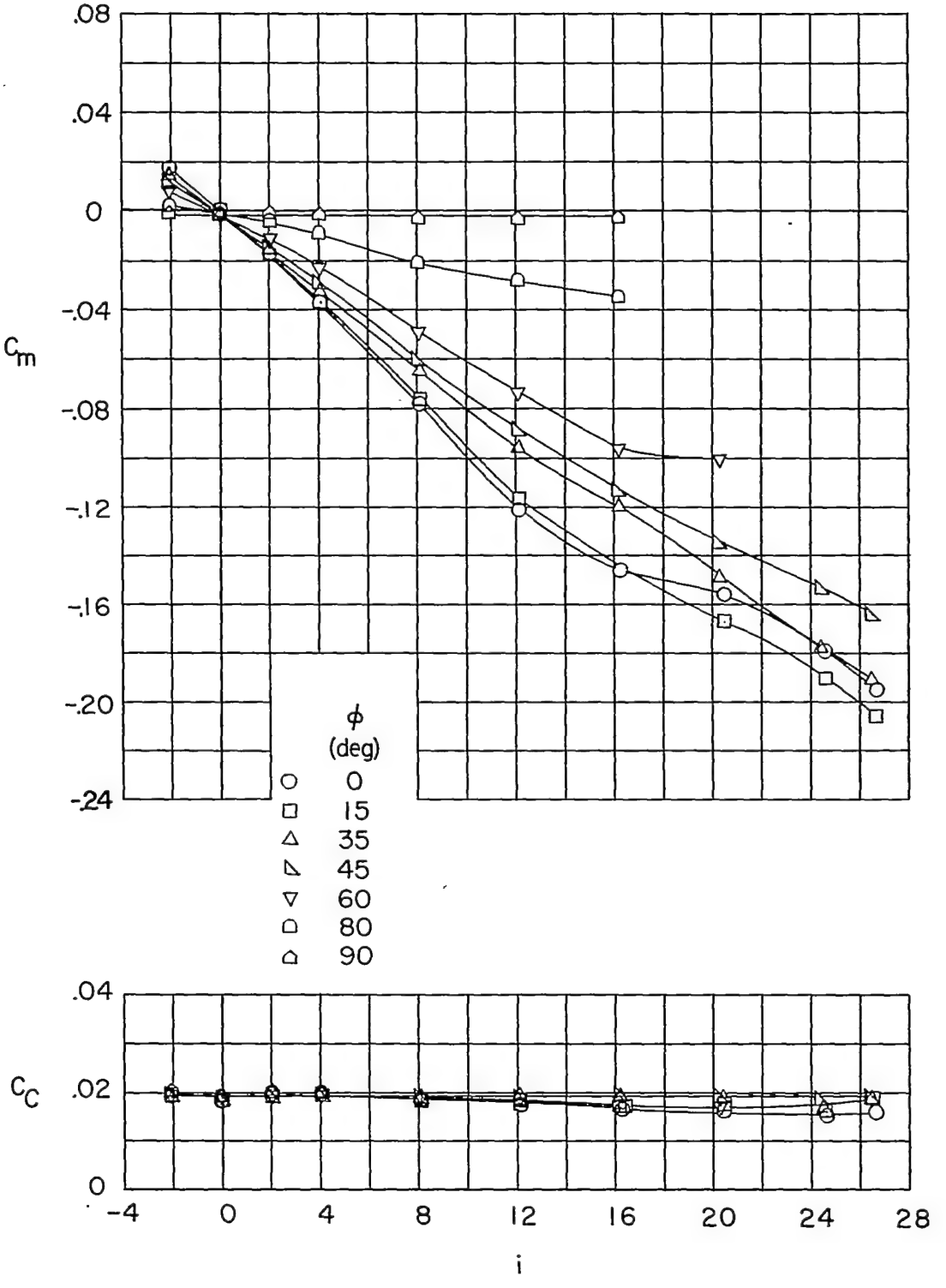

(a) Continued.

Figure 9.- Continued.

[redacted]

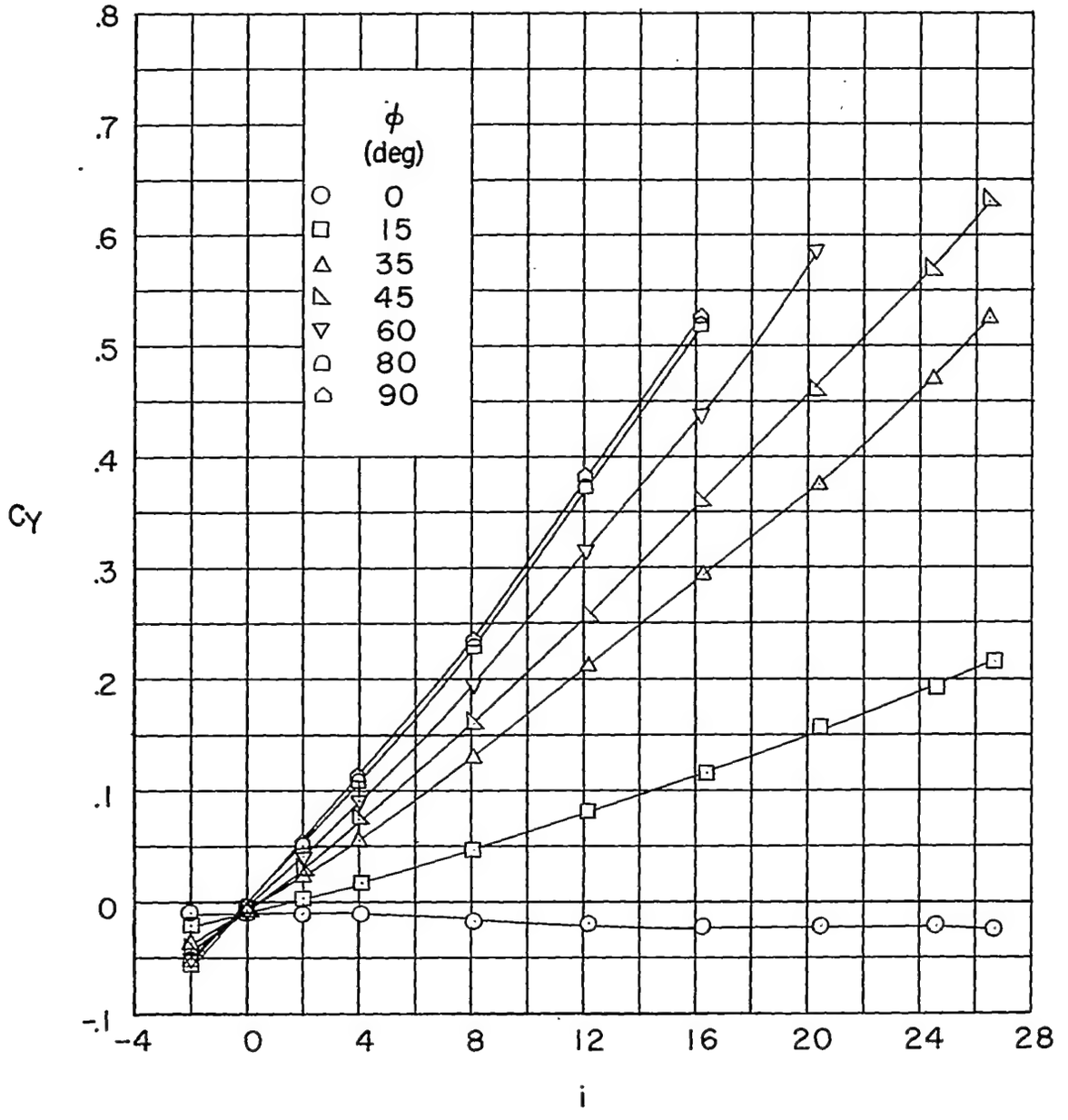

(a) Continued.

Figure 9.- Continued.

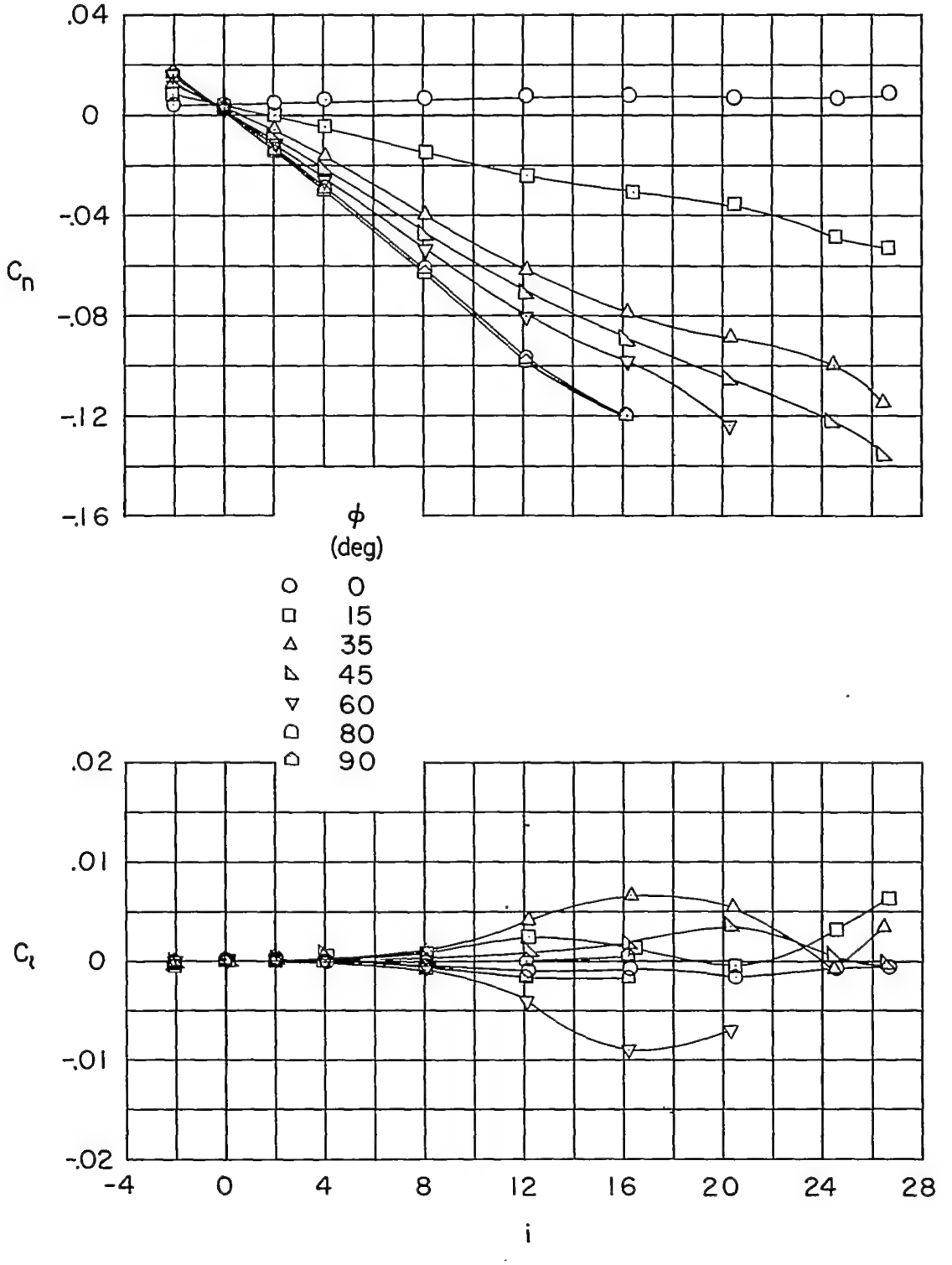

(a) Concluded.

Figure 9.- Continued.

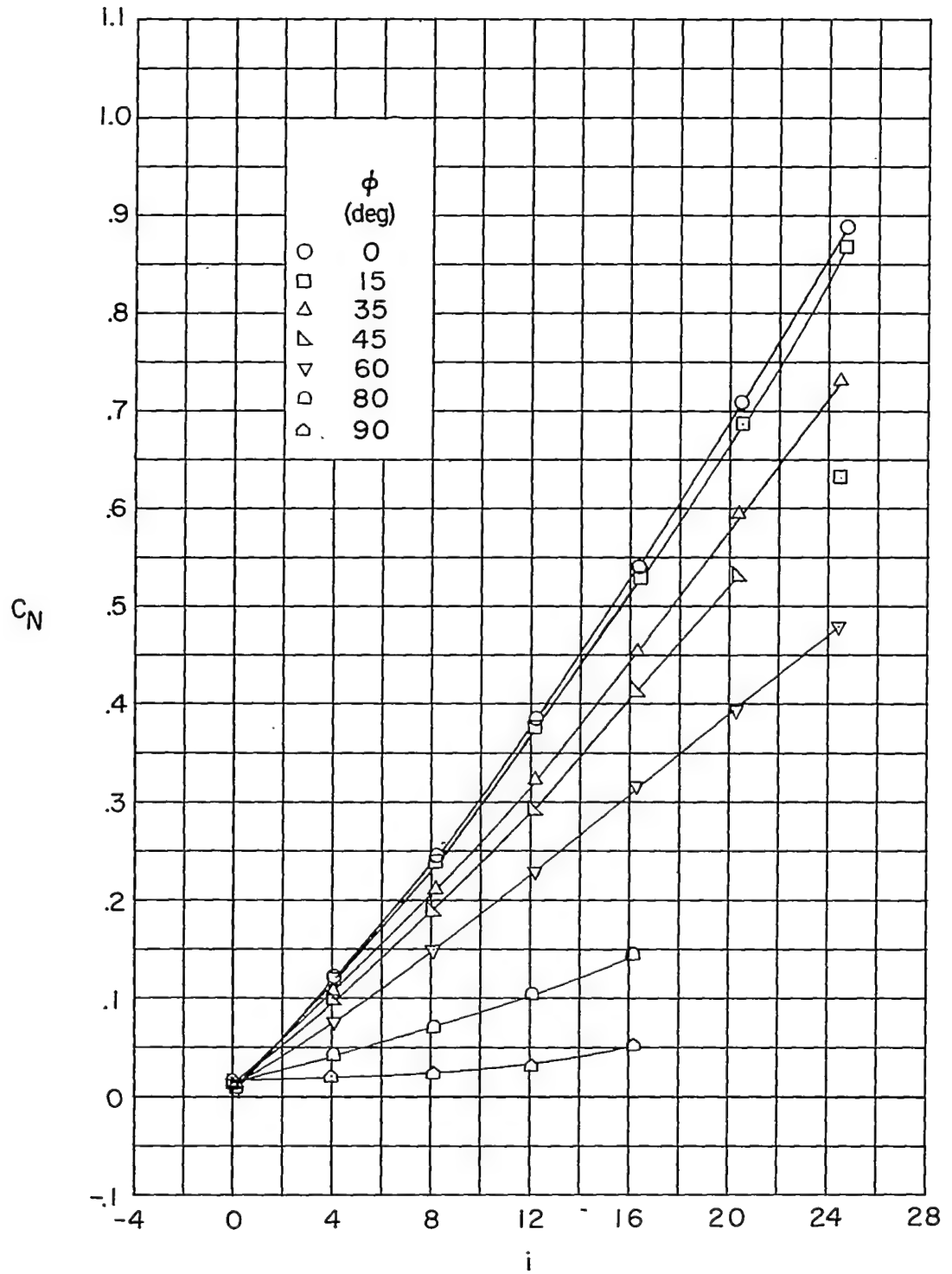

(b) $\delta_H = 8^\circ$.

Figure 9.- Continued.

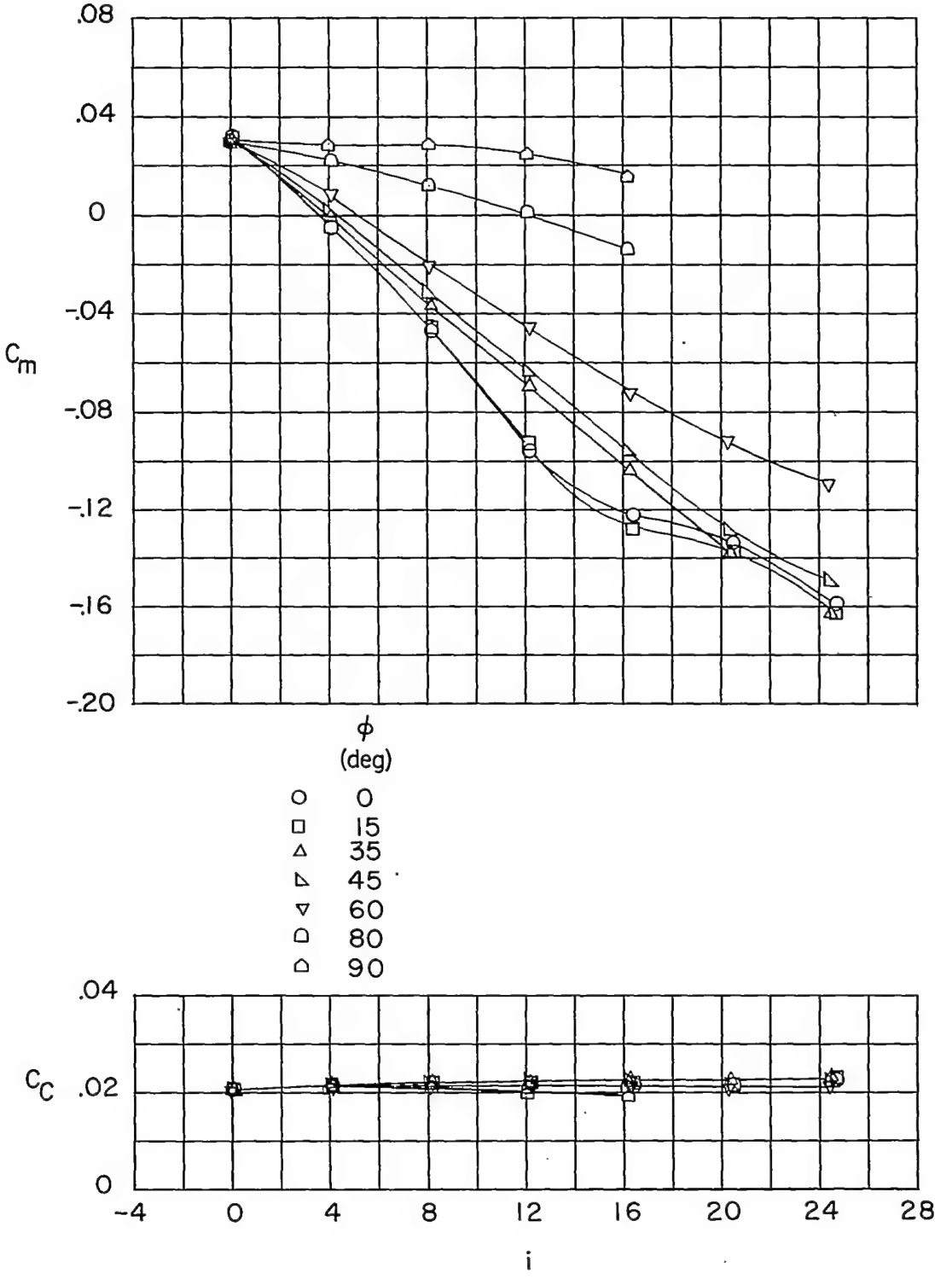

(b) Continued.

Figure 9.- Continued.

[redacted]

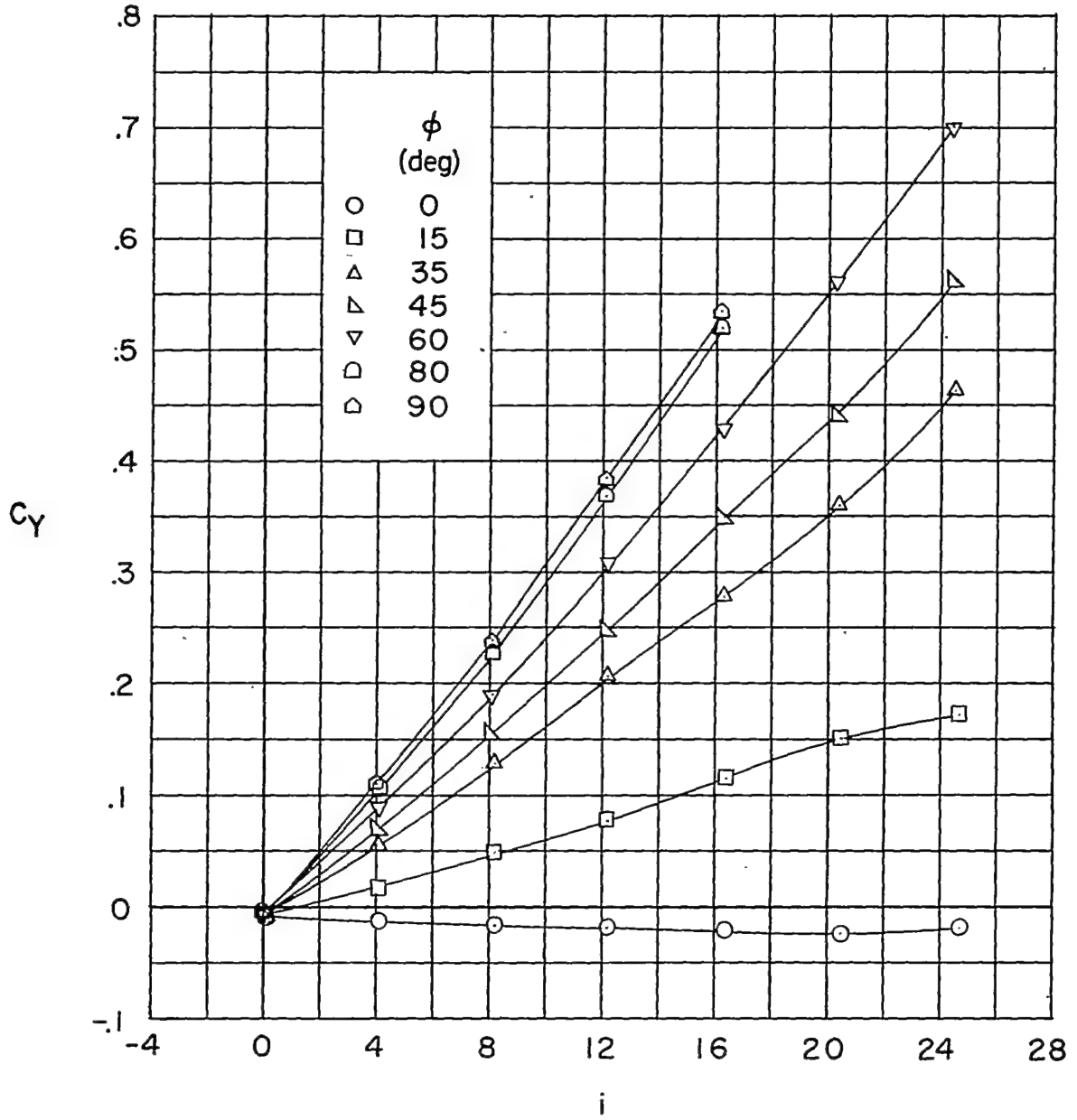

(b) Continued.

Figure 9.- Continued.

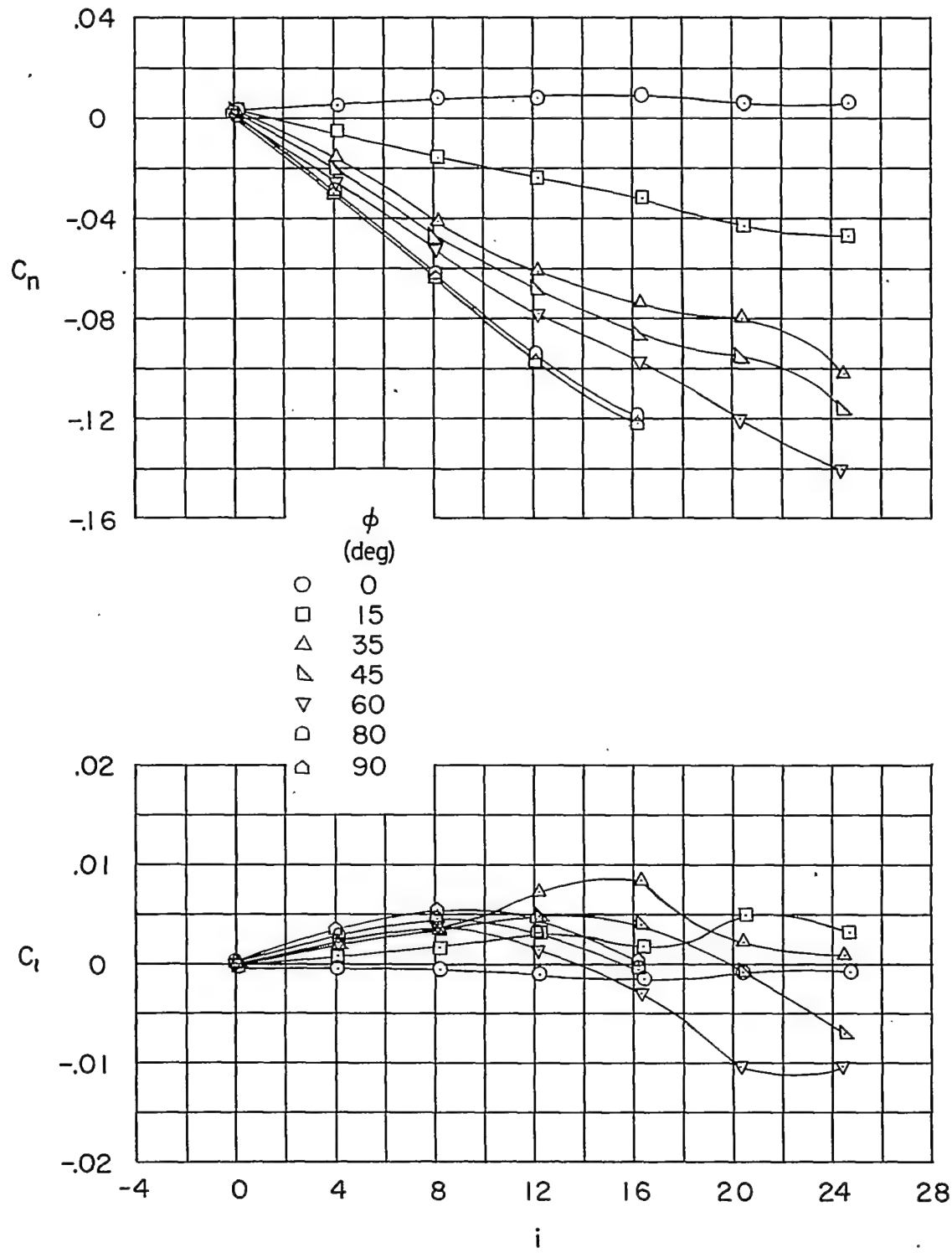

(b) Concluded.

Figure 9.- Continued.

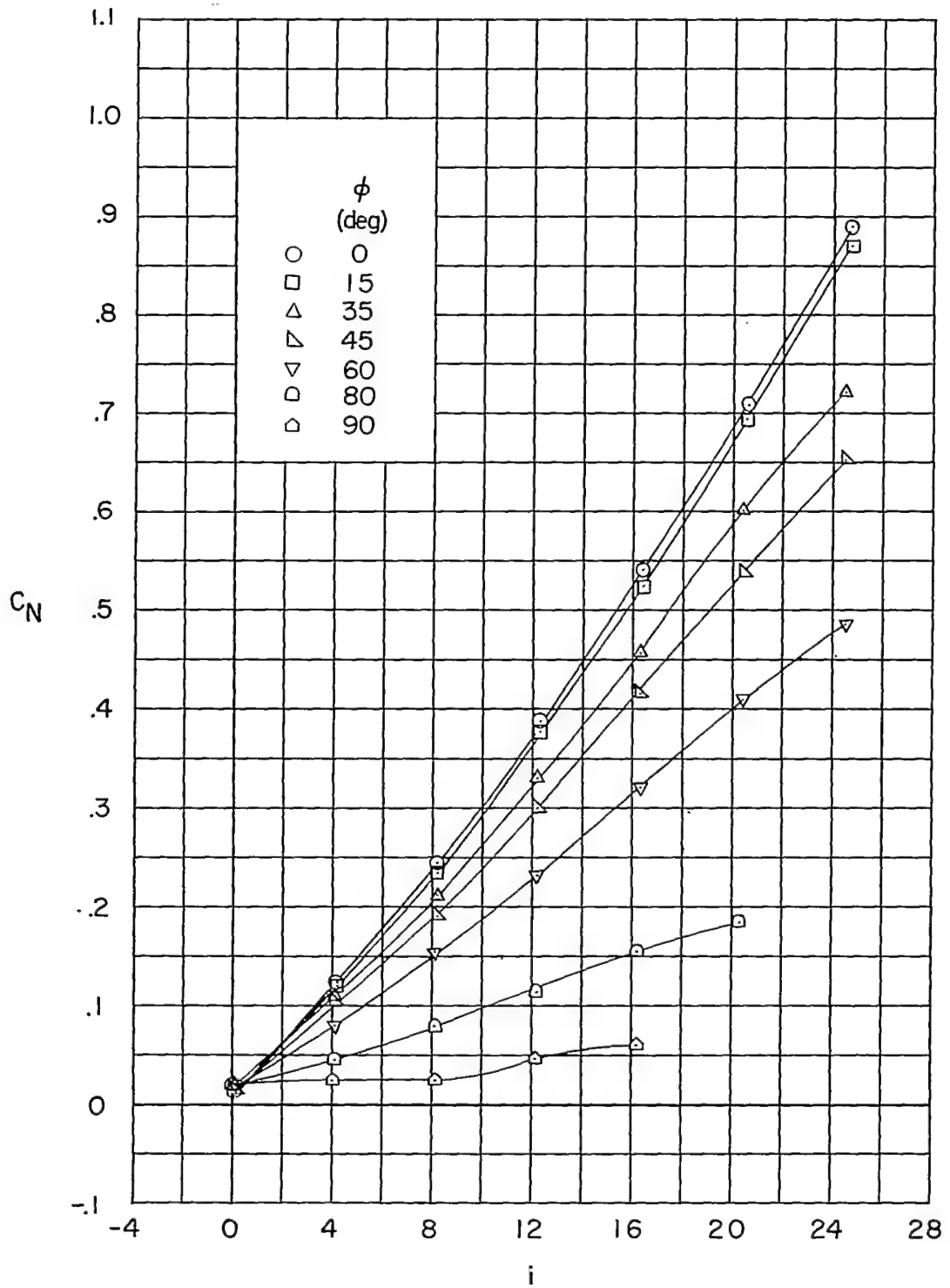

(c) $\delta_H = 12^o$.

Figure 9.- Continued.

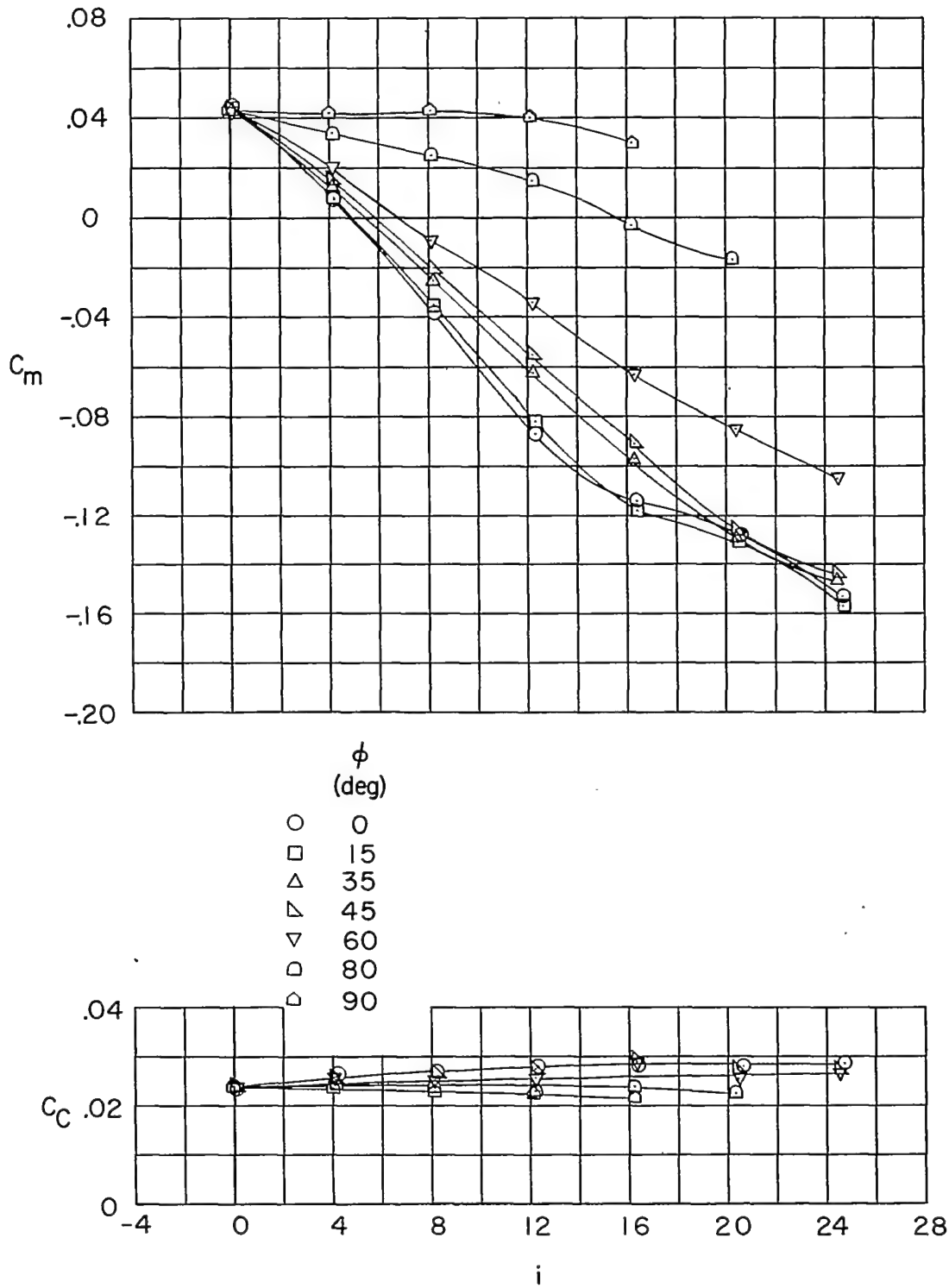

(c) Continued.

Figure 9.- Continued.

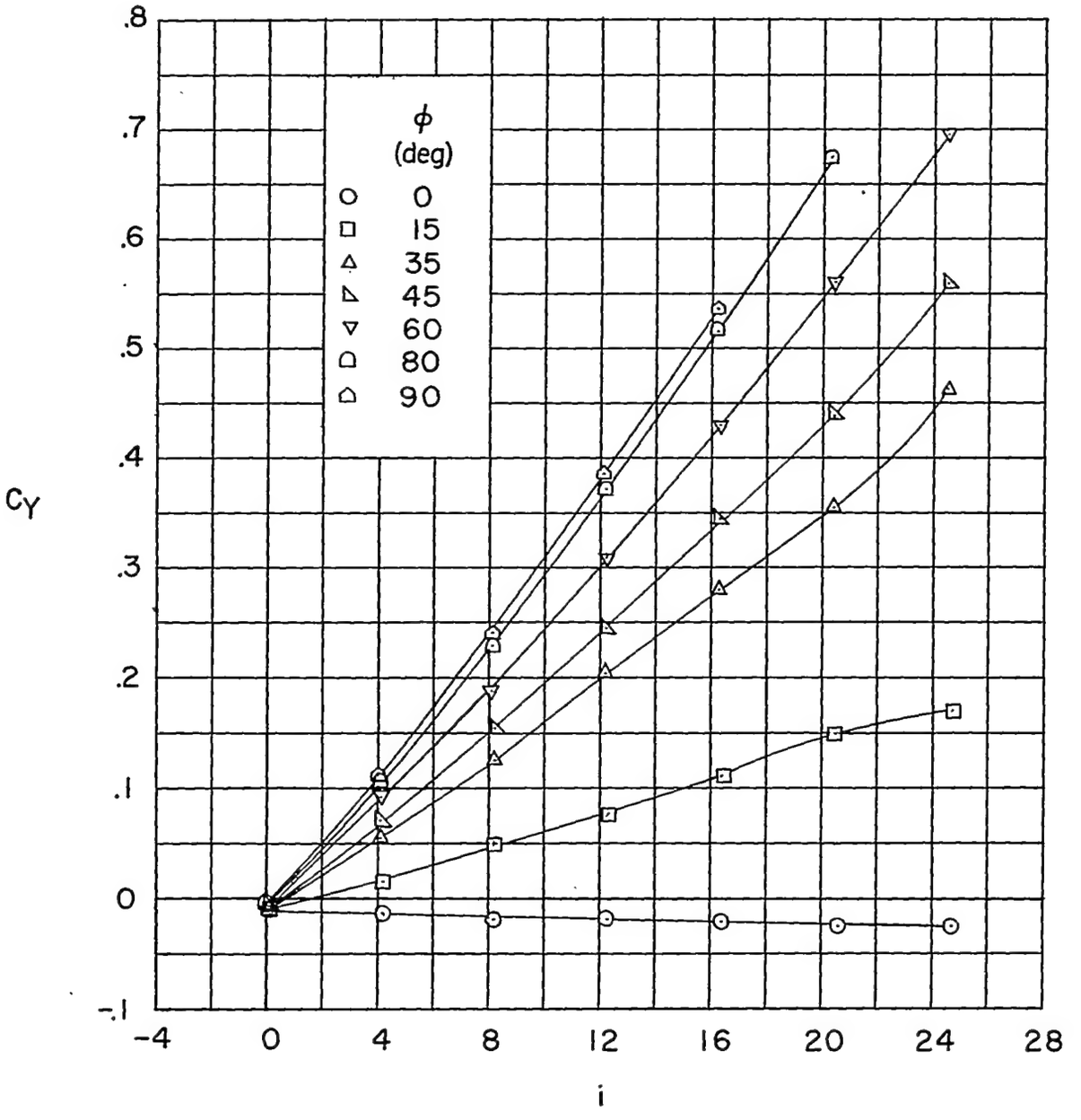

(c) Continued.

Figure 9.- Continued.

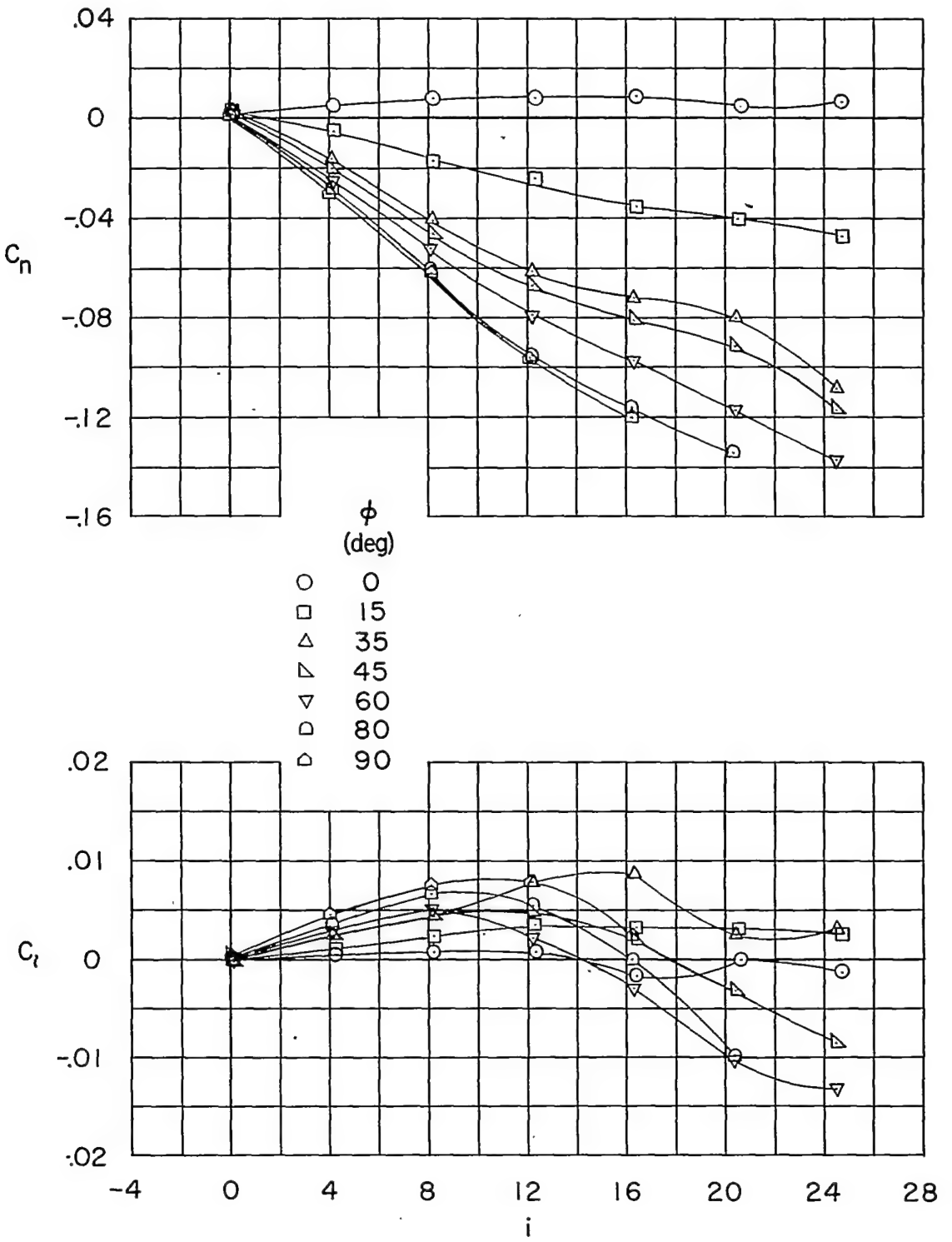

(c) Concluded.

Figure 9.- Concluded.

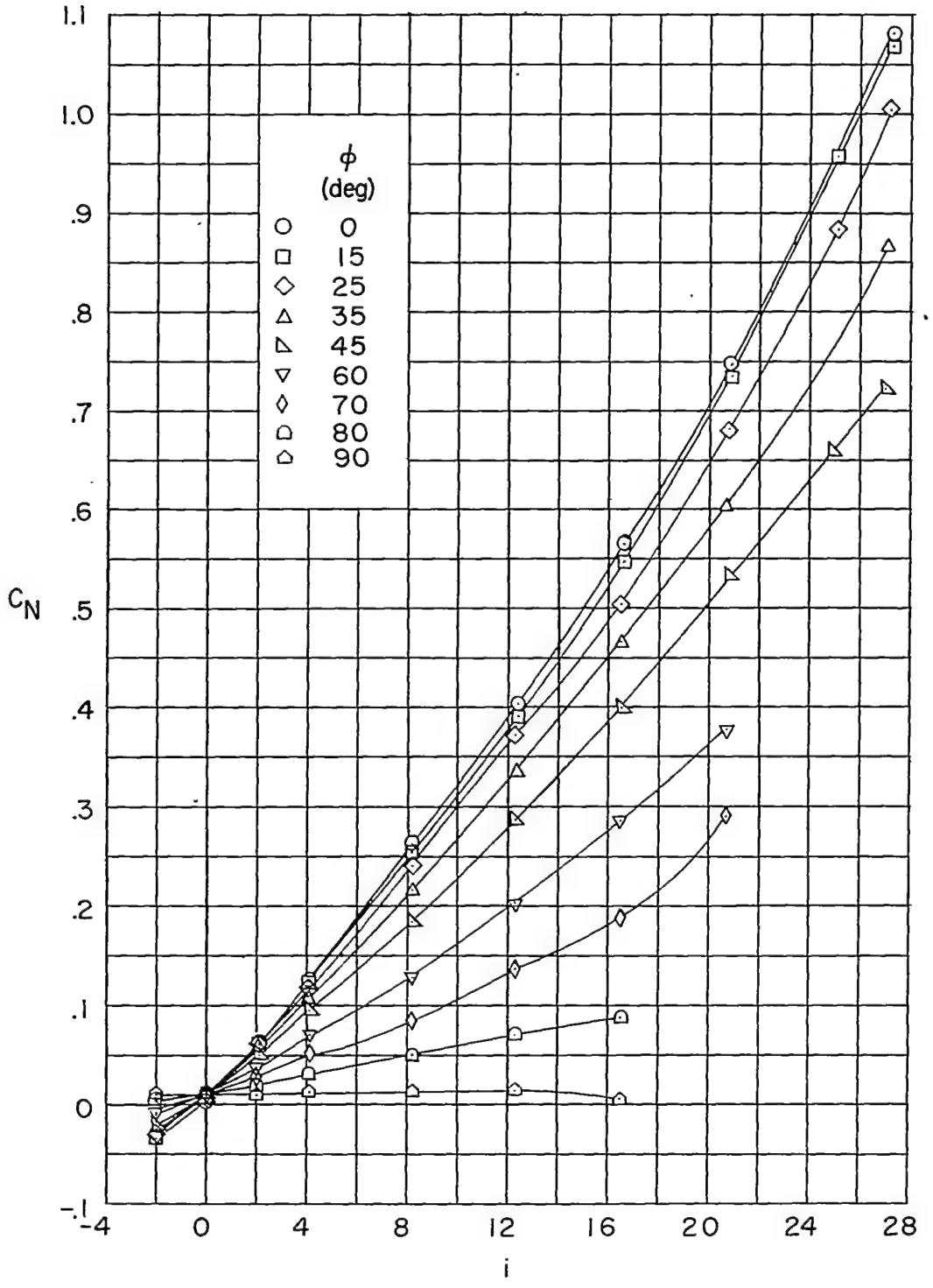

(a) $\delta_H = 0.$

Figure 10.- Body-wing-canard. $l/d = 19.1$; inline wings.

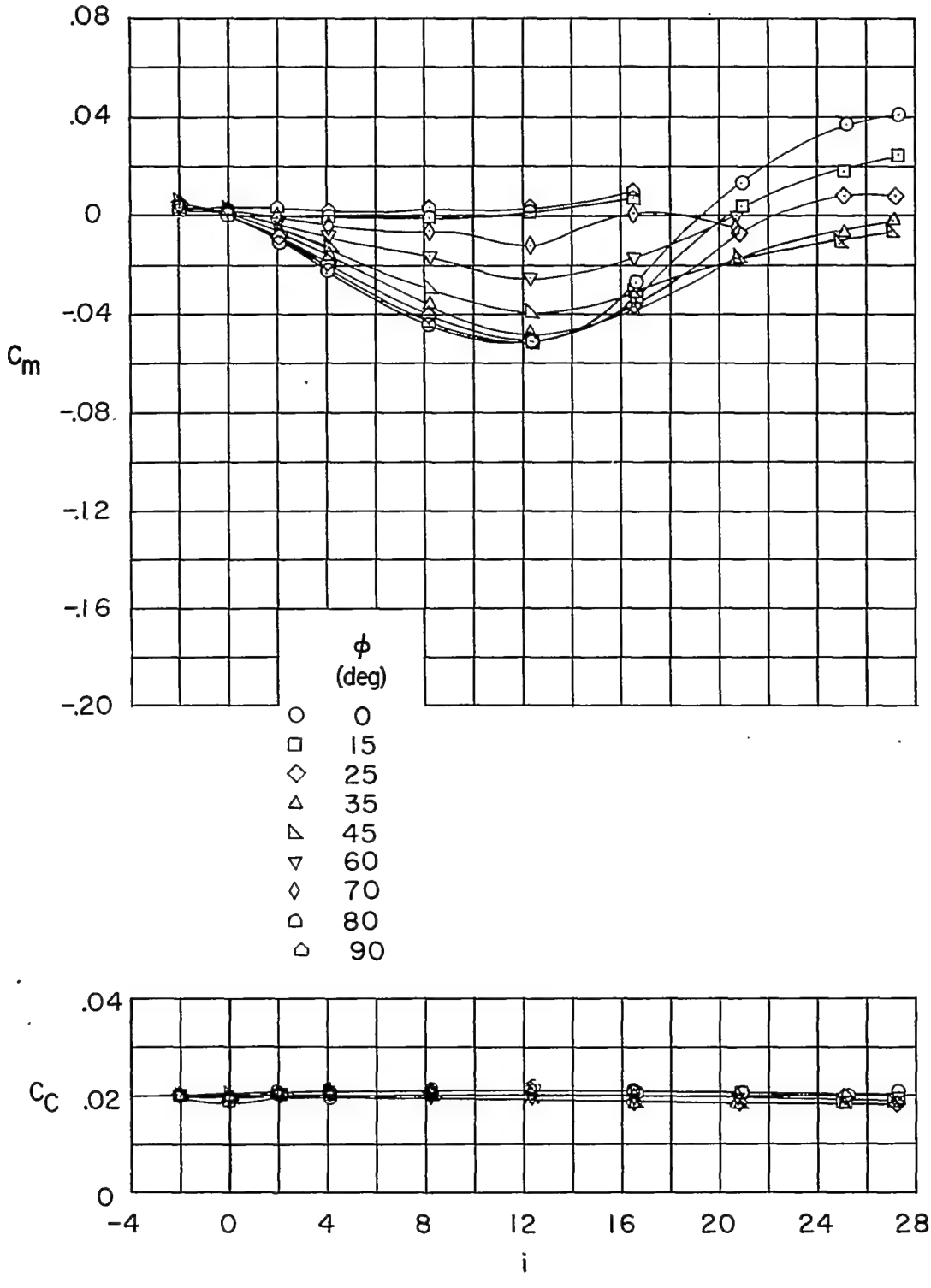

(a) Continued.

Figure 10.- Continued.

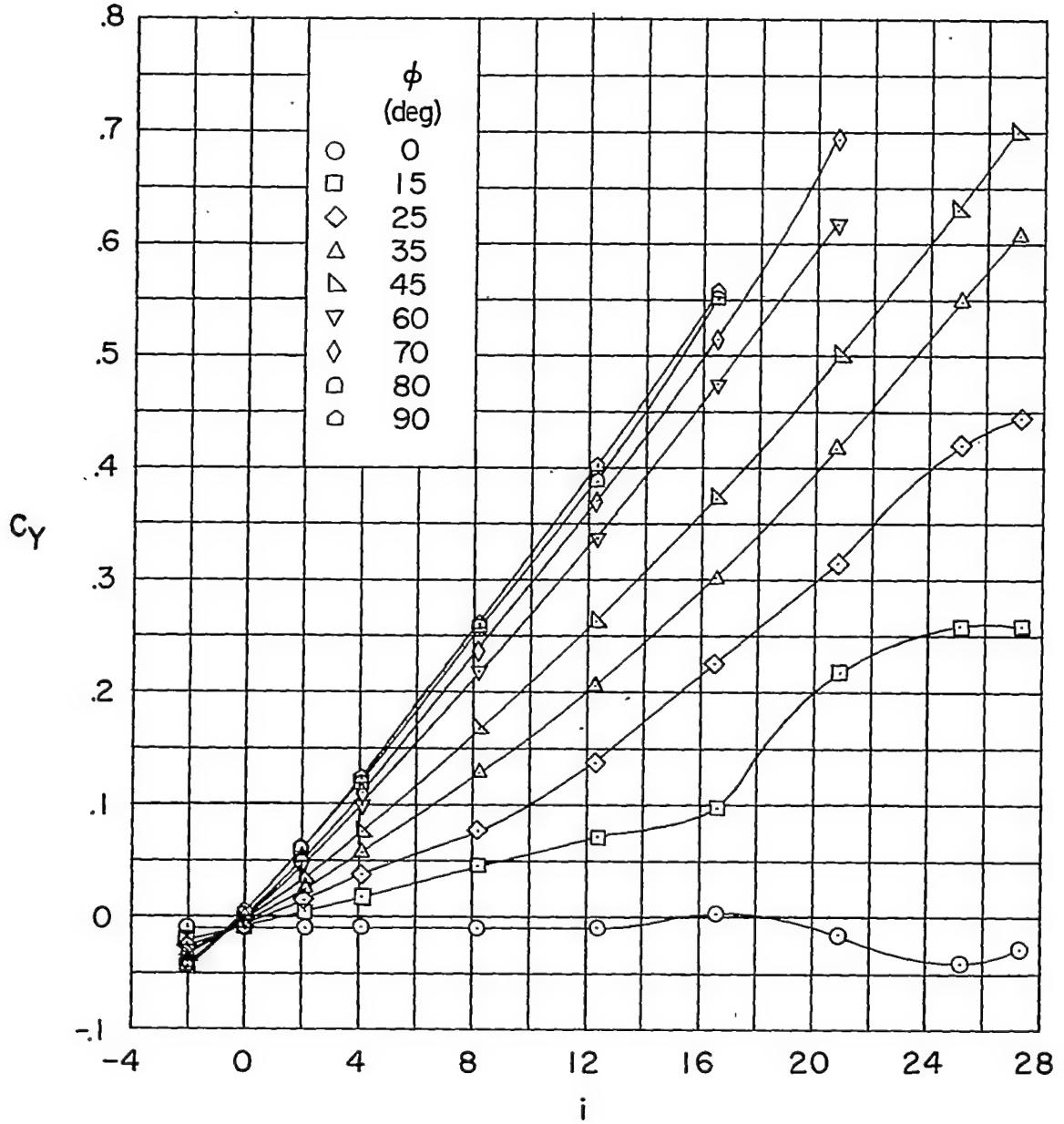

(a) Continued.

Figure 10.- Continued.

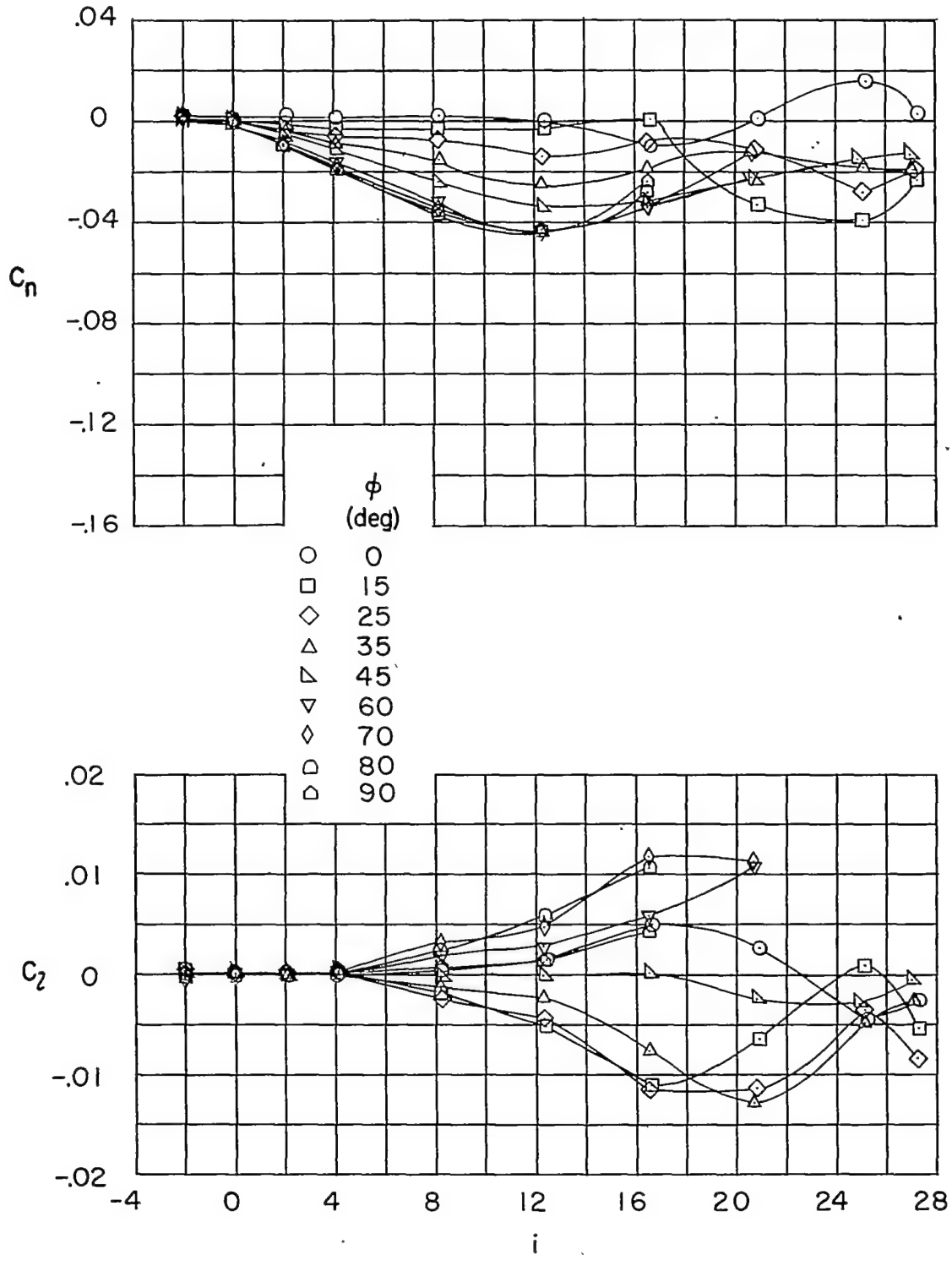

(a) Concluded.

Figure 10.- Continued.

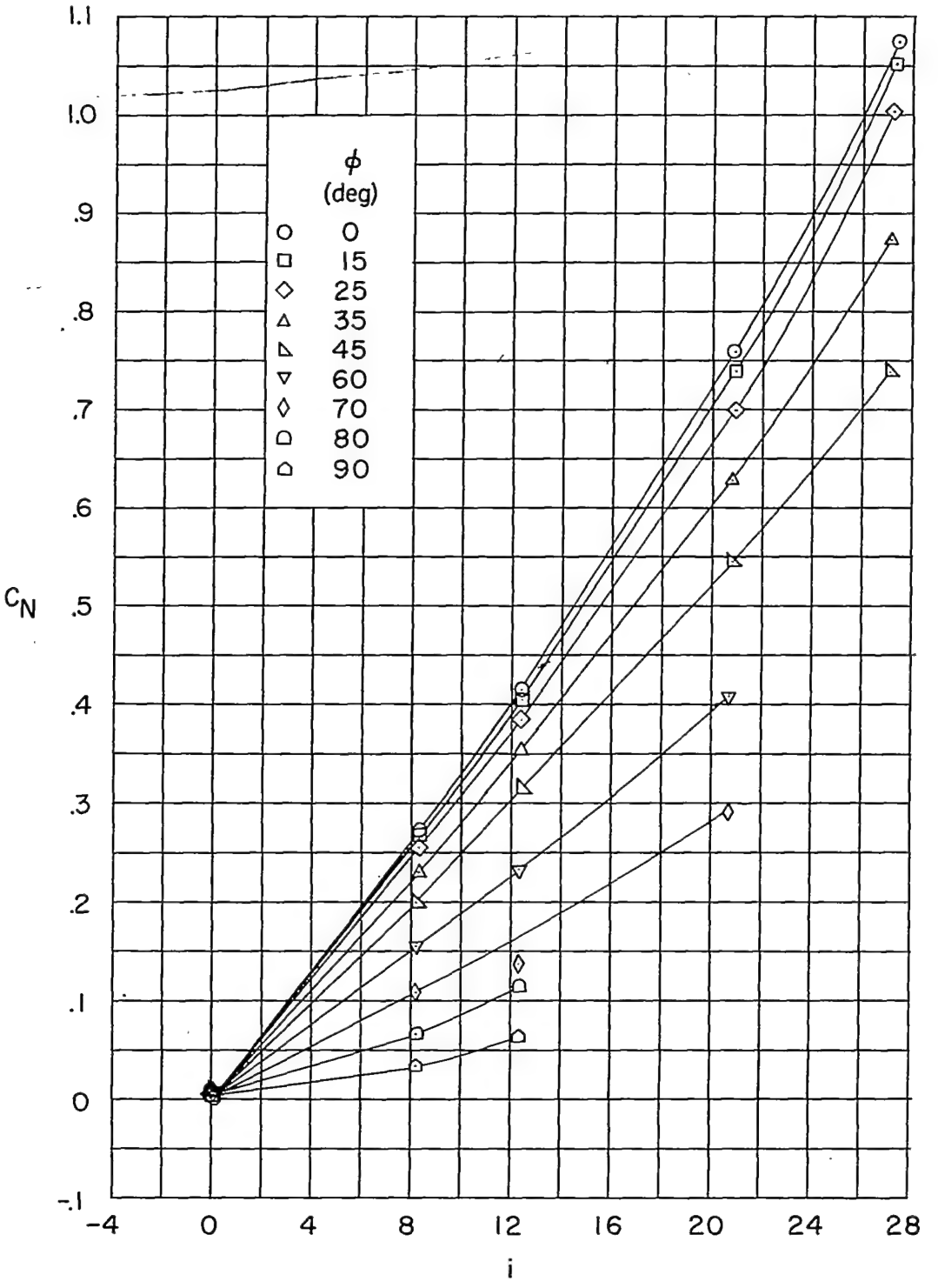

(b) $\delta_H = 8^\circ$.

Figure 10.- Continued.

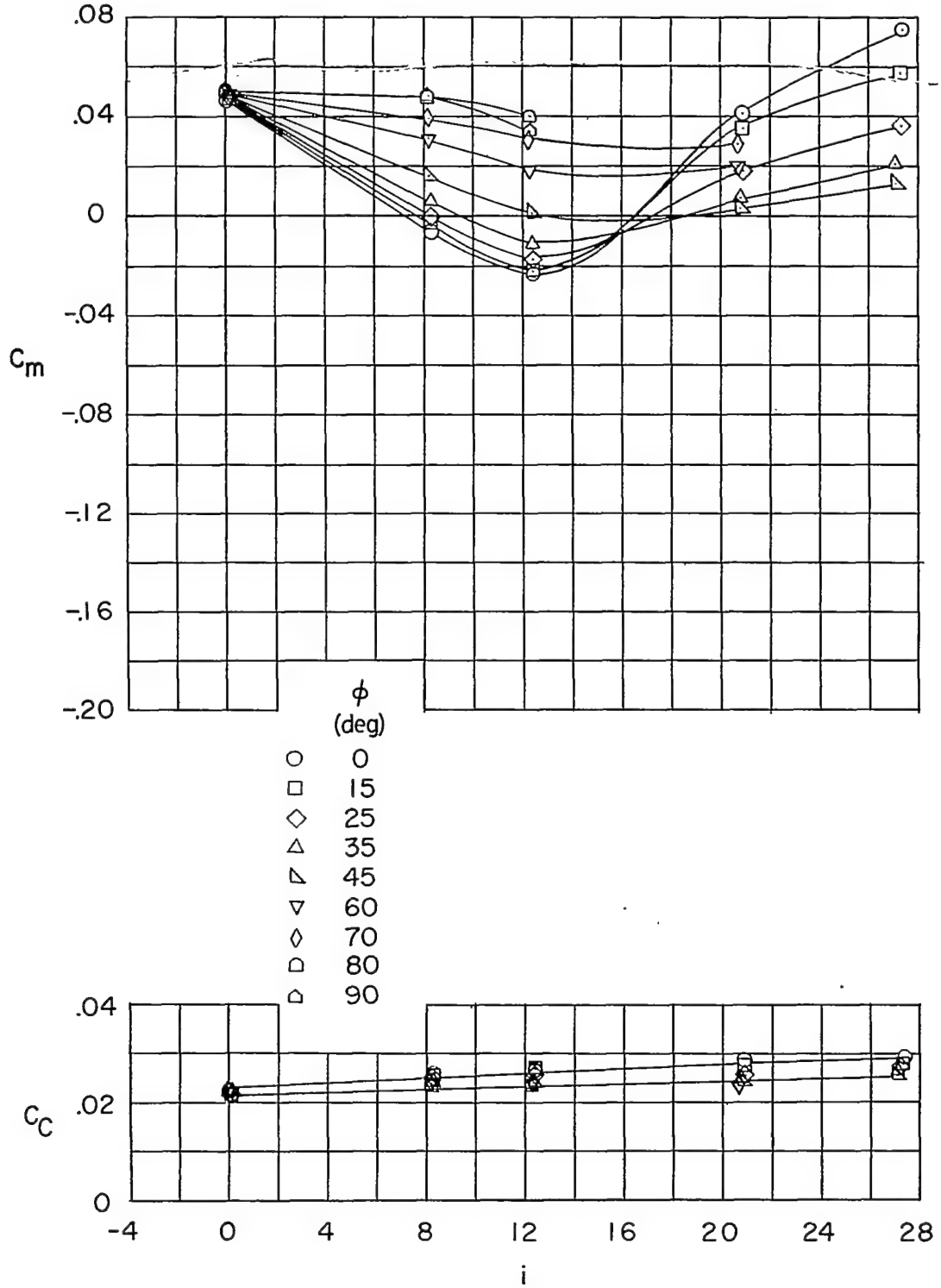

(b) Continued.

Figure 10.- Continued.

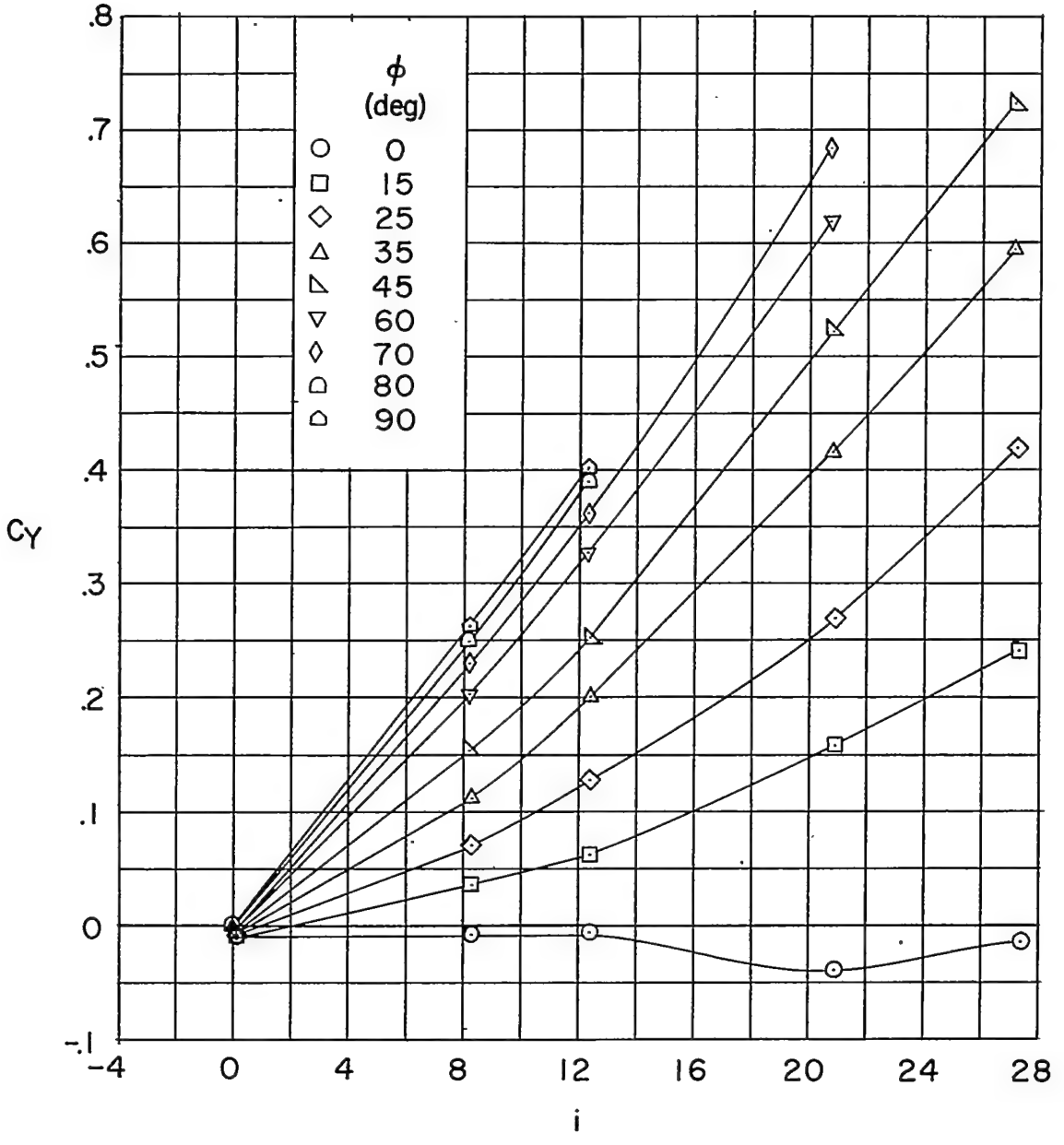

(b) Continued.

Figure 10.- Continued.

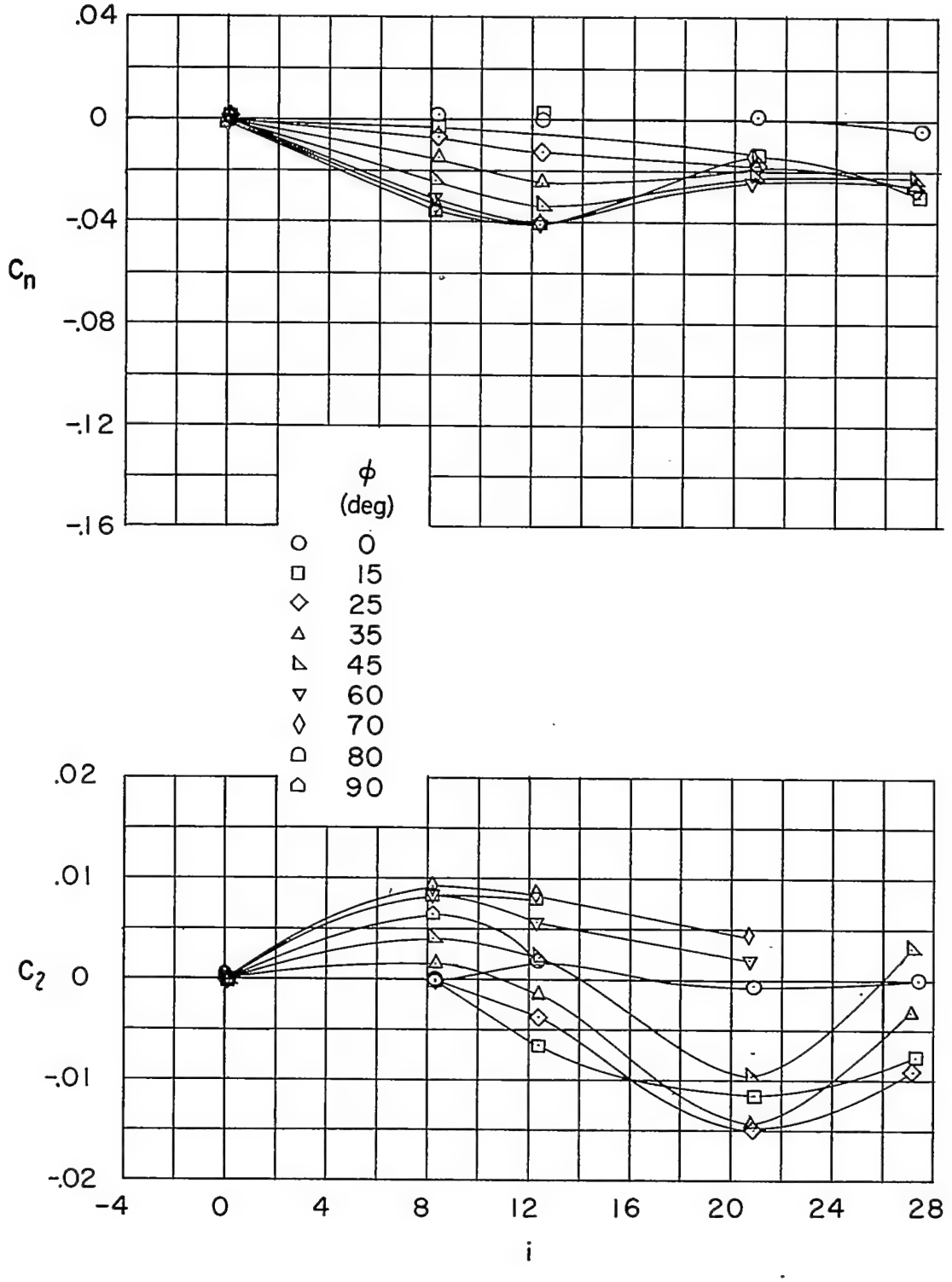

(b) Concluded.

Figure 10.- Continued.

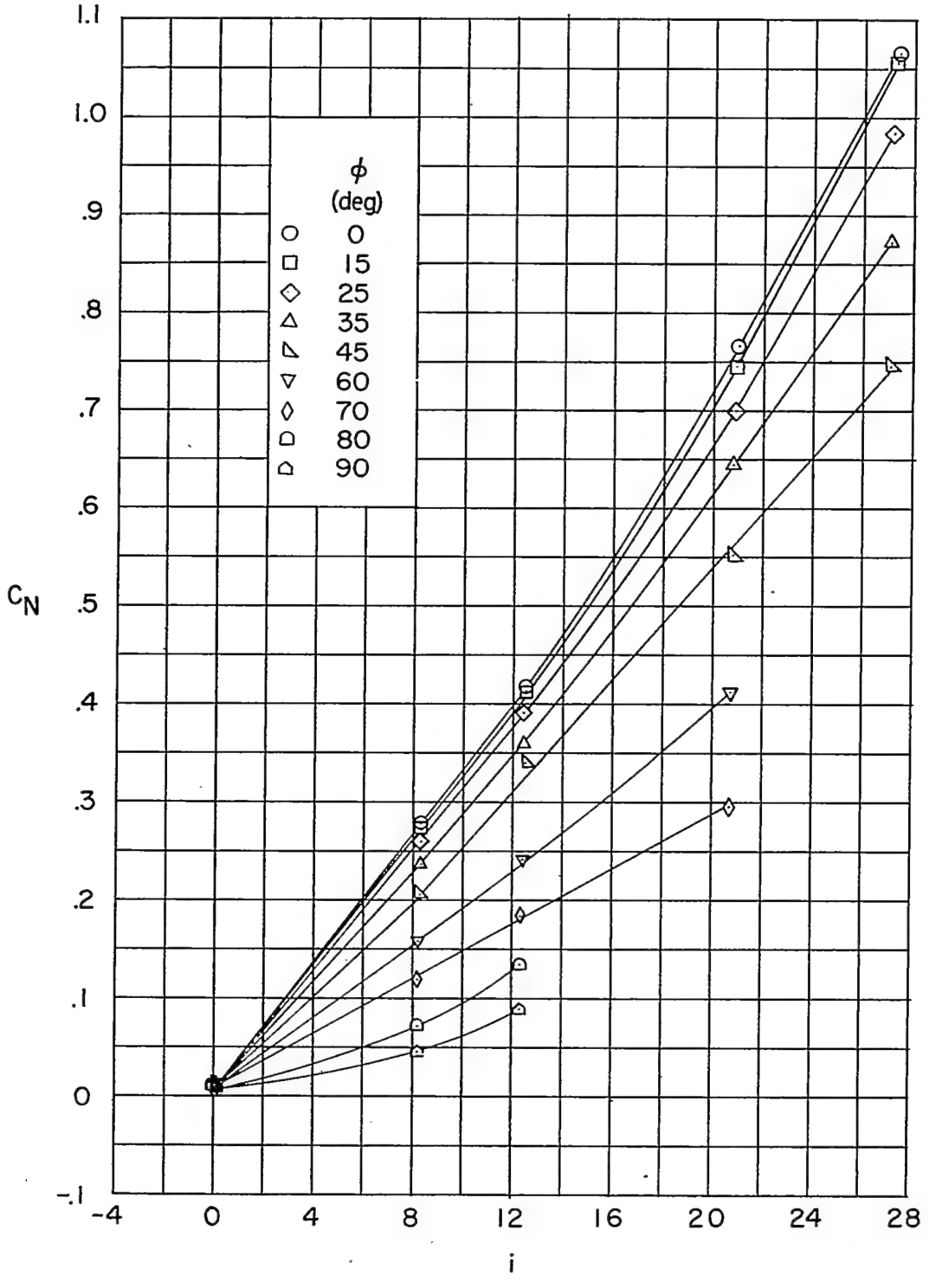

(c) $\delta_H = 12^\circ$.

Figure 10.- Continued.

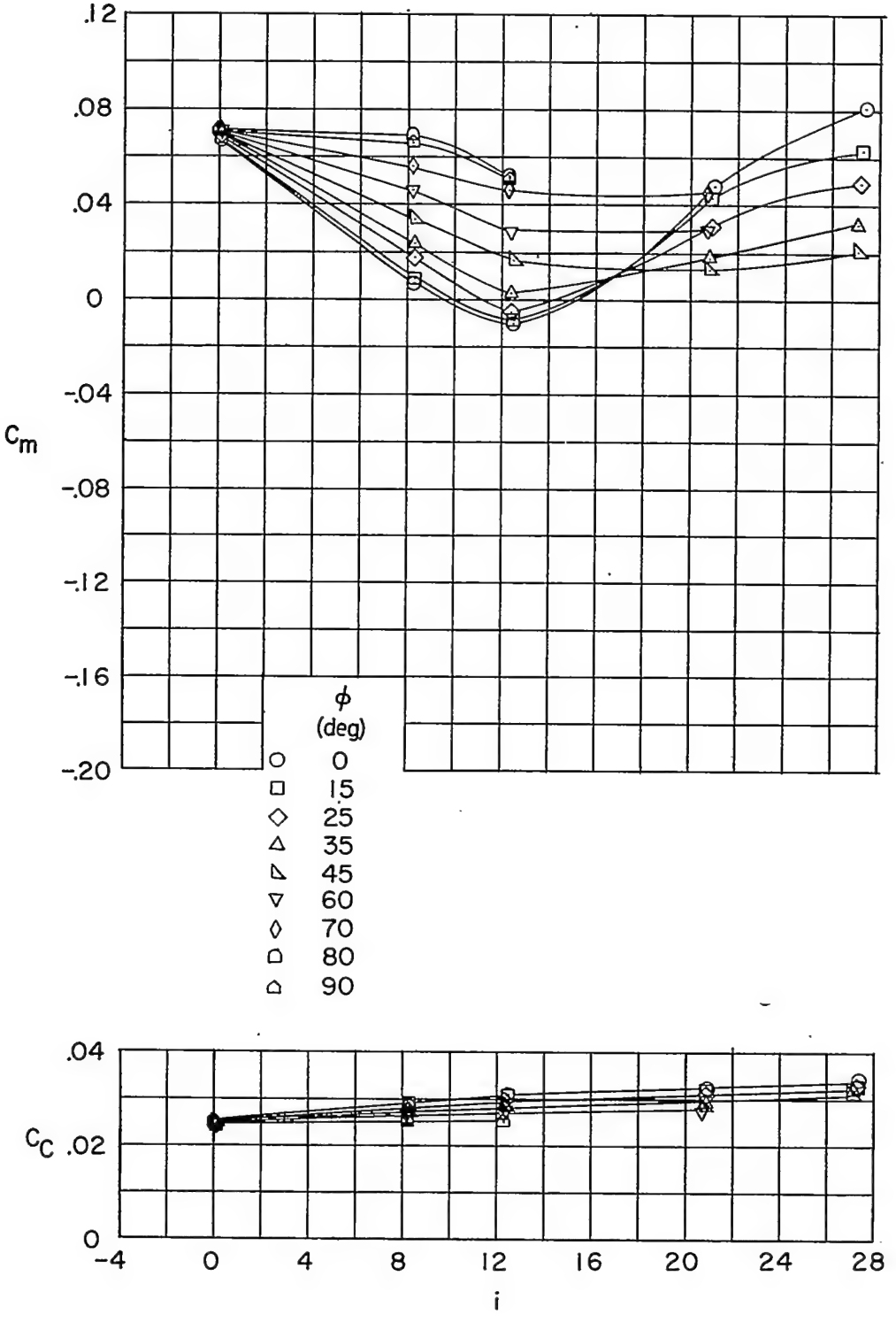

(c) Continued.

Figure 10.- Continued.

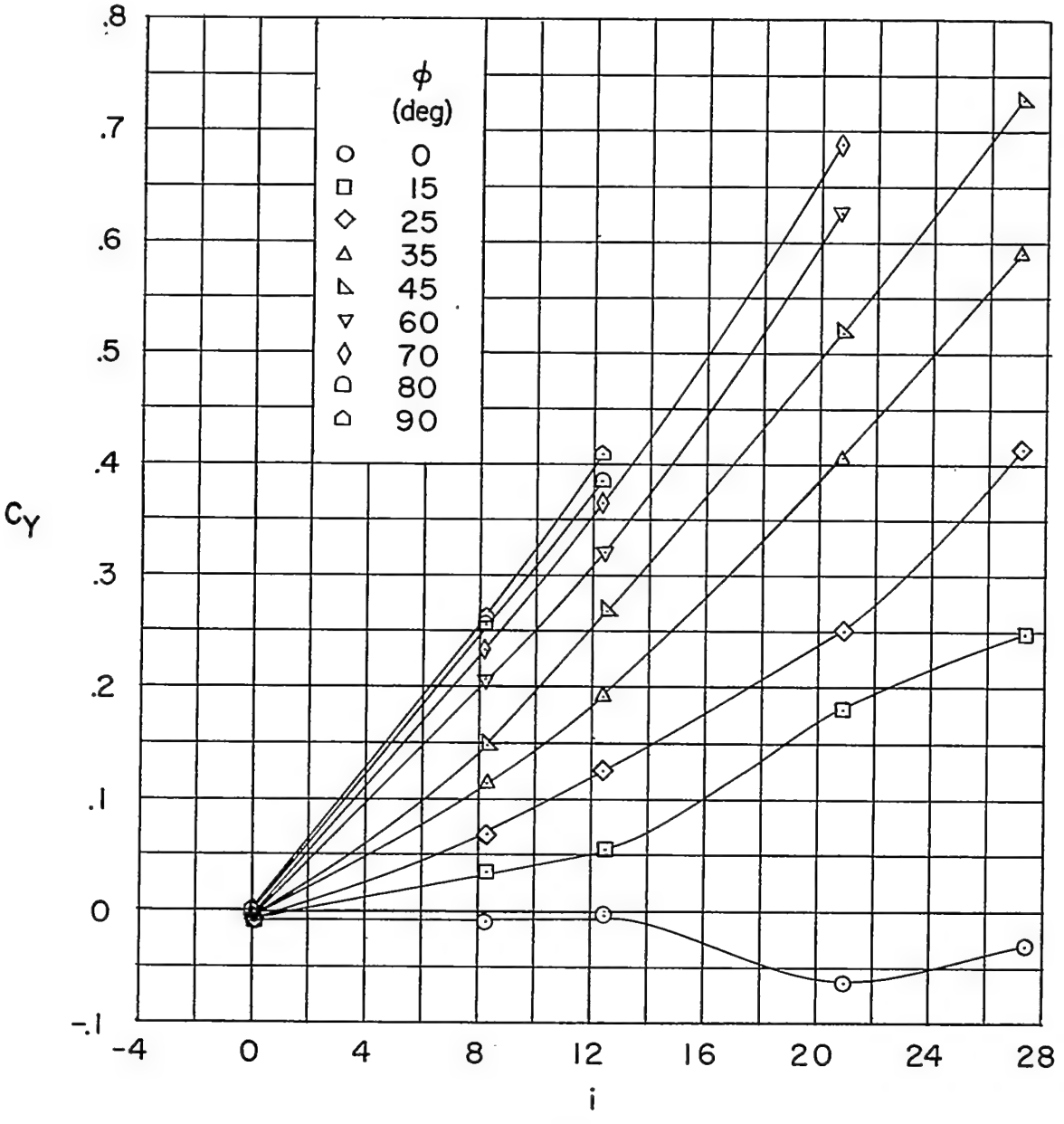

(c) Continued.

Figure 10.-Continued.

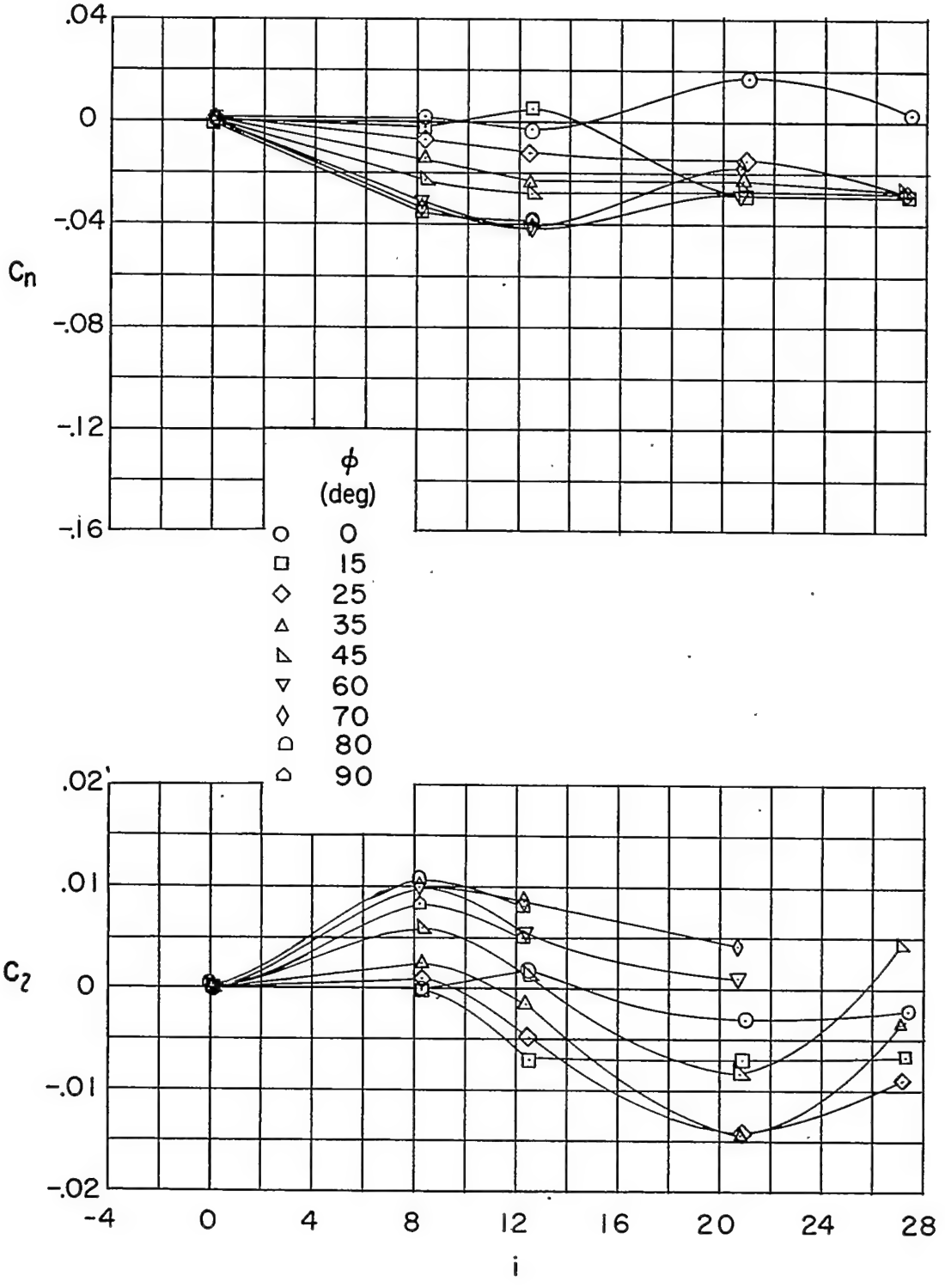

(c) Concluded.

Figure 10.-Concluded.

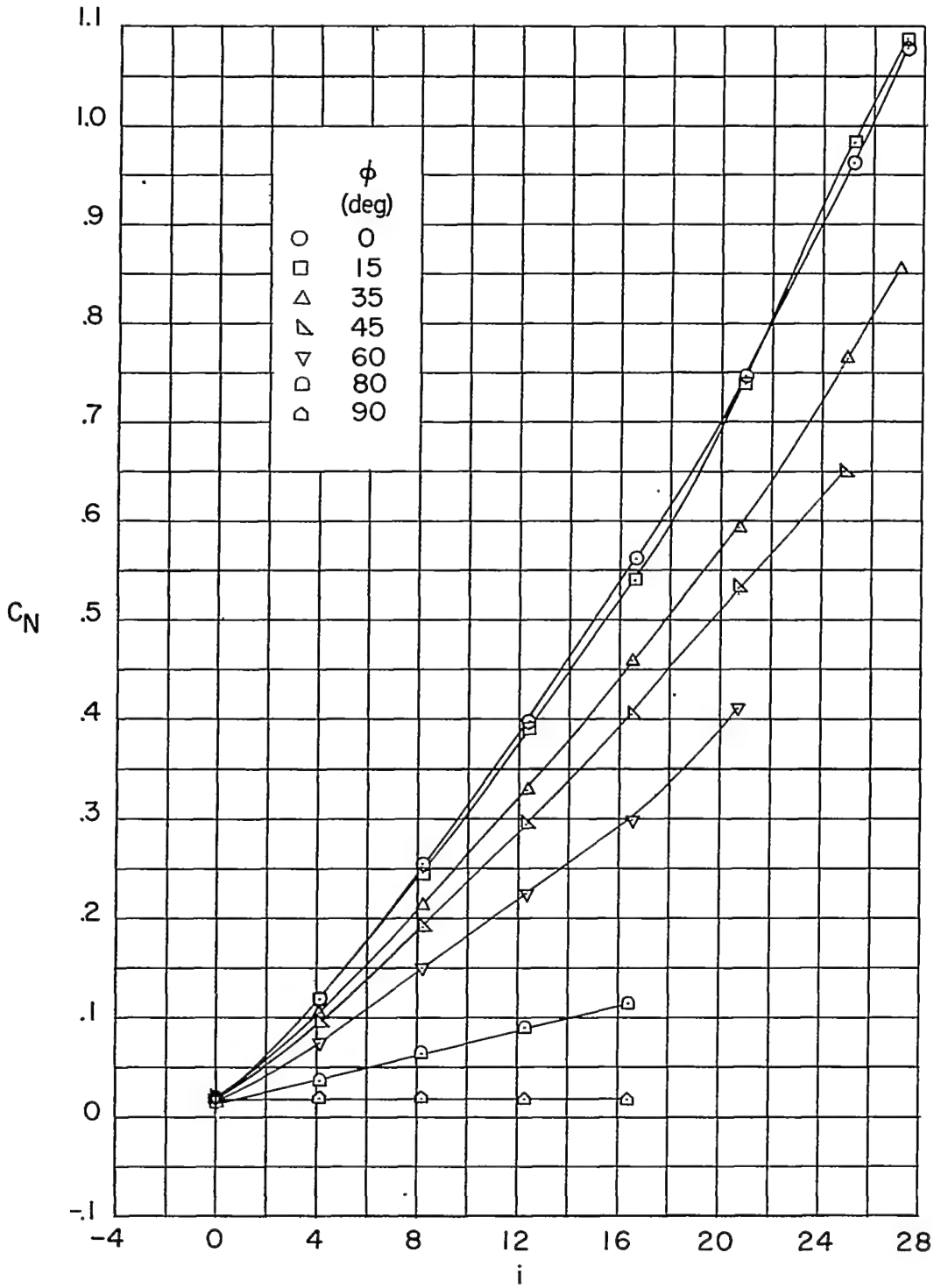

(a) $\delta_H = 0^\circ$.

Figure 11.- Body-wing-canard. $l/d = 19.1$; indexed wings.

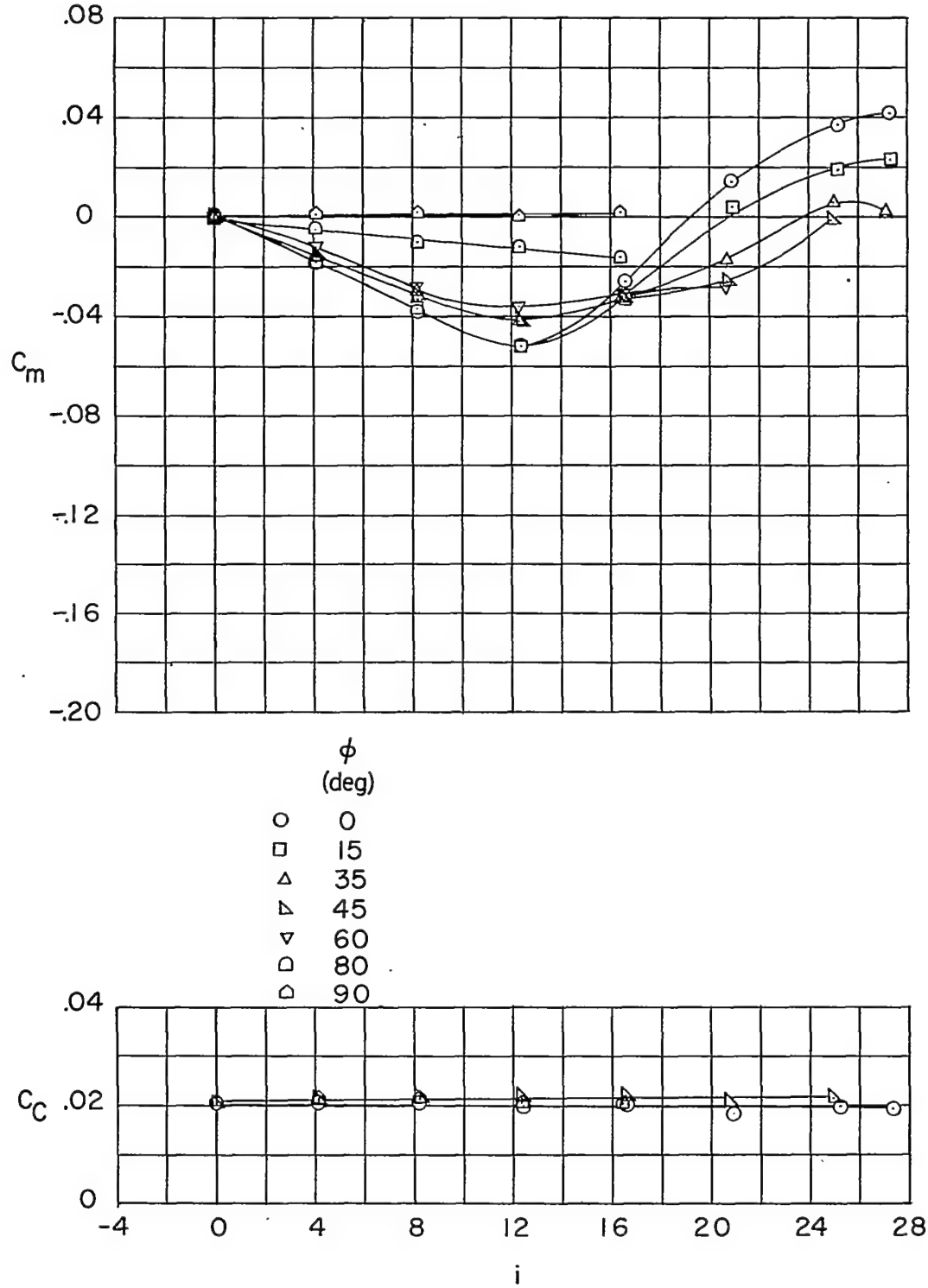

(a) Continued.

Figure 11.- Continued.

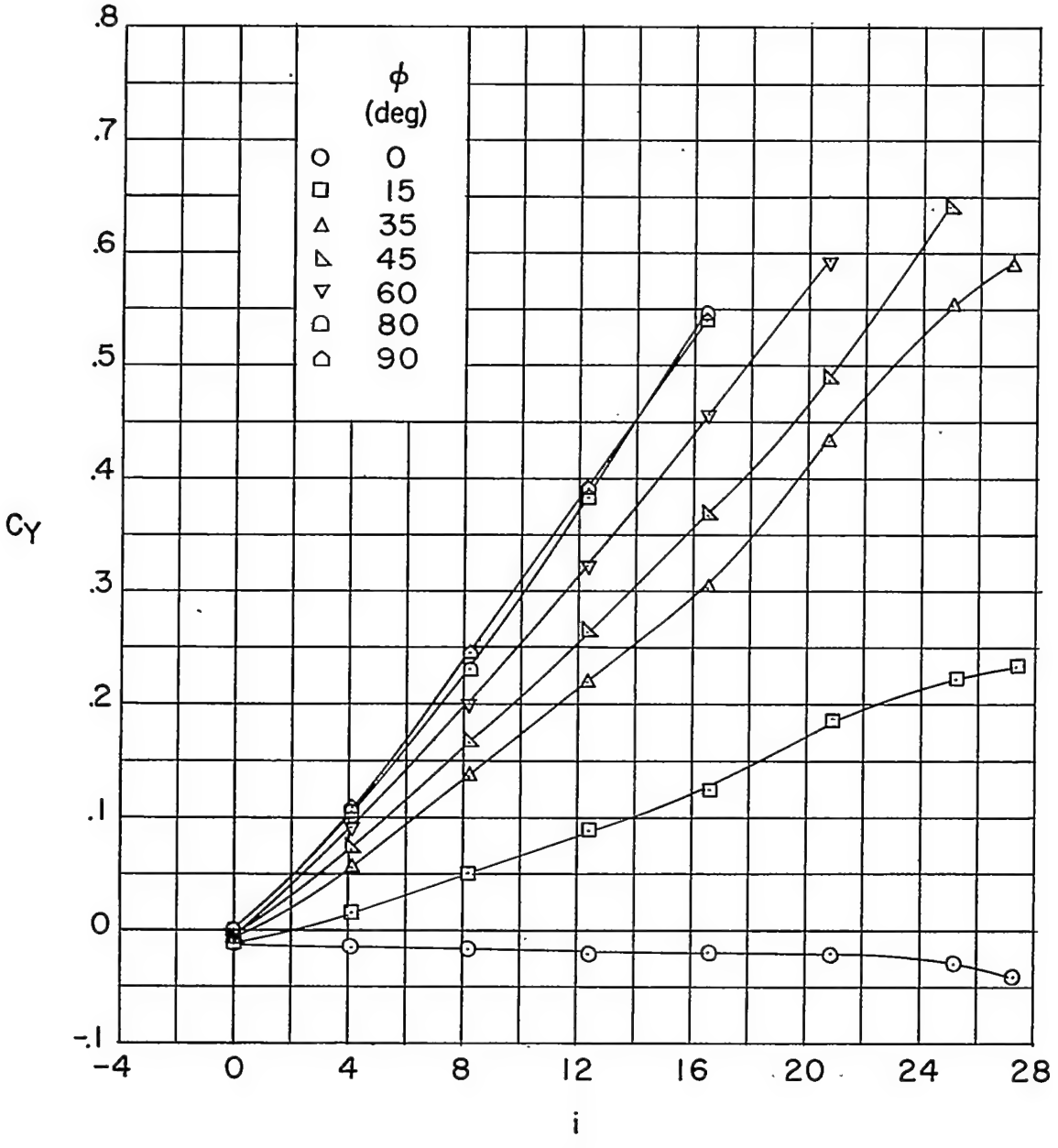

(a) Continued.

Figure 11.- Continued.

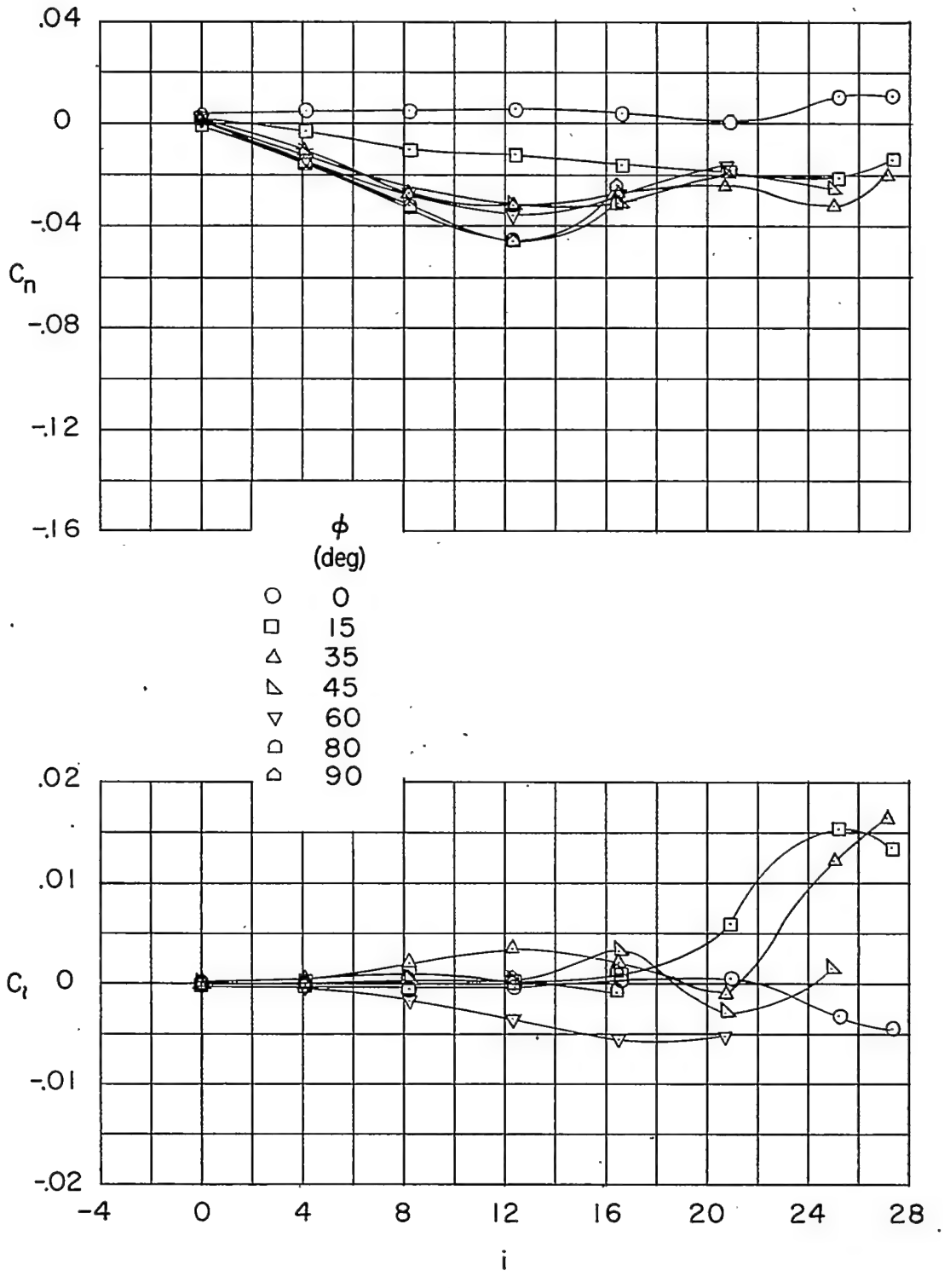

(a) Concluded.

Figure 11.- Continued.

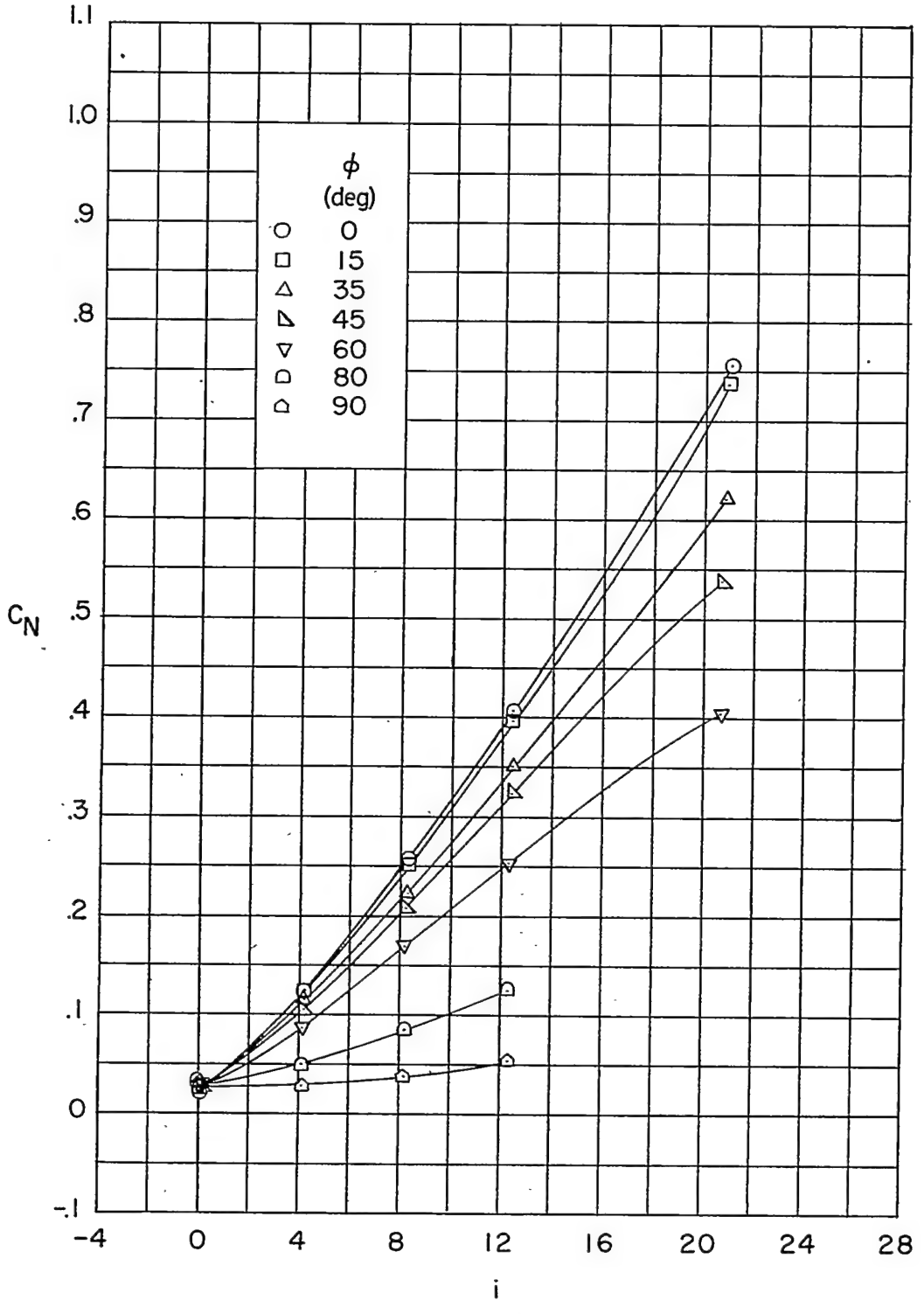

(b) $\delta_H = 8^\circ$.

Figure 11.- Continued.

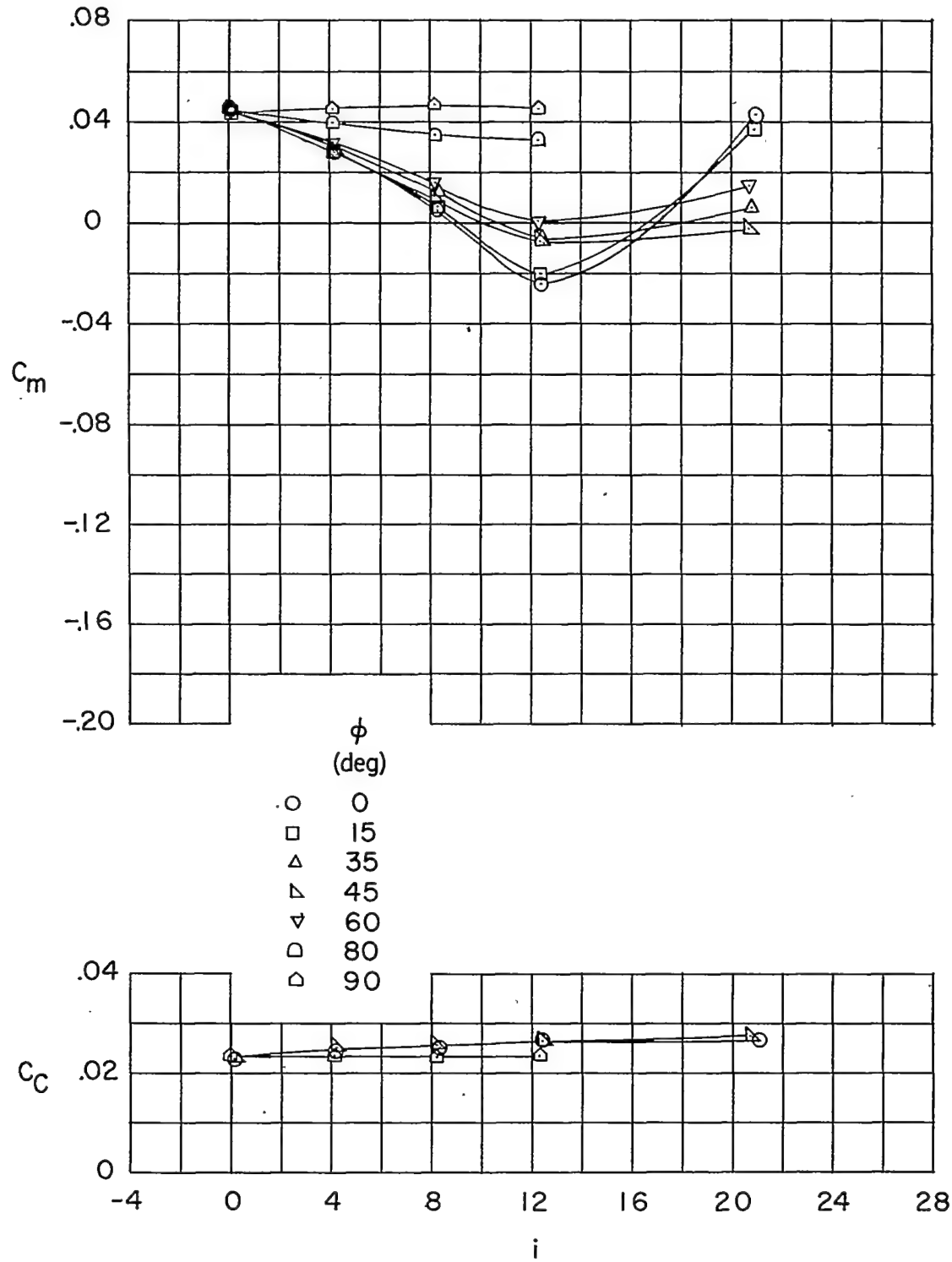

(b) Continued.

Figure 11.- Continued.

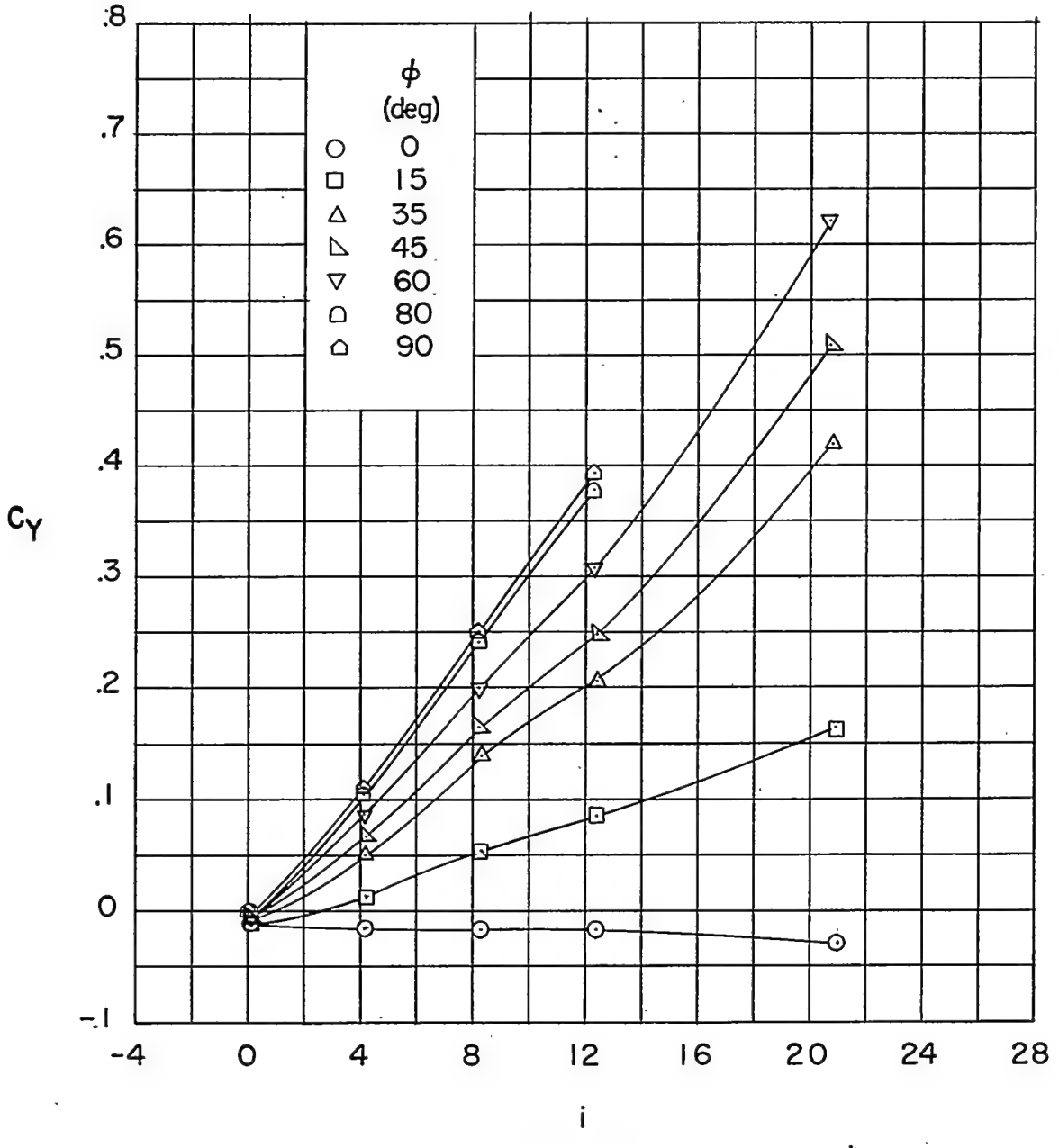

(b) Continued.

Figure 11.- Continued.

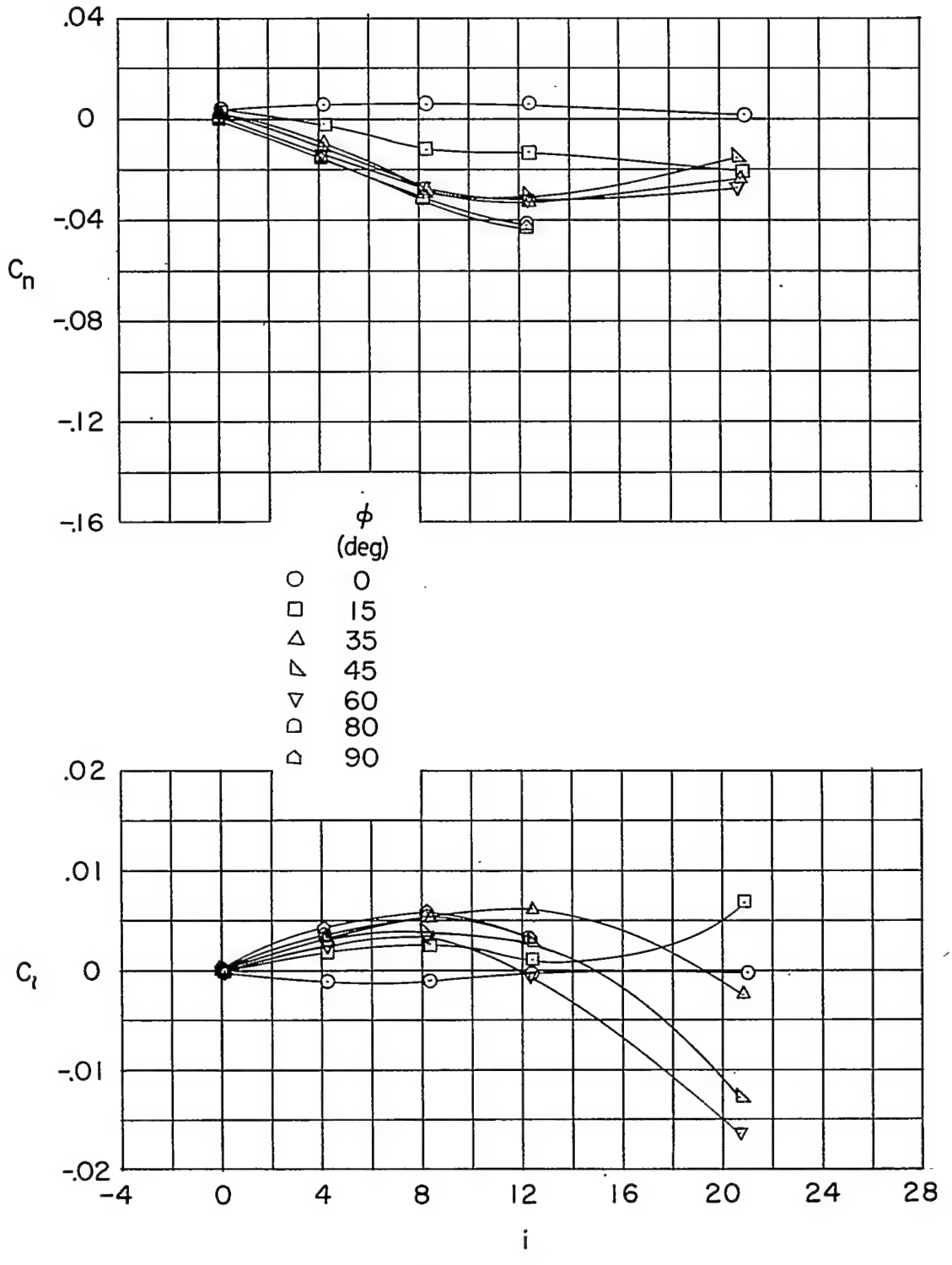

(b) Concluded.

Figure 11.- Continued.

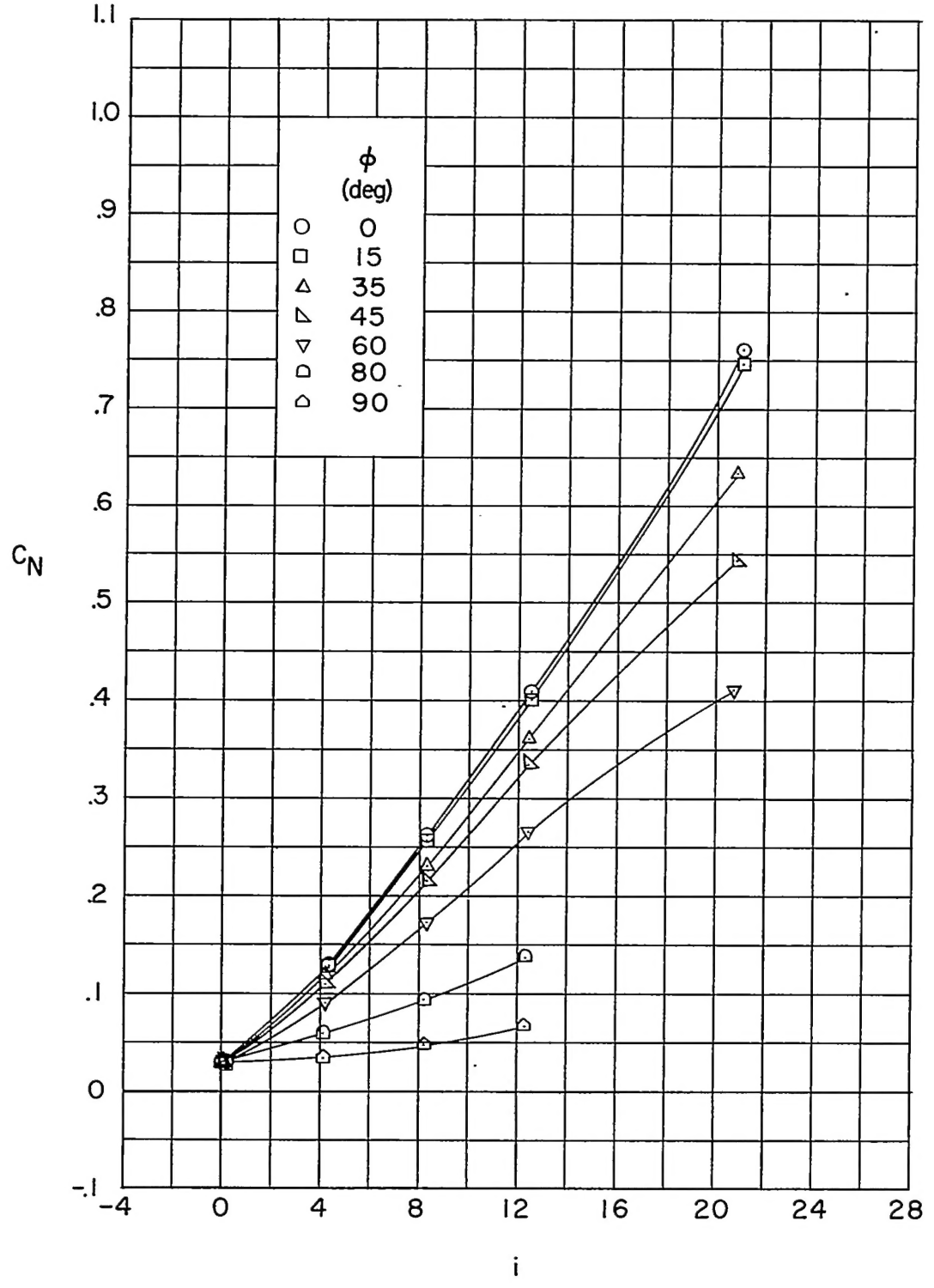

(c) $\delta_H = 12^\circ$.

Figure 11.- Continued.

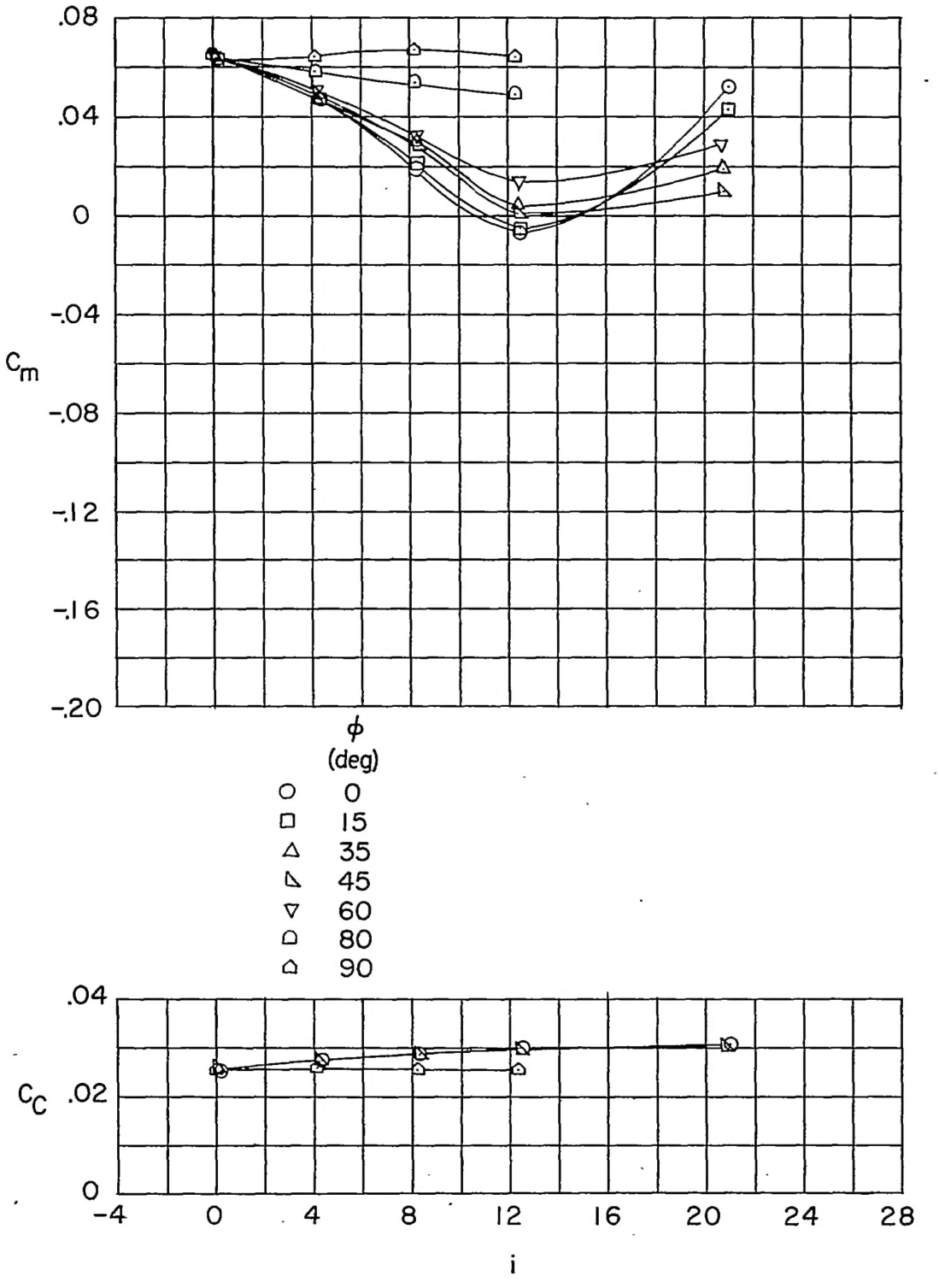

(c) Continued.

Figure 11.- Continued.

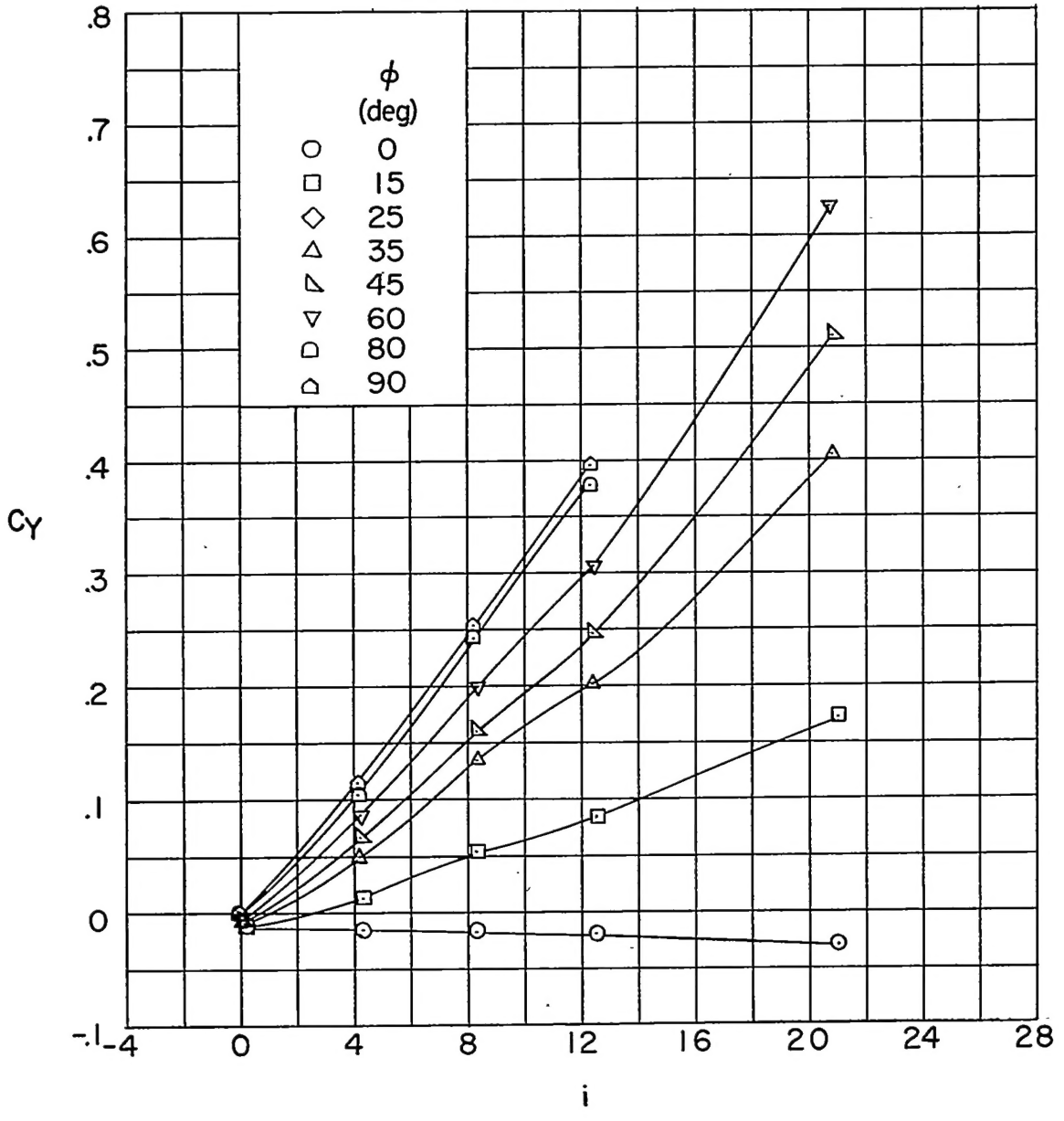

(c) Continued.

Figure 11.- Continued.

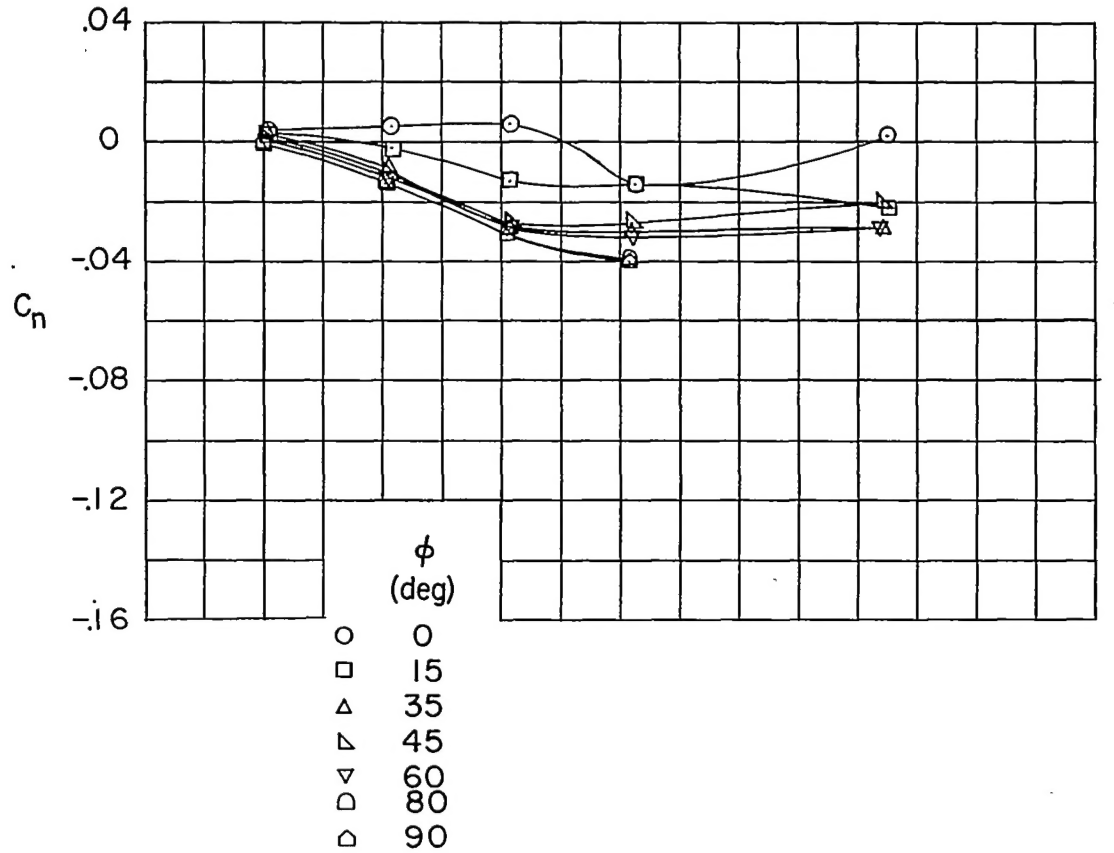

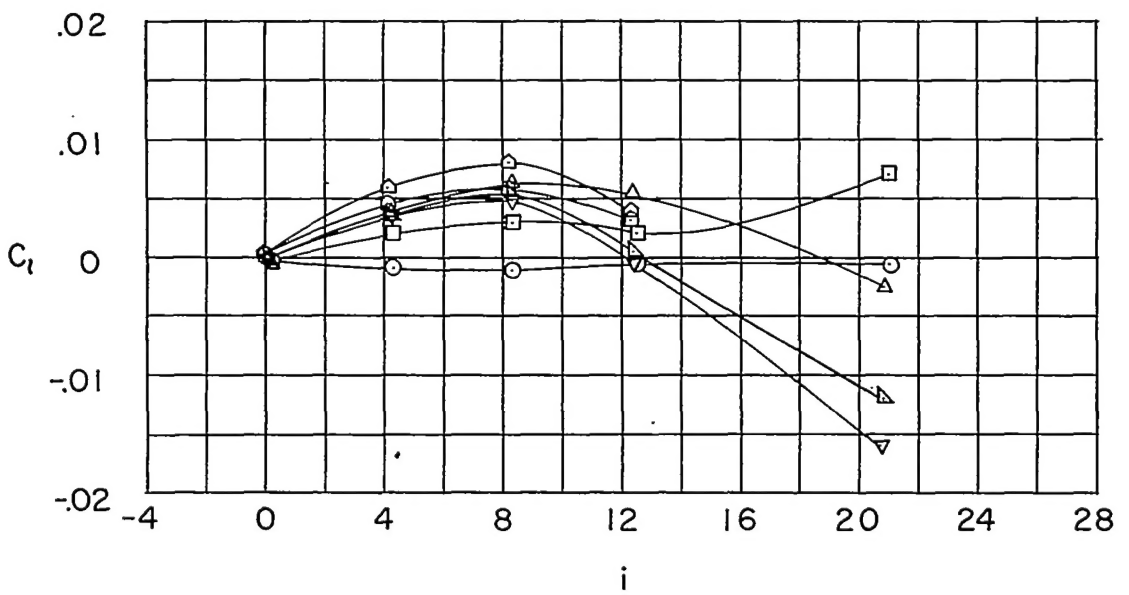

(c) Concluded.

Figure 11.- Concluded.

NACA-Langley - 8-23-54 - 325